



Forest Service

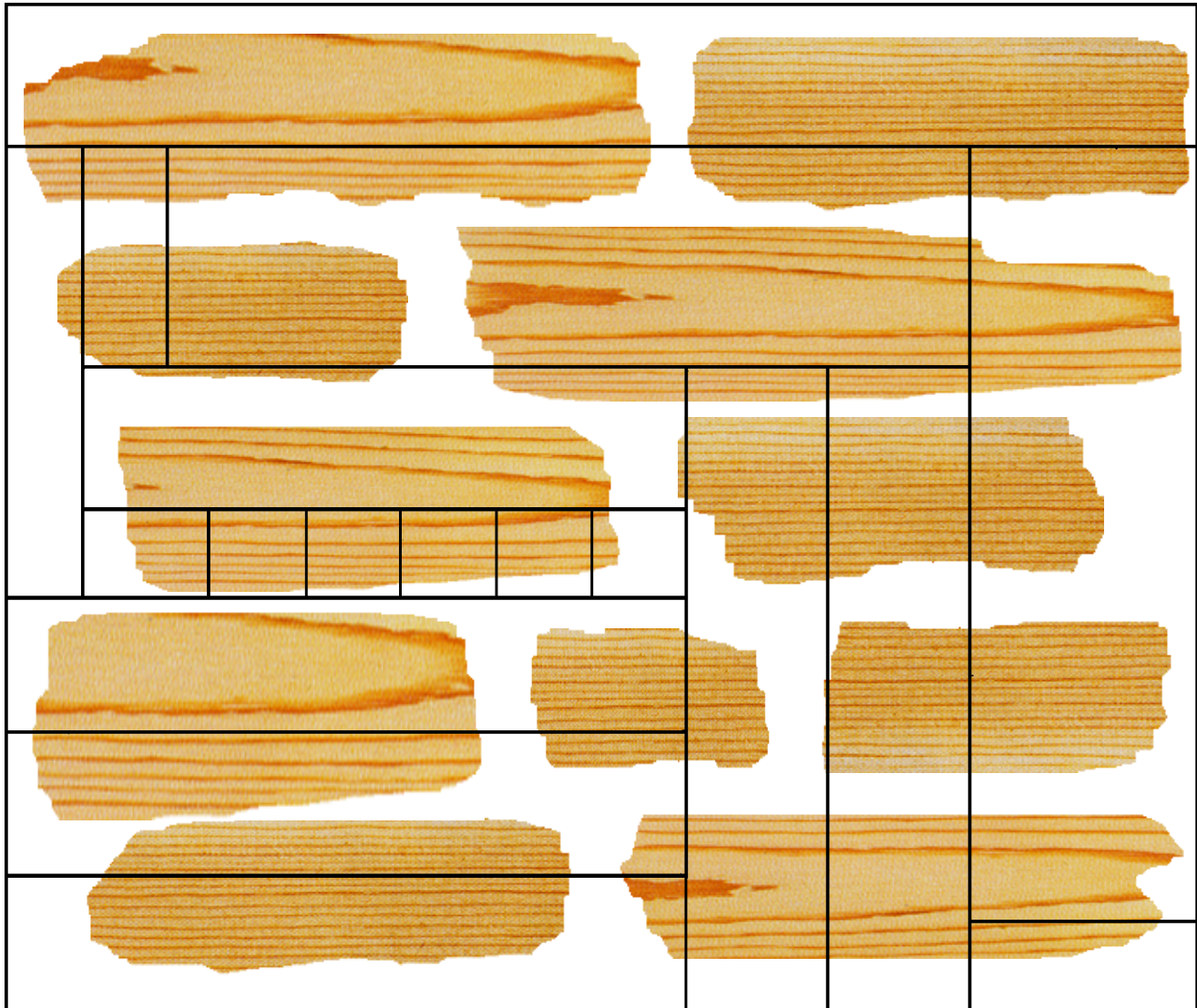
Forest Products Laboratory

Research Paper  
FPL-RP-577



# Flake Furnish Characterization Modeling Board Properties With Geometric Descriptors

Robert L. Geimer  
James W. Evans  
Dody Setiabudi



## Abstract

Four flake furnishes differing in either target length and width or in production methods were combined and degraded to establish 13 different furnish types. Samples from each furnish type were then examined using image analysis techniques. By ranking the data from smallest to largest, percentile values were obtained for long chord, width, area, and perimeter. Cumulative distribution curves visually presented the difference in these geometric descriptors between furnish types. Data were analyzed to determine the descriptors most useful in predicting the flake alignment potential as well as the board properties of bending modulus of elasticity, shear stress, thickness swell, and linear expansion.

Keywords: flake furnish, characterization, image analysis, flake geometry, board properties

September 1999

---

Geimer, Robert L.; Evans, James W.; Setiabudi, Dody. 1999. Flake furnish characterization—Modeling board properties with geometric descriptors. Res. Pap. FPL–RP–577. Madison, WI: U.S. Department of Agriculture, Forest Service, Forest Products Laboratory. 36 p.

A limited number of free copies of this publication are available to the public from the Forest Products Laboratory, One Gifford Pinchot Drive, Madison, WI 53705–2398. Laboratory publications are sent to hundreds of libraries in the United States and elsewhere.

The Forest Products Laboratory is maintained in cooperation with the University of Wisconsin.

The use of trade or firm names in this publication is for reader information and does not imply endorsement by the U.S. Department of Agriculture of any product or service.

The United States Department of Agriculture (USDA) prohibits discrimination in all its programs and activities on the basis of race, color, national origin, gender, religion, age, disability, political beliefs, sexual orientation, or marital or familial status. (Not all prohibited bases apply to all programs.) Persons with disabilities who require alternative means for communication of program information (braille, large print, audiotape, etc.) should contact the USDA's TARGET Center at (202) 720–2600 (voice and TDD). To file a complaint of discrimination, write USDA, Director, Office of Civil Rights, Room 326-W, Whitten Building, 14th and Independence Avenue, SW, Washington, DC 20250–9410, or call (202) 720–5964 (voice and TDD). USDA is an equal employment opportunity employer.

## Contents

|  | <i>Page</i> |
|--|-------------|
| Introduction .....   | 1           |
| Background .....   | 1           |
| Objective .....  | 2           |
| Procedure.....   | 2           |
| Flake Preparation.....   | 2           |
| Flake Characterization.....                                      | 3           |
| Board Fabrication.....   | 4           |
| Testing .....  | 4           |
| Results and Discussion .....                                     | 6           |
| Furnish Characterization.....                                    | 6           |
| Flake Alignment .....  | 11          |
| Board Properties.....  | 14          |
| Models.....  | 23          |
| Predicting Board Properties Using Flake<br>Characteristics ..... | 27          |
| Determining Sample Sizes.....                                    | 35          |
| Conclusions .....  | 35          |
| References .....   | 35          |

# Flake Furnish Characterization

## Modeling Board Properties With Geometric Descriptors

**Robert L. Geimer**, Research Forest Products Technologist (retired)

**James W. Evans**, Supervisory Mathematical Statistician  
Forest Products Laboratory, Madison, Wisconsin

**Dody Setiabudi**, Research Wood Scientist

Agency for Forestry Research and Development, Samarinda, East Kalimantan, Indonesia

### Introduction

In 1999, 35 years after the commercialization of structural flakeboard, the combined annual flakeboard production capacity of Canada and the United States is projected to reach 18.7 million cubic meters, capturing 50% of the mammoth commodity sheathing market (Spelter 1997, Tansey 1994) (Spelter 1997, personal communication). As with most commodity products, competition has motivated product and process optimization. Fabrication techniques have been altered, incorporating flake alignment to achieve high bending stiffness in oriented strandboard (OSB), which is a variation of structural flakeboard. Layered board configurations have been developed to control linear expansion and further the economic use of lower grade material. Major improvements made in flake production (whole-log, ring type flakers) and resin blending (spinning disk atomization) have permitted manufacturers to reduce board density and glue consumption. The efficiency thus gained has reduced the margin for manufacturing error.

A major problem manufacturers are facing, both now and into the future, is maintaining board quality and controlling production costs in the face of a changing and more heterogeneous forest resource (combinations of factors such as species, size, age class, plantation grown material, and residues) and greater competition for finite wood supplies. The problem has become more acute since 1995 with the construction of 22 new OSB mills increasing net production capabilities by 94%. Two recourses for the industry are to increase the use of chipable forest residues and to more efficiently use smaller flakes.

Basic investigations have shown the potential and the limitations of converting maxi chips or “fingerlings” to usable flakes with a ring flaker (Heebink and others 1977, Geimer and others 1974, Geimer and Price 1978).

Important requirements for the successful integration of these ring flakes with disk flakes or strands include a means to measure the flake furnish and development of criteria that determine the relative quality of the furnish. Previous research has shown that image analysis techniques can supply geometrical information useful in the statistical description of a flake furnish (Geimer and Link 1988). The following research addresses the problem of determining the relative importance of a number of flake furnish descriptors. These descriptors are used to estimate flake alignment potential and to predict bending, shear, and dimensional stability properties of the flakeboard, which affect final product performance and, hence, board quality.

### Background

Early structural composite wood research demonstrated the strong relationship between flake geometry and the major physical and mechanical properties of flakeboards constructed from uniform flakes and mixtures of flake types (Turner 1954, Lehmann and Geimer 1974). Early studies included the effect of flake geometry on the potential to align flakes and subsequently the effect of flake alignment on board properties (Geimer 1976, 1979, 1980). Recent work directed at modeling the consolidation of flakeboard by measuring the vertical and horizontal density distribution has shown that board properties are affected by changes in flake packing arrangement (Steiner and Dai 1993; Dai and Steiner 1994a,b; Lang and Wolcott 1995; Lu and others 1998; Suchland and Xu-Hong 1989; Winistorfer and others 1996; Winistorfer and Xu 1996). Packing arrangement, resulting from changes in flake geometry, also changes in predictable fashion with changes in flake alignment. Being able to define a furnish type and to detect changes in flake geometry is extremely important in the design and manufacture of a structural flakeboard.

Disk-cut flake furnishes, because of their relative uniformity, have in most cases been adequately defined by average length, width, and thickness measurements. However, increasing demand on wood supply has prompted the use of lower quality material and in some cases the addition of ring flakes to the structural board furnish. Heebink and Chern (1975, unpublished data) first realized the potential of a ring flaker to manufacture flakes suitable for the production of structural board from residues. Large maxi-chips with a relatively high aspect ratio, 40 to 80 mm long and approximately 20 mm wide, are oriented by centrifugal force and machine design with the grain direction parallel to the cutting edge of the knives. The resulting furnish comprises larger flakes and has less fines than that produced by small pulp chips, which are often cut perpendicular to the grain. Heebink termed these large chips “fingerlings” because they were approximately the size of a human finger.

Because of the variability of flake size and shape associated with ring flakes, the quality of this type of furnish is more difficult to ascertain or define than a disk flake furnish. Using image analysis (IA) techniques, Geimer and Link (1988) explored the use of geometric descriptors to characterize ring flake furnishes. Q–Q type plots, developed from cumulative distribution relations, were used to compare different flake furnishes. This work showed the potential of using descriptors such as long chord, width, surface area, and form factors to predict board properties.

The rapid conversion of industrial plants from the production of waferboard and flakeboard, which both have random distribution of flakes, to OSB demonstrated the importance of flake orientation in achieving and maintaining desirable board properties. Flake orientation, which is directly dependent on flake geometry, is also extremely critical in achieving the high bending properties necessary in oriented strand lumber (OSL). To obtain sufficient orientation with present day equipment, it is necessary to use very long (300 mm) flakes. However, the high cost of manufacturing associated with long flakes will eventually lead to the development of equipment capable of achieving acceptable alignment with shorter flakes. The need then arises to distinguish a flake furnish in respect to its direct effect on random board properties and on the ability to achieve good alignment.

## Objective

The objective of this research was to determine the ability of flake furnish descriptors, derived from image analysis, to predict flake alignment potential and resulting board properties.

## Procedure

Thirteen flake furnishes, including mixtures of furnish types and degraded furnishes, were characterized using both screen

analysis and IA. Each flake furnish was used to fabricate boards with random flake orientation and at least two levels (high and low) of flake alignment. Alignment was measured using four methods: IA, James V-Meter, grain angle indicator (GAI) (Geimer and others 1993), and directional bending property data. The boards were tested for bending, shear, and dimensional stability. Flake furnish descriptors obtained from the IA were correlated to the board properties considering the various levels of alignment.

## Flake Preparation

Twenty aspen (*Populus* spp.) logs with average diameters of 250 mm were obtained at a local Wisconsin sawmill. Four basic flake types designated A, B, C, and D were manufactured.

- Type A (0.762 by 13 by 73 mm; disk). A portion of the logs were band-sawed into 13-mm-thick boards, ripped to eliminate the bark, and cross-cut to 73-mm lengths. These “cutoffs” were then oriented with the grain direction parallel to the knives of a disk flaker and cut into flakes measuring 13 mm wide by 73 mm long. Target thickness was 0.762 mm.
- Type B (0.762 by 13 by 38 mm; disk). Additional 13-mm-thick boards were cross-cut into 114.3-mm cutoffs and were processed in a manner similar to that described for Type A except that scoring knives were inserted in the disk flaker to cut 13-mm-wide by 38-mm-long flakes.
- Type C (0.762 by 3.2 by 73 mm; disk). Another portion of the logs was band-sawed to 3.2-mm-thick boards, ripped to eliminate the bark, and cross-cut to 73-mm lengths. These cutoffs were then disk-cut into flakes measuring 3.2 mm wide and 73 mm long. Target thickness was again 0.762 mm.
- Type D (0.762 by 70 mm; ring). The final portion of the logs was slabbed to 20-mm thickness and then ripped and cross-cut into 20- by 20- by 70-mm blocks. These blocks were then cut into flakes in a ring flaker. Target thickness was 0.762 mm.

The material for the four basic flake types was then dried to approximately 2% moisture and screened on a 1.59-mm mesh screen to eliminate the fines.

By combining several of these flake types, two additional furnish types were available to study.

Type A+B — This furnish consisted of 50% type A and 50% type B flakes

Type A+B+C — This furnish consisted of 33.3% type A, 33.3% type B, and 33.3% type C flakes

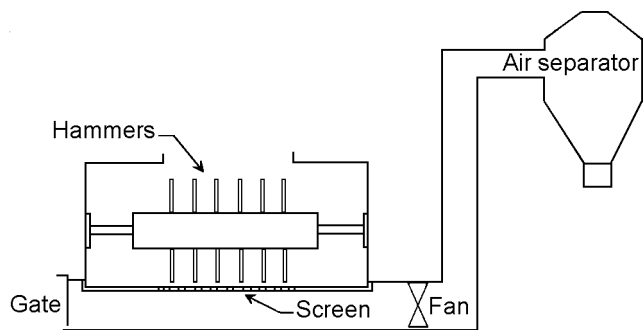


**Figure 1—Hammermill and fan assembly used to prepare flakes.**

Three of the four basic flake types (A, B, and D) were then subjected to milling treatments to provide seven more furnish types. Several options existed for processing the material through the hammermill machine (Fig. 1). These included, in order of increasing severity, passing the material through the fan, passing the material through the hammers without the screen in place, and passing the material through the hammers and a screen. A pass through the hammermill necessitates a pass through the fan. The treatments used to mill the furnishes were not intended to mimic any commercial plant operation but were arrived at by exploratory trials using visual observations and screen analysis as guides. The objective was to create an observable difference in furnish composition without completely destroying its integrity. Ultimately, no hammermill screens were used. However, variations used to refine the degree of treatment included multiple passes using the same or different procedure. The treatments are described as follows:

- Type A<sub>1</sub> — Type A flakes passed once through the fan
- Type A<sub>2</sub> — Type A flakes passed twice through the fan
- Type A<sub>3</sub> — Type A flakes passed once through the hammermill and once through the fan
- Type A<sub>4</sub> — Type A flakes passed once through the hammermill and twice through the fan
- Type B<sub>1</sub> — Type B flakes passed twice through the fan
- Type D<sub>1</sub> — Type D flakes passed once through the fan
- Type A<sub>1</sub>+B<sub>1</sub> — Mixture of 50% type A<sub>1</sub> and 50% type B<sub>1</sub>

The fines passing through a 1.59-mm screen were eliminated following collection of IA samples but prior to board manufacture.

## Flake Characterization

With the exception of type A<sub>1</sub>+B<sub>1</sub>, three screen analyses of approximately 15 kg each were performed for each furnish type (Table 1). Screen mesh sizes used were 12.7, 6.35, 3.175, and 1.59 mm, hereafter referred to as 1/2, 1/4, 1/8, and 1/16 screens (after their mesh sites in inches). A sample of the fraction remaining on each screen, equal in weight to the percentage that the screen type represented of the total, was obtained for IA. For example, if a screen contained 25% of the weight, then 25 g of our sample would come from that screen. This provided three replicate IA sets, each consisting of four screen fractions for each flake type (except type A<sub>1</sub>+B<sub>1</sub>). Each IA set had a total weight equal to 100 g minus the weight fraction equivalent that passed through the

**Table 1—Screen analysis by furnish type**

| Screen <sup>a</sup> | Furnish type                  |                |                |                |                |       |                |       |       |                |       | (A <sub>1</sub> +B <sub>1</sub> )<br>calc | A+B+C |  |
|---------------------|-------------------------------|----------------|----------------|----------------|----------------|-------|----------------|-------|-------|----------------|-------|---|-------|--|
|                     | A                             | A <sub>1</sub> | A <sub>2</sub> | A <sub>3</sub> | A <sub>4</sub> | B     | B <sub>1</sub> | C     | D     | D <sub>1</sub> | A+B   |   |       |  |
|                     | Weight (%) <sup>b</sup>       |                |                |                |                |       |                |       |       |                |       |   |       |  |
| -1/16               | 0.11                          | 2.53           | 5.51           | 8.46           | 13.07          | 0.05  | 3.54           | 0.66  | 1.00  | 7.57           | 0.08  | 3.04                                      | 0.26  |  |
| +1/16               | 0.78                          | 6.79           | 12.04          | 15.56          | 20.97          | 0.03  | 6.94           | 3.96  | 3.66  | 11.26          | 0.40  | 6.86                                      | —     |  |
| 1/8                 | 3.69                          | 14.99          | 26.82          | 37.58          | 49.52          | 0.17  | 23.99          | 26.36 | 10.14 | 27.87          | 1.93  | 19.49                                     | 10.08 |  |
| 1/4                 | 22.08                         | 31.06          | 34.92          | 27.46          | 13.27          | 13.49 | 44.38          | 46.92 | 29.37 | 31.17          | 17.79 | 37.72                                     | 27.50 |  |
| 1/2                 | 73.34                         | 44.63          | 20.71          | 10.94          | 3.17           | 86.26 | 21.15          | 22.10 | 55.83 | 22.13          | 79.80 | 32.89                                     | 60.57 |  |
|                     | Number of flakes <sup>b</sup> |                |                |                |                |       |                |       |       |                |       |   |       |  |
| +1/16               | 192                           | 1,476          | 2,719          | 4,239          | 6,433          | 15    | 1,440          | 553   | 1,118 | 4,398          | 104   | 1,458                                     | 253   |  |
| 1/8                 | 111                           | 736            | 1,567          | 3,013          | 5,218          | 22    | 973            | 475   | 718   | 3,717          | 66    | 855                                       | 203   |  |
| 1/4                 | 158                           | 351            | 555            | 578            | 426            | 99    | 937            | 732   | 505   | 1,470          | 129   | 644                                       | 330   |  |
| 1/2                 | 306                           | 338            | 241            | 186            | 152            | 614   | 344            | 328   | 549   | 664            | 460   | 341                                       | 416   |  |

<sup>a</sup>1/16 = 1.59 mm, 1/8 = 3.175 mm, 1/4 = 6.35 mm, 1/2 = 12.7 mm.

<sup>b</sup>Average of three samples.

1/16 screen. Screen analysis and the resulting IA samples on the unmilled furnish types were obtained after most of the material passing the 1/16 screen was removed in a preliminary screening. Screen analysis and IA samples on the milled furnishes were obtained prior to removing the fraction passing the 1/16 screen.

The IA data were obtained with a Cambridge Quantinet 970 instrument. Field of view was 15 by 20 cm with a magnification factor of 28. To avoid overlap, the flakes were individually placed on a black sheet of paper with their long dimension generally oriented in one direction. The number of flakes measured with each image varied with flake size. In general, between 20 and 30 flakes from the 1/2 screen were viewed at any one time. Approximately 30 to 40, 40 to 70, and 80 to 120 flakes were viewed for the 1/4, 1/8, and 1/16 screen fractions, respectively. Data measured with the IA included the long chord, width, perimeter, and top surface area. Long chord (LC) is defined as the longest chord that can be drawn within the described image. Width is computed as the greatest distance within a flake at right angles to the LC. Perimeter is the distance described by the flake edges. Area is the space enclosed within the perimeter. Image analysis data were not obtained for those flake furnishes that were a mixture of other furnishes, A+B, A+B+C, and A<sub>1</sub>+B<sub>1</sub>. With the exception of the mixed furnishes, flake thickness was measured on 10 flakes drawn randomly from each screen fraction, from each IA replication.

## Board Fabrication

A series of 13- by 660- by 715-mm single layer boards having random (R) distribution, low alignment (LA), and high alignment (HA) of the flakes was constructed using each of the 13 furnish types. Three replications were made at each level of alignment. In addition, three medium aligned (MA) boards were made using the B furnish. Flakes were aligned in a machine having a series of horizontal vibrating fins (Geimer 1976). Plate spacing (25 mm), vibration amplitude (5 mm), and vibration rate (20 Hz) were held constant for all board constructions. Alignment was varied by changing free-fall distance. This adjustment was made by raising and lowering the alignment machine, which was mounted on a motorized hoist. The elevation of the alignment machine was adjusted to maintain a constant free-fall distance throughout the forming process. The distance between the bottom of the alignment fins to the top of the mat was maintained at 102 mm, 70 mm, and 38 mm, respectively, for LA, MA, and HA. Keeping the alignment settings the same for all furnish types permitted the development of relations between flake geometry and degree of alignment. The MA free-fall distance was chosen to obtain an alignment for the B furnish, nearly equal to the LA level in the boards made from type A furnish. This provided the opportunity to compare properties of boards made from different furnish types at the same level of alignment.

All boards were single layer and were constructed to an oven-dry (OD) specific gravity (SG) of 0.64 using 4% of phenolic resin. Target mat moisture before pressing was 10%. Boards were pressed in a conventional manner for 8 min at 190°C.

## Testing

All boards were weighed and measured for thickness immediately following removal from the press. The boards were then equilibrated to constant weight in a 27°C 60% relative humidity (RH) environment.

### Alignment Measurement

After trimming the boards to 638 mm in the direction parallel (Pa) to flake alignment and to 559 mm in the direction perpendicular (Pe) to flake alignment, they were measured in each direction with a James V-meter to determine the sonic velocity ratio. Three measurements were taken in each direction.

Flake alignment was also estimated by measuring the angle that selected surface flakes made with the cardinal direction of alignment. Sixty flakes were measured on the top surface of each board. These flakes were selected by overlaying the board with a clear plastic sheet that contained a 10 (Pe) × 6 (Pa) matrix of dots.

The board was then cut into specimens as shown in Figure 2. The 121- by 432-mm specimens, one cut Pa and one cut Pe to the cardinal alignment direction, were used to determine alignment using the GAI. The GAI data are not included in this report.

### Physical and Mechanical Board Properties

From each board, four 76- by 356-mm specimens were tested for bending modulus of elasticity (MOE) and modulus of rupture (MOR). Two specimens were cut Pa and two Pe to the cardinal alignment direction. Four 50- by 57-mm specimens from each board were tested for shear properties using the Minnesota shear tester. Bending and shear tests followed ASTM D1037 (ASTM 1991) procedures. One 76- by 305-mm specimen cut Pa to the cardinal alignment direction and one similar-sized specimen derived from the Pe alignment specimen were tested for the dimensional stability properties of thickness swell (TS), water adsorption (WA), and linear expansion (LE). After determining weights, thicknesses, and lengths at OD conditions, these specimens were progressively equilibrated and measured at 50%, 65%, and 90% RH and were exposed to a vacuum pressure soak (VPS). Finally, the specimens were measured following a second OD exposure (OD2), to determine nonrecoverable TS and LE. All dimensional stability tests were conducted according to ASTM D1037.

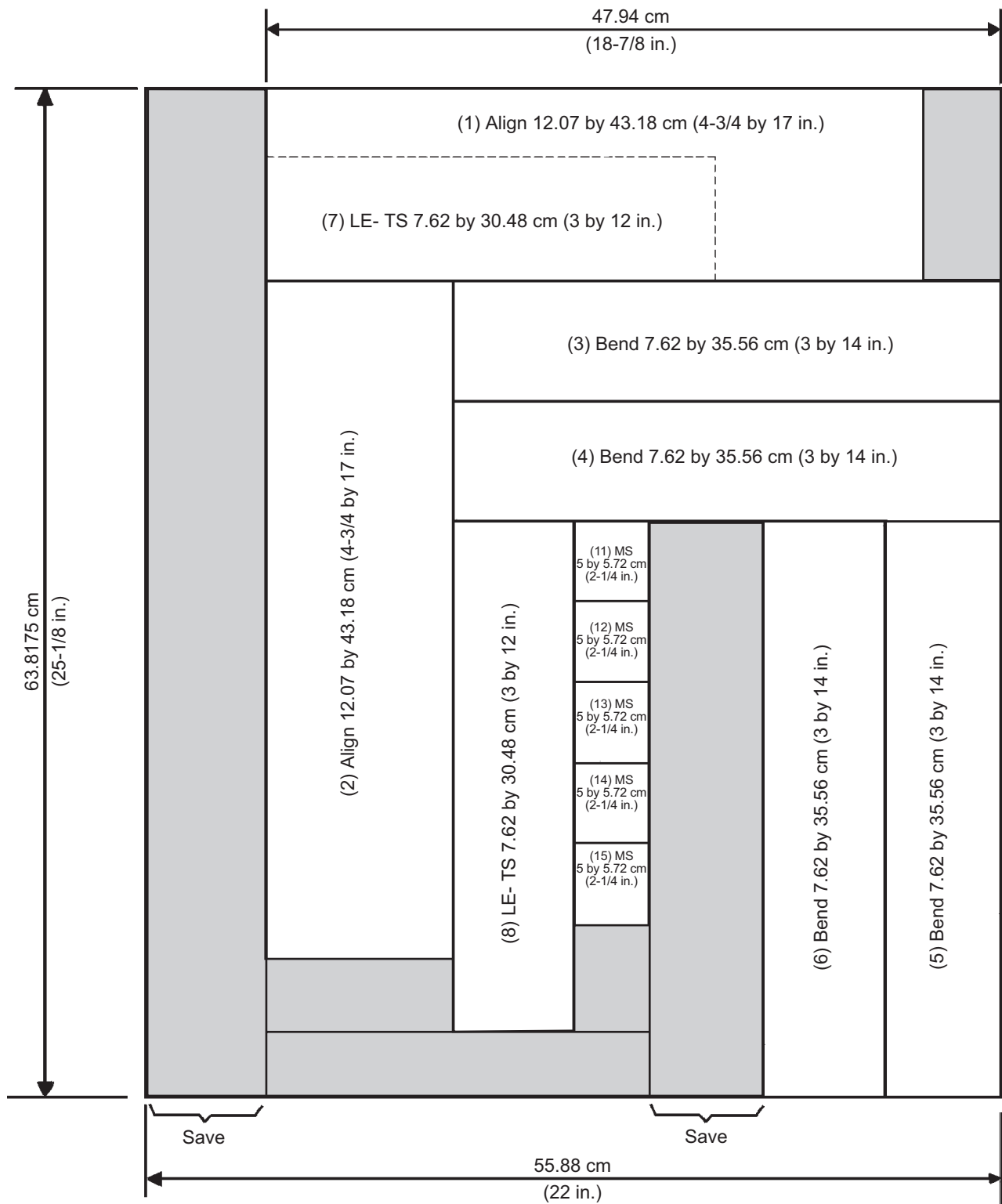


Figure 2—Board cut-up diagram (LE, linear expansion; TS, thickness swell; MS, Minnesota shear).

# Results and Discussion

## Furnish Characterization

Classification of a wood composite furnish has traditionally been described using screen analysis. This method, comparing the weights of a succession of screen fractions, has proven adequate for particleboard, where the variation in particle geometry is relatively small. However, IA, which defines the furnish by geometry, is particularly suited to OSB because a large difference in flake size has a profound influence on board properties and the flake alignment potential. We have intentionally segregated the image data by screen fractions to distinguish the differences in the two classification methods.

## Screen Analysis

Average weight and number of flakes contained in each fraction of the screen analysis are given in Table 1 by furnish type. The sheer volume of data permitted the detection of very small differences in average flake descriptor values (Table 2). Initial analysis implied that, despite precautions taken to assure sample uniformity, the descriptors (area, perimeter, length, and width) were statistically different between the three sample replications. This was true for all flake types and for the majority of the screen fractions. Therefore, in-depth analysis was conducted using the combined data sets, which totaled three times the average number of flakes shown in Table 1. The data suggest that more samples containing less flakes would provide a better representation of the furnish. Procedural recommendations to determine minimum sample size are discussed later in this report.

**Table 2—Descriptor average by screen size and furnish type**

| Screen                  | Furnish type |                |                |                |                |       |                |       |       |                |
|-------------------------|--------------|----------------|----------------|----------------|----------------|-------|----------------|-------|-------|----------------|
|                         | A            | A <sub>1</sub> | A <sub>2</sub> | A <sub>3</sub> | A <sub>4</sub> | B     | B <sub>1</sub> | C     | D     | D <sub>1</sub> |
| Length (mm)             |              |                |                |                |                |       |                |       |       |                |
| 1/16                    | 12           | 11             | 11             | 11             | 11             | 13    | 12             | 15    | 12    | 11             |
| 1/8                     | 37           | 25             | 23             | 21             | 17             | 20    | 28             | 62    | 25    | 18             |
| 1/4                     | 66           | 52             | 46             | 41             | 34             | 39    | 34             | 69    | 51    | 31             |
| 1/2                     | 71           | 56             | 47             | 39             | 29             | 40    | 36             | 68    | 58    | 37             |
| Width (mm)              |              |                |                |                |                |       |                |       |       |                |
| 1/16                    | 2            | 2              | 2              | 2              | 2              | 2     | 2              | 3     | 3     | 2              |
| 1/8                     | 5            | 4              | 4              | 3              | 3              | 3     | 4              | 4     | 4     | 3              |
| 1/4                     | 9            | 7              | 6              | 6              | 5              | 12    | 6              | 4     | 8     | 5              |
| 1/2                     | 12           | 9              | 7              | 6              | 4              | 13    | 7              | 4     | 11    | 6              |
| Area (mm <sup>2</sup> ) |              |                |                |                |                |       |                |       |       |                |
| 1/16                    | 20           | 20             | 20             | 19             | 16             | 18    | 21             | 31    | 21    | 17             |
| 1/8                     | 127          | 73             | 65             | 53             | 40             | 39    | 84             | 190   | 79    | 43             |
| 1/4                     | 470          | 278            | 211            | 180            | 121            | 424   | 160            | 215   | 301   | 115            |
| 1/2                     | 744          | 414            | 286            | 196            | 90             | 447   | 225            | 220   | 523   | 177            |
| Perimeter (mm)          |              |                |                |                |                |       |                |       |       |                |
| 1/16                    | 26           | 26             | 26             | 26             | 24             | 30    | 27             | 34    | 28    | 25             |
| 1/8                     | 82           | 55             | 51             | 46             | 39             | 44    | 62             | 132   | 59    | 41             |
| 1/4                     | 152          | 118            | 102            | 92             | 75             | 100   | 79             | 147   | 122   | 72             |
| 1/2                     | 170          | 131            | 108            | 88             | 65             | 101   | 85             | 145   | 147   | 87             |
| Thickness (mm)          |              |                |                |                |                |       |                |       |       |                |
| 1/16                    | 0.634        | 0.683          | 0.665          | 0.679          | 0.741          | 0.511 | 0.646          | 0.726 | 0.499 | 0.537          |
| 1/8                     | 0.729        | 0.753          | 0.722          | 0.753          | 0.723          | 0.720 | 0.666          | 0.772 | 0.476 | 0.473          |
| 1/4                     | 0.733        | 0.836          | 0.725          | 0.758          | 0.741          | 0.718 | 0.733          | 0.782 | 0.529 | 0.474          |
| 1/2                     | 0.773        | 0.749          | 0.739          | 0.770          | 0.748          | 0.721 | 0.711          | 0.793 | 0.517 | 0.491          |
| Specific gravity        |              |                |                |                |                |       |                |       |       |                |
| 1/16                    | 0.429        | 0.347          | 0.339          | 0.291          | 0.270          | 0.223 | 0.362          | 0.306 | 0.321 | 0.286          |
| 1/8                     | 0.382        | 0.375          | 0.369          | 0.317          | 0.332          | 0.289 | 0.443          | 0.386 | 0.382 | 0.371          |
| 1/4                     | 0.411        | 0.382          | 0.413          | 0.350          | 0.346          | 0.448 | 0.404          | 0.389 | 0.375 | 0.395          |
| 1/2                     | 0.423        | 0.430          | 0.417          | 0.389          | 0.310          | 0.436 | 0.390          | 0.388 | 0.387 | 0.387          |

**Table 3—Tukey test separation of furnish by descriptors**

| Descriptor <sup>a</sup> | Significance level | (Low)          |                |                |                |                |                |                |                |                | (High)         |
|-------------------------|--------------------|----------------|----------------|----------------|----------------|----------------|----------------|----------------|----------------|----------------|----------------|
| 1/16 screen             |                    |                |                |                |                |                |                |                |                |                |                |
| Area                    | 0.0511             | A <sub>4</sub> | D <sub>1</sub> | A <sub>3</sub> | A <sub>1</sub> | B              | A <sub>2</sub> | B <sub>1</sub> | D              | C              | A              |
| Perimeter               | 0.1475             | A <sub>4</sub> | D <sub>1</sub> | A <sub>3</sub> | A <sub>1</sub> | A <sub>2</sub> | B <sub>1</sub> | D              | B              | C              | A              |
| Length                  | 0.1500             | A <sub>4</sub> | D <sub>1</sub> | A <sub>1</sub> | A <sub>3</sub> | A <sub>2</sub> | B <sub>1</sub> | D              | B              | C              | A              |
| Width                   | 0.0357             | A <sub>4</sub> | D <sub>1</sub> | A <sub>3</sub> | A <sub>1</sub> | B <sub>1</sub> | A <sub>2</sub> | B              | D              | C              | A              |
| Thickness               | 0.0030             | D              | B              | D <sub>1</sub> | A              | B <sub>1</sub> | A <sub>2</sub> | A <sub>3</sub> | A <sub>1</sub> | C              | A <sub>4</sub> |
| Weight (%)              | 0.0001             | B              | A              | D              | C              | A <sub>1</sub> | B <sub>1</sub> | D <sub>1</sub> | A <sub>2</sub> | A <sub>3</sub> | A <sub>4</sub> |
| 1/8 screen              |                    |                |                |                |                |                |                |                |                |                |                |
| Area                    | 0.0001             | A <sub>4</sub> | D <sub>1</sub> | A <sub>3</sub> | A <sub>2</sub> | A <sub>1</sub> | D              | B              | B <sub>1</sub> | A              | C              |
| Perimeter               | 0.0001             | A <sub>4</sub> | D <sub>1</sub> | A <sub>3</sub> | A <sub>2</sub> | A <sub>1</sub> | D              | B <sub>1</sub> | B              | A              | C              |
| Length                  | 0.0001             | A <sub>4</sub> | D <sub>1</sub> | A <sub>3</sub> | A <sub>2</sub> | D              | A <sub>1</sub> | B <sub>1</sub> | B              | A              | C              |
| Width                   | 0.0166             | A <sub>4</sub> | D <sub>1</sub> | A <sub>3</sub> | B              | A <sub>2</sub> | B <sub>1</sub> | A <sub>1</sub> | C              | D              | A              |
| Thickness               | 0.0001             | D <sub>1</sub> | D              | B <sub>1</sub> | B              | A <sub>2</sub> | A <sub>4</sub> | A              | A <sub>1</sub> | A <sub>3</sub> | C              |
| Weight (%)              | 0.0001             | B              | A              | D              | A <sub>1</sub> | B <sub>1</sub> | C              | A <sub>2</sub> | D <sub>1</sub> | A <sub>3</sub> | A <sub>4</sub> |
| 1/4 screen              |                    |                |                |                |                |                |                |                |                |                |                |
| Area                    | 0.0001             | D <sub>1</sub> | A <sub>4</sub> | B <sub>1</sub> | A <sub>3</sub> | A <sub>2</sub> | C              | A <sub>1</sub> | D              | B              | A              |
| Perimeter               | 0.0001             | D <sub>1</sub> | A <sub>4</sub> | B <sub>1</sub> | A <sub>3</sub> | B              | A <sub>2</sub> | A <sub>1</sub> | D              | C              | A              |
| Length                  | 0.0001             | D <sub>1</sub> | A <sub>4</sub> | B <sub>1</sub> | B              | A <sub>3</sub> | A <sub>2</sub> | D              | A <sub>1</sub> | A              | C              |
| Width                   | 0.0001             | C              | A <sub>4</sub> | D <sub>1</sub> | B <sub>1</sub> | A <sub>2</sub> | A <sub>3</sub> | A <sub>1</sub> | D              | A              | B              |
| Thickness               | 0.0001             | D <sub>1</sub> | D              | B              | A <sub>2</sub> | A              | B <sub>1</sub> | A <sub>4</sub> | A <sub>3</sub> | C              | A <sub>1</sub> |
| Weight (%)              | 0.0001             | B              | A <sub>4</sub> | A              | D              | A <sub>3</sub> | A <sub>1</sub> | D <sub>1</sub> | A <sub>2</sub> | B <sub>1</sub> | C              |
| 1/2 screen              |                    |                |                |                |                |                |                |                |                |                |                |
| Area                    | 0.0001             | A <sub>4</sub> | D <sub>1</sub> | A <sub>3</sub> | C              | B <sub>1</sub> | A <sub>2</sub> | A <sub>1</sub> | B              | D              | A              |
| Perimeter               | 0.0001             | A <sub>4</sub> | B <sub>1</sub> | D <sub>1</sub> | A <sub>3</sub> | B              | A <sub>2</sub> | A <sub>1</sub> | C              | D              | A              |
| Length                  | 0.0001             | A <sub>4</sub> | B <sub>1</sub> | D <sub>1</sub> | A <sub>3</sub> | B              | A <sub>2</sub> | A <sub>1</sub> | D              | C              | A              |
| Width                   | 0.0001             | A <sub>4</sub> | C              | D <sub>1</sub> | A <sub>3</sub> | A <sub>2</sub> | B <sub>1</sub> | A <sub>1</sub> | D              | A              | B              |
| Thickness               | 0.0001             | D <sub>1</sub> | D              | B <sub>1</sub> | B              | A <sub>2</sub> | A <sub>4</sub> | A <sub>1</sub> | A <sub>3</sub> | A              | C              |
| Weight (%)              | 0.0001             | A <sub>4</sub> | A <sub>3</sub> | A <sub>2</sub> | B <sub>1</sub> | C              | D <sub>1</sub> | A <sub>1</sub> | D              | A              | B              |

<sup>a</sup>Descriptors are averages except for weight.

In most cases, the screening adequately separated flakes by descriptors (such as area, perimeter, etc.) within a furnish type (Table 2). However, an analysis of variance (ANOVA) indicated that the descriptor averages of fractions retained on screen sizes of 1/8 and larger varied considerably between furnish types. A Tukey's test separation of furnish type by flake descriptors is shown in Table 3. Furnish types that are

not significantly different are connected by a continuous underline. Because there was almost no statistical difference between furnishes in any of the visual descriptors on the 1/16 screen, this portion could appropriately be described using a screen analysis weight fraction. However, we elected to retain this portion in our IA-derived cumulative distribution furnish descriptions.

Flake thickness is averaged by flake type and screen fraction in Table 2. As described earlier, thickness information was derived from a separate data source. In this case, ANOVA indicated that there was little or no difference in average flake thickness derived from the three replicate samples but there was a difference in flake thickness between flake types. Tukey's test showed that the ring flakes, types D and D<sub>1</sub>, were thinner than the others on all screens except the 1/16 screen. This gave them some advantage in achieving higher values of board properties. After the ring flakes, the B and B<sub>1</sub> disk flakes were the thinnest. This is probably caused by the scoring knives preventing the wood blocks from riding directly on the surface of the disk flaker. Further statistical analysis, grouping all flake furnishes, showed that the flakes in the 1/16 screen fractions were thinner than flakes in the other screen fractions. Previous work (Geimer and Link 1988) has shown that flake thickness and SG decrease as flake size (by screen fraction) decreases. A possible explanation is that more breakage occurs in lower SG material; however, this relation was not statistically verified.

### Image Analysis

Image-analysis-derived characteristics of a flake furnish can be readily described by cumulative distribution functions. The flake data are first sorted by the variable in question and arranged in ascending rank from the smallest to the largest. The data are then split into the desired number of equal groups or percentiles. The measured value of the variable corresponding to the percentile point is then recorded and plotted against its respective percentile. Cumulative distribution functions of LC for the four basic flake types are shown in Figure 3a. Except for a slightly greater amount of very short flakes in the type A furnish, the cumulative distribution curves depicting flake length for the type A and C furnishes are almost identical. This is a considerably different characterization than is obtained from comparing average length of the flakes retained on the 1/8 and 1/4 screen for these furnishes. The average length of the A flakes on the 1/8 screen is only 37 mm, compared with the 62 mm recorded for the C flakes on this screen. In contrast, the average length of the A flakes on the 1/4 screen is 66 mm compared with 69 mm for the C flakes. Apparently, screen classification is highly dependent on the interaction of length and width, and the larger width of the A flakes (9 mm compared with 4 mm on the 1/4 screen) has prevented many of the A flakes from passing through the 1/4 screen.

In a cumulative distribution function plot based on number of flakes, each observation has equal weight. To account for the increased contribution of larger flakes to board properties, we can obtain a cumulative distribution function "weighted" by area. To obtain an area-weighted property like LC, assume we have  $n$  flakes that we have arranged from the smallest LC to the largest LC and each flake has an area. The  $\alpha \times 100$ th weighted percentile would be the LC where the sum of the areas of all the flakes up to and including this

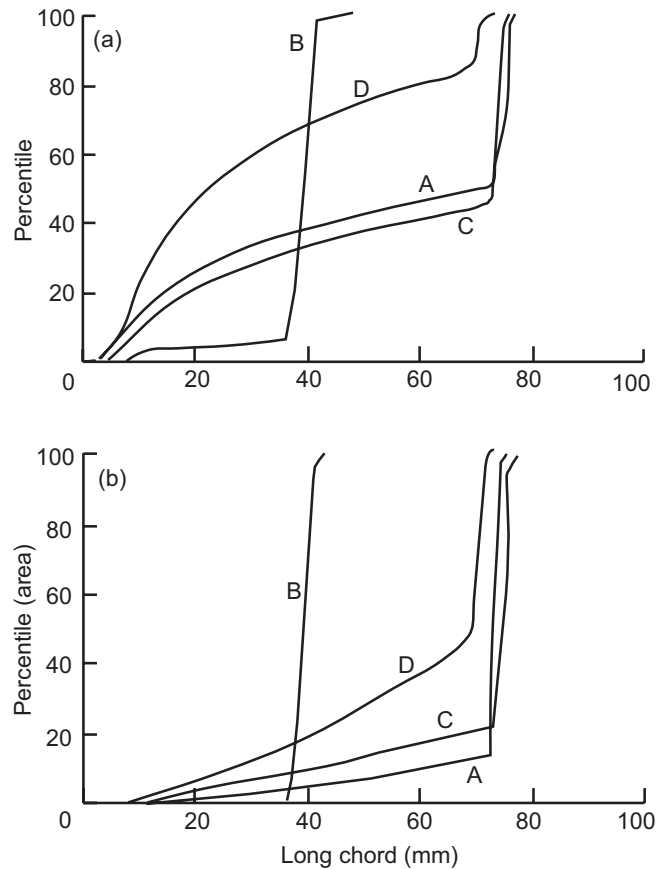


**Figure 3—Long chord percentiles (a) nonweighted and (b) weighted by area for the primary furnishes (A, B, C, and D).**

flake is  $\alpha$  times the total area of all the flakes. In Figure 3b, the ranked LC data are plotted against the percentile of their respective accumulative area. The position of the curve is shifted to reflect the importance of the large flakes. The curves for those furnishes that have a large portion of short particles, such as type D, are affected the most.

Data describing selected number-derived and area-weighted percentiles for the LC, width, area, and perimeter descriptors are given in Tables 4, 5, 6, and 7 for all furnish types. Also given (Table 8) are aspect ratio percentiles calculated using LC and width measurements on individual flakes. Width, area, and perimeter cumulative distribution plots, all calculated by number and weighted by area, for the four basic flake types are shown in Figures 4a, 4b, 5a, 5b, 6a, and 6b, respectively. Similarity or difference of cumulative distribution curves for two furnishes depends on the descriptor under consideration. Furnish types A and C have similar LC and perimeter curves but very different width and area curves.

**Table 4—Long chord percentiles by furnish type**

| Percentile                                  | Furnish type |                |                |                |                |      |                |      |      |                |      |                                |       |
|---|--------------|----------------|----------------|----------------|----------------|------|----------------|------|------|----------------|------|--------------------------------|-------|
|   | A            | A <sub>1</sub> | A <sub>2</sub> | A <sub>3</sub> | A <sub>4</sub> | B    | B <sub>1</sub> | C    | D    | D <sub>1</sub> | A+B  | A <sub>1</sub> +B <sub>1</sub> | A+B+C |
| Long chord percentiles (mm)                 |              |                |                |                |                |      |                |      |      |                |      |                                |       |
| 1   | 3.4          | 4.2            | 4.2            | 4.4            | 4.6            | 8.4  | 4.3            | 5.0  | 4.1  | 3.8            | 4.3  | 4.3                            | 4.7   |
| 10  | 8.1          | 6.4            | 6.6            | 6.9            | 6.7            | 37.2 | 7.1            | 10.3 | 7.0  | 6.2            | 12.6 | 6.8                            | 10.9  |
| 20  | 14.5         | 8.2            | 8.3            | 8.5            | 8.1            | 38.1 | 9.4            | 18.8 | 9.8  | 8.2            | 35.7 | 8.8                            | 23.0  |
| 25  | 19.3         | 9.1            | 9.1            | 9.3            | 8.7            | 38.4 | 10.7           | 26.1 | 11.4 | 9.1            | 37.5 | 9.8                            | 33.2  |
| 30  | 26.4         | 10.0           | 9.9            | 10.1           | 9.3            | 38.7 | 12.3           | 35.1 | 13.1 | 10.1           | 38.3 | 11.0                           | 38.0  |
| 40  | 46.2         | 12.1           | 11.6           | 11.8           | 10.5           | 39.1 | 17.2           | 54.7 | 17.3 | 12.0           | 39.2 | 14.2                           | 40.0  |
| 50  | 72.1         | 15.4           | 13.9           | 13.8           | 11.9           | 39.5 | 25.8           | 72.9 | 22.6 | 14.2           | 39.9 | 19.4                           | 46.0  |
| 60  | 73.7         | 19.9           | 16.9           | 16.2           | 13.6           | 39.9 | 33.0           | 73.4 | 31.2 | 16.8           | 40.7 | 27.7                           | 72.9  |
| 70  | 74.8         | 27.5           | 21.5           | 19.3           | 15.9           | 40.2 | 36.2           | 73.7 | 43.0 | 20.5           | 48.2 | 35.4                           | 73.5  |
| 75  | 75.1         | 34.0           | 25.0           | 21.4           | 17.4           | 40.3 | 36.8           | 73.8 | 50.0 | 23.0           | 72.9 | 36.7                           | 73.7  |
| 80  | 75.4         | 43.0           | 30.0           | 24.4           | 19.1           | 40.6 | 37.3           | 74.0 | 58.8 | 26.0           | 73.8 | 37.5                           | 74.0  |
| 90  | 75.7         | 66.8           | 45.6           | 33.6           | 25.2           | 41.2 | 38.2           | 74.4 | 70.0 | 35.5           | 75.4 | 39.9                           | 74.6  |
| 99  | 76.5         | 74.3           | 73.1           | 70.0           | 47.5           | 42.5 | 39.8           | 75.3 | 71.6 | 66.7           | 76.3 | 74.0                           | 76.0  |
| Average                                     | 50.3         | 24.8           | 20.3           | 17.6           | 14.4           | 38.4 | 23.9           | 53.0 | 31.1 | 18.0           | 44.4 | 24.3                           | 49.4  |
| Long chord percentiles (area weighted) (mm) |              |                |                |                |                |      |                |      |      |                |      |                                |       |
| 1   | 17.9         | 6.9            | 6.2            | 6.1            | 5.7            | 36.4 | 7.1            | 12.1 | 8.6  | 5.5            | 25.6 | 7.0                            | 16.6  |
| 10  | 59.7         | 18.0           | 12.2           | 11.2           | 9.2            | 37.7 | 20.2           | 44.2 | 26.9 | 11.6           | 38.1 | 19.0                           | 38.3  |
| 20  | 73.4         | 31.6           | 18.5           | 15.1           | 11.5           | 38.4 | 30.8           | 69.6 | 41.9 | 16.0           | 39.1 | 31.0                           | 39.6  |
| 25  | 73.6         | 38.5           | 22.1           | 17.0           | 12.7           | 38.7 | 33.3           | 72.8 | 47.3 | 18.3           | 39.5 | 34.4                           | 40.1  |
| 30  | 73.8         | 44.5           | 26.3           | 19.0           | 13.8           | 38.9 | 35.0           | 73.1 | 52.2 | 20.6           | 39.8 | 35.9                           | 40.6  |
| 40  | 74.5         | 55.1           | 34.7           | 23.6           | 16.3           | 39.3 | 36.3           | 73.4 | 62.6 | 25.4           | 40.5 | 37.2                           | 53.5  |
| 50  | 75.1         | 64.5           | 42.0           | 28.9           | 19.1           | 39.6 | 37.0           | 73.6 | 69.3 | 30.3           | 41.8 | 38.1                           | 73.3  |
| 60  | 75.4         | 71.3           | 49.9           | 34.6           | 22.6           | 40.0 | 37.4           | 73.8 | 70.0 | 35.9           | 73.4 | 39.2                           | 73.7  |
| 70  | 75.6         | 73.2           | 59.1           | 41.5           | 27.1           | 40.3 | 37.9           | 74.0 | 70.4 | 41.9           | 74.5 | 53.3                           | 74.1  |
| 75  | 75.7         | 73.4           | 63.6           | 45.8           | 29.7           | 40.4 | 38.2           | 74.1 | 70.6 | 45.3           | 75.1 | 63.3                           | 74.4  |
| 80  | 75.8         | 73.7           | 67.2           | 50.8           | 32.7           | 40.7 | 38.4           | 74.2 | 70.8 | 49.1           | 75.4 | 70.3                           | 74.8  |
| 90  | 76.0         | 74.1           | 72.7           | 67.1           | 42.6           | 41.3 | 39.0           | 74.6 | 71.3 | 61.5           | 75.8 | 73.6                           | 75.6  |
| 99  | 76.7         | 74.8           | 75.6           | 75.6           | 73.2           | 42.6 | 40.9           | 75.4 | 72.2 | 70.5           | 76.5 | 74.7                           | 76.4  |
| Average                                     | 71.3         | 54.7           | 42.4           | 33.3           | 23.1           | 39.5 | 33.7           | 67.5 | 57.7 | 33.2           | 55.4 | 43.9                           | 59.6  |

**Table 5—Width percentiles by furnish type**

| Percentile                             | Furnish type |                |                |                |                |      |                |     |      |                |      |                                |       |
|--|--------------|----------------|----------------|----------------|----------------|------|----------------|-----|------|----------------|------|--------------------------------|-------|
|  | A            | A <sub>1</sub> | A <sub>2</sub> | A <sub>3</sub> | A <sub>4</sub> | B    | B <sub>1</sub> | C   | D    | D <sub>1</sub> | A+B  | A <sub>1</sub> +B <sub>1</sub> | A+B+C |
| Width percentiles (mm)                 |              |                |                |                |                |      |                |     |      |                |      |                                |       |
| 1                                      | 1.5          | 0.3            | 1.3            | 1.1            | 1.2            | 1.5  | 1.2            | 1.6 | 1.4  | 1.0            | 1.5  | 0.3                            | 1.5   |
| 10                                     | 2.3          | 1.8            | 1.8            | 1.7            | 1.6            | 11.6 | 1.8            | 2.5 | 2.1  | 1.5            | 2.6  | 1.8                            | 2.5   |
| 20                                     | 2.8          | 2.1            | 2.1            | 2.0            | 1.8            | 12.1 | 2.1            | 3.2 | 2.5  | 1.8            | 4.7  | 2.1                            | 3.4   |
| 25                                     | 3.2          | 2.3            | 2.2            | 2.1            | 1.9            | 12.3 | 2.3            | 3.4 | 2.6  | 2.0            | 6.6  | 2.3                            | 3.5   |
| 30                                     | 3.9          | 2.4            | 2.3            | 2.2            | 2.0            | 12.3 | 2.5            | 3.5 | 2.8  | 2.1            | 8.5  | 2.4                            | 3.7   |
| 40                                     | 5.7          | 2.7            | 2.6            | 2.3            | 2.2            | 12.5 | 2.9            | 3.7 | 3.3  | 2.3            | 11.9 | 2.8                            | 4.0   |
| 50                                     | 7.6          | 3.1            | 2.8            | 2.6            | 2.4            | 12.7 | 3.4            | 3.9 | 4.0  | 2.6            | 12.3 | 3.1                            | 4.4   |
| 60                                     | 10.3         | 3.5            | 3.1            | 2.9            | 2.6            | 12.8 | 3.9            | 4.2 | 5.0  | 3.0            | 12.6 | 3.7                            | 5.0   |
| 70                                     | 12.3         | 4.3            | 3.6            | 3.3            | 2.9            | 13.0 | 4.7            | 4.4 | 6.4  | 3.4            | 12.8 | 4.5                            | 8.0   |
| 75                                     | 12.7         | 4.9            | 4.0            | 3.5            | 3.1            | 13.1 | 5.2            | 4.5 | 7.3  | 3.7            | 13.0 | 5.0                            | 11.9  |
| 80                                     | 13.0         | 5.7            | 4.4            | 3.8            | 3.3            | 13.2 | 5.7            | 4.7 | 8.4  | 4.1            | 13.1 | 5.7                            | 12.4  |
| 90                                     | 13.6         | 8.3            | 5.9            | 4.9            | 4.0            | 13.5 | 7.3            | 5.0 | 11.6 | 5.4            | 13.5 | 7.6                            | 13.1  |
| 99                                     | 15.2         | 13.5           | 11.2           | 9.3            | 6.2            | 14.9 | 12.5           | 6.4 | 18.5 | 9.8            | 15.1 | 13.1                           | 14.4  |
| Average                                | 8.0          | 4.1            | 3.4            | 3.0            | 2.6            | 12.2 | 4.0            | 3.9 | 5.5  | 3.1            | 10.1 | 4.1                            | 6.5   |
| Width percentiles (area weighted) (mm) |              |                |                |                |                |      |                |     |      |                |      |                                |       |
| 1                                      | 3.0          | 1.7            | 1.6            | 1.5            | 1.3            | 9.1  | 1.8            | 2.5 | 2.1  | 1.3            | 3.7  | 1.7                            | 2.9   |
| 10                                     | 7.2          | 3.2            | 2.6            | 2.2            | 2.0            | 11.9 | 2.9            | 3.4 | 4.4  | 2.3            | 9.3  | 3.0                            | 3.9   |
| 20                                     | 9.6          | 4.4            | 3.2            | 2.7            | 2.3            | 12.3 | 3.7            | 3.7 | 6.2  | 2.8            | 11.9 | 4.0                            | 4.4   |
| 25                                     | 11.0         | 5.1            | 3.6            | 2.9            | 2.5            | 12.3 | 4.1            | 3.8 | 7.0  | 3.1            | 12.1 | 4.4                            | 4.7   |
| 30                                     | 11.8         | 5.7            | 3.9            | 3.1            | 2.6            | 12.5 | 4.4            | 3.9 | 7.6  | 3.3            | 12.3 | 4.9                            | 5.0   |
| 40                                     | 12.4         | 6.9            | 4.7            | 3.6            | 2.9            | 12.6 | 5.1            | 4.1 | 9.0  | 4.0            | 12.5 | 5.7                            | 8.6   |
| 50                                     | 12.7         | 8.1            | 5.4            | 4.3            | 3.3            | 12.8 | 5.8            | 4.2 | 10.3 | 4.7            | 12.8 | 6.7                            | 12.0  |
| 60                                     | 13.1         | 9.4            | 6.4            | 5.0            | 3.6            | 12.9 | 6.6            | 4.4 | 11.8 | 5.4            | 13.0 | 7.7                            | 12.5  |
| 70                                     | 13.3         | 11.0           | 7.4            | 5.9            | 4.1            | 13.1 | 7.5            | 4.7 | 13.1 | 6.3            | 13.2 | 8.9                            | 12.8  |
| 75                                     | 13.5         | 11.9           | 7.9            | 6.4            | 4.3            | 13.1 | 8.0            | 4.8 | 14.1 | 6.9            | 13.3 | 9.7                            | 13.0  |
| 80                                     | 13.7         | 12.5           | 8.7            | 7.1            | 4.7            | 13.2 | 8.6            | 4.9 | 14.9 | 7.5            | 13.4 | 10.9                           | 13.1  |
| 90                                     | 14.2         | 13.3           | 10.9           | 9.0            | 5.7            | 13.6 | 10.7           | 5.3 | 17.6 | 9.3            | 13.8 | 12.8                           | 13.6  |
| 99                                     | 16.3         | 14.7           | 13.7           | 13.5           | 8.9            | 15.1 | 13.2           | 7.0 | 20.6 | 14.5           | 15.6 | 14.2                           | 15.3  |
| Average                                | 11.8         | 8.3            | 6.1            | 5.1            | 3.6            | 12.7 | 6.3            | 4.4 | 10.6 | 5.3            | 12.2 | 7.3                            | 9.5   |

**Table 6—Area percentiles by furnish type**

| Percentile | Furnish type  |                |                |                |                |       |                |       |         |                |       |                                |       |
|------------|---|----------------|----------------|----------------|----------------|-------|----------------|-------|---------|----------------|-------|--------------------------------|-------|
|            | A   | A <sub>1</sub> | A <sub>2</sub> | A <sub>3</sub> | A <sub>4</sub> | B     | B <sub>1</sub> | C     | D       | D <sub>1</sub> | A+B   | A <sub>1</sub> +B <sub>1</sub> | A+B+C |
|            | Area percentiles (mm <sup>2</sup> )                 |                |                |                |                |       |                |       |         |                |       |                                |       |
| 1          | 3.8   | 5.6            | 5.6            | 5.6            | 5.5            | 7.2   | 5.6            | 6.5   | 5.8     | 5.4            | 5.3   | 5.6                            | 5.9   |
| 10         | 12.5  | 9.2            | 9.7            | 9.2            | 8.3            | 397.4 | 10.7           | 17.3  | 10.8    | 8.4            | 20.7  | 9.9                            | 18.2  |
| 20         | 26.4  | 12.9           | 13.5           | 12.4           | 10.9           | 418.6 | 16.3           | 40.4  | 16.6    | 11.4           | 119.6 | 14.5                           | 52.9  |
| 25         | 40.4  | 15.2           | 15.3           | 14.0           | 12.1           | 424.2 | 19.4           | 65.5  | 20.2    | 13.1           | 243.7 | 17.2                           | 93.5  |
| 30         | 68.7  | 17.4           | 17.3           | 15.7           | 13.5           | 429.1 | 23.0           | 96.7  | 24.4    | 14.9           | 376.1 | 20.1                           | 140.1 |
| 40         | 185.1   | 22.9           | 21.9           | 19.5           | 16.4           | 437.7 | 34.4           | 160.6 | 36.6    | 19.2           | 424.5 | 27.7                           | 208.2 |
| 50         | 346.2   | 31.0           | 27.5           | 24.3           | 19.8           | 445.4 | 56.6           | 204.6 | 57.8    | 24.6           | 440.9 | 41.2                           | 224.6 |
| 60         | 519.2   | 45.3           | 35.9           | 30.8           | 24.4           | 451.6 | 89.1           | 217.3 | 100.6   | 32.7           | 454.3 | 69.0                           | 240.0 |
| 70         | 762.8   | 78.3           | 51.2           | 41.3           | 30.8           | 458.6 | 120.6          | 225.7 | 186.4   | 45.3           | 470.3 | 108.7                          | 366.3 |
| 75         | 828.5   | 109.9          | 65.0           | 48.8           | 35.7           | 462.8 | 139.4          | 229.6 | 246.4   | 55.0           | 483.5 | 132.6                          | 426.3 |
| 80         | 856.4   | 158.6          | 86.6           | 59.1           | 41.9           | 467.1 | 160.5          | 234.1 | 327.2   | 69.0           | 542.2 | 160.3                          | 445.4 |
| 90         | 896.7   | 350.6          | 177.7          | 104.0          | 64.0           | 478.6 | 221.0          | 246.7 | 545.7   | 120.7          | 857.3 | 251.0                          | 488.3 |
| 99         | 986.3   | 841.4          | 538.4          | 366.7          | 179.7          | 528.3 | 421.8          | 348.7 | 1,058.9 | 374.3          | 958.4 | 728.8                          | 925.6 |
| Average    | 416.5   | 110.5          | 67.4           | 47.1           | 31.0           | 423.6 | 91.6           | 161.3 | 179.4   | 50.7           | 420.0 | 99.9                           | 270.1 |
|            | Area percentiles (area weighted) (mm <sup>2</sup> ) |                |                |                |                |       |                |       |         |                |       |                                |       |
| 1          | 39.4  | 10.6           | 9.4            | 8.1            | 6.9            | 293.5 | 11.2           | 21.2  | 15.1    | 7.7            | 74.6  | 10.9                           | 34.4  |
| 10         | 328.9   | 42.0           | 24.9           | 19.0           | 13.9           | 412.7 | 45.2           | 138.8 | 91.6    | 20.1           | 402.8 | 43.7                           | 200.8 |
| 20         | 502.0   | 108.0          | 44.2           | 29.8           | 20.0           | 425.1 | 88.6           | 191.9 | 202.1   | 34.0           | 429.6 | 94.3                           | 224.8 |
| 25         | 584.7   | 148.8          | 58.8           | 36.1           | 23.1           | 429.7 | 103.4          | 202.8 | 251.6   | 42.2           | 437.6 | 114.0                          | 233.2 |
| 30         | 664.3   | 191.4          | 77.1           | 43.6           | 26.6           | 434.4 | 116.2          | 209.5 | 301.8   | 51.8           | 444.9 | 133.9                          | 243.9 |
| 40         | 793.7   | 276.3          | 119.9          | 61.2           | 34.7           | 441.5 | 143.0          | 217.6 | 394.1   | 74.5           | 456.7 | 171.7                          | 395.1 |
| 50         | 840.7   | 365.0          | 172.7          | 87.2           | 44.9           | 448.2 | 168.0          | 223.9 | 488.3   | 102.1          | 471.7 | 217.1                          | 436.0 |
| 60         | 863.0   | 450.4          | 229.4          | 121.3          | 57.8           | 454.4 | 197.5          | 229.5 | 580.7   | 137.7          | 525.0 | 268.4                          | 455.7 |
| 70         | 884.1   | 557.2          | 300.2          | 172.0          | 75.8           | 461.4 | 228.9          | 235.9 | 694.2   | 186.9          | 797.5 | 352.4                          | 482.0 |
| 75         | 891.5   | 608.9          | 342.6          | 203.3          | 88.3           | 465.7 | 246.7          | 239.7 | 746.6   | 217.2          | 841.1 | 408.9                          | 572.6 |
| 80         | 900.9   | 681.9          | 389.9          | 242.4          | 105.2          | 469.0 | 269.7          | 244.0 | 811.2   | 255.4          | 863.4 | 456.7                          | 784.8 |
| 90         | 929.2   | 819.4          | 538.4          | 381.9          | 162.0          | 481.0 | 344.5          | 263.1 | 985.0   | 369.4          | 901.0 | 672.0                          | 883.5 |
| 99         | 1,045.0   | 919.3          | 864.6          | 797.0          | 376.9          | 534.9 | 463.6          | 377.3 | 1,256.1 | 667.0          | 994.6 | 906.4                          | 978.6 |
| Average    | 725.9   | 395.8          | 230.9          | 150.3          | 71.2           | 445.6 | 184.3          | 215.8 | 516.9   | 154.5          | 586.2 | 287.1                          | 458.1 |

**Table 7—Perimeter percentiles by furnish type**

| Percentile | Furnish type                               |                |                |                |                |       |                |       |       |                |       |                                |       |
|------------|--|----------------|----------------|----------------|----------------|-------|----------------|-------|-------|----------------|-------|--------------------------------|-------|
|            | A  | A <sub>1</sub> | A <sub>2</sub> | A <sub>3</sub> | A <sub>4</sub> | B     | B <sub>1</sub> | C     | D     | D <sub>1</sub> | A+B   | A <sub>1</sub> +B <sub>1</sub> | A+B+C |
|            | Perimeter percentiles (mm)                 |                |                |                |                |       |                |       |       |                |       |                                |       |
| 1          | 9.0  | 11.0           | 11.1           | 11.2           | 11.5           | 18.4  | 11.1           | 12.7  | 11.1  | 10.5           | 11.2  | 11.0                           | 12.1  |
| 10         | 19.1                                       | 15.6           | 16.1           | 16.1           | 15.8           | 95.6  | 17.3           | 24.0  | 17.3  | 15.3           | 28.6  | 16.4                           | 25.1  |
| 20         | 32.8                                       | 19.6           | 19.8           | 19.7           | 18.7           | 97.9  | 22.2           | 41.8  | 23.3  | 19.3           | 81.6  | 20.9                           | 51.1  |
| 25         | 43.6                                       | 21.4           | 21.4           | 21.3           | 19.9           | 98.7  | 25.0           | 57.4  | 26.8  | 21.4           | 96.1  | 23.0                           | 73.7  |
| 30         | 59.2                                       | 23.2           | 23.2           | 23.1           | 21.2           | 99.4  | 28.5           | 76.4  | 30.4  | 23.4           | 98.1  | 25.6                           | 94.8  |
| 40         | 102.5                                      | 28.0           | 27.0           | 26.8           | 23.8           | 100.4 | 38.7           | 117.0 | 39.6  | 27.5           | 100.4 | 32.5                           | 101.2 |
| 50         | 157.6                                      | 34.7           | 31.8           | 30.9           | 26.9           | 101.1 | 57.4           | 154.1 | 52.6  | 32.2           | 102.0 | 43.3                           | 106.2 |
| 60         | 166.3                                      | 45.0           | 38.2           | 36.1           | 30.6           | 102.0 | 74.3           | 155.4 | 71.9  | 38.3           | 103.7 | 61.8                           | 154.1 |
| 70         | 172.5                                      | 61.6           | 48.1           | 43.0           | 35.4           | 102.8 | 80.7           | 156.3 | 100.7 | 46.3           | 111.2 | 78.7                           | 156.0 |
| 75         | 174.3                                      | 76.7           | 55.8           | 47.8           | 38.7           | 103.2 | 82.3           | 156.7 | 118.2 | 51.8           | 158.2 | 82.1                           | 156.7 |
| 80         | 175.8                                      | 96.6           | 66.9           | 54.0           | 42.8           | 103.7 | 83.9           | 157.1 | 138.7 | 58.9           | 166.5 | 84.7                           | 157.6 |
| 90         | 178.8                                      | 151.6          | 101.5          | 74.5           | 55.7           | 105.0 | 88.3           | 158.3 | 164.6 | 80.4           | 175.8 | 97.3                           | 162.6 |
| 99         | 221.5                                      | 180.7          | 163.5          | 155.3          | 104.9          | 110.4 | 101.3          | 162.6 | 220.1 | 150.8          | 206.5 | 172.1                          | 188.8 |
| Average    | 117.3                                      | 56.7           | 46.0           | 39.6           | 32.4           | 98.1  | 54.7           | 113.3 | 74.7  | 41.4           | 107.8 | 55.6                           | 111.0 |
|            | Perimeter percentiles (area weighted) (mm) |                |                |                |                |       |                |       |       |                |       |                                |       |
| 1          | 41.5                                       | 16.9           | 15.5           | 14.8           | 13.7           | 91.8  | 17.4           | 27.5  | 20.8  | 14.1           | 59.9  | 17.1                           | 37.6  |
| 10         | 140.3                                      | 41.2           | 28.7           | 25.7           | 21.2           | 97.2  | 45.9           | 95.2  | 65.1  | 27.1           | 98.2  | 43.3                           | 98.0  |
| 20         | 165.1                                      | 72.5           | 42.3           | 34.2           | 26.3           | 98.7  | 70.8           | 148.4 | 100.6 | 37.3           | 100.4 | 71.3                           | 101.1 |
| 25         | 167.7                                      | 89.1           | 50.3           | 38.4           | 28.8           | 99.4  | 76.4           | 153.8 | 114.3 | 42.4           | 101.1 | 78.2                           | 102.2 |
| 30         | 169.9                                      | 102.3          | 59.5           | 43.0           | 31.4           | 99.9  | 79.0           | 154.4 | 126.7 | 47.4           | 101.9 | 81.3                           | 103.4 |
| 40         | 172.7                                      | 126.0          | 79.0           | 53.2           | 36.9           | 100.8 | 82.1           | 155.4 | 149.9 | 58.7           | 103.4 | 85.1                           | 119.4 |
| 50         | 174.6                                      | 148.3          | 95.4           | 65.1           | 43.3           | 101.5 | 84.1           | 156.0 | 158.2 | 70.1           | 106.5 | 89.4                           | 155.3 |
| 60         | 175.8                                      | 158.7          | 112.6          | 78.1           | 50.6           | 102.4 | 86.1           | 156.6 | 165.1 | 82.9           | 165.1 | 96.9                           | 157.0 |
| 70         | 177.1                                      | 163.8          | 133.1          | 94.1           | 60.3           | 103.0 | 88.6           | 157.2 | 171.4 | 97.5           | 172.8 | 123.8                          | 160.5 |
| 75         | 177.9                                      | 166.1          | 143.3          | 103.8          | 66.3           | 103.4 | 89.9           | 157.6 | 175.3 | 105.5          | 174.6 | 145.5                          | 167.4 |
| 80         | 178.8                                      | 169.2          | 151.3          | 115.5          | 73.2           | 103.9 | 91.4           | 158.0 | 180.3 | 115.3          | 175.8 | 158.3                          | 172.5 |
| 90         | 185.7                                      | 175.3          | 162.2          | 151.8          | 94.5           | 105.2 | 96.9           | 159.4 | 196.2 | 146.7          | 178.8 | 169.0                          | 177.1 |
| 99         | 241.9                                      | 213.0          | 188.0          | 178.9          | 158.4          | 110.7 | 108.4          | 164.5 | 262.5 | 186.2          | 221.5 | 197.5                          | 213.1 |
| Average    | 168.7                                      | 126.8          | 96.5           | 75.5           | 51.7           | 101.3 | 78.9           | 143.8 | 144.8 | 77.8           | 135.1 | 102.2                          | 138.1 |

**Table 8—Aspect ratio percentiles by furnish type**

| Percentile | Furnish type                            |                |                |                |                |      |                |      |      |                |      |                                |       |  |
|------------|---|----------------|----------------|----------------|----------------|------|----------------|------|------|----------------|------|--------------------------------|-------|--|
|            | A                                       | A <sub>1</sub> | A <sub>2</sub> | A <sub>3</sub> | A <sub>4</sub> | B    | B <sub>1</sub> | C    | D    | D <sub>1</sub> | A+B  | A <sub>1</sub> +B <sub>1</sub> | A+B+C |  |
|            | Aspect percentiles (mm)                 |                |                |                |                |      |                |      |      |                |      |                                |       |  |
| 1          | 1.7                                     | 1.6            | 1.6            | 1.7            | 1.9            | 2.7  | 1.7            | 2.0  | 1.4  | 1.4            | 1.9  | 1.7                            | 1.9   |  |
| 10         | 3.2                                     | 2.6            | 2.6            | 2.9            | 2.9            | 2.9  | 2.8            | 4.0  | 2.4  | 2.4            | 2.9  | 2.7                            | 3.0   |  |
| 20         | 4.4                                     | 3.3            | 3.2            | 3.5            | 3.5            | 3.0  | 3.5            | 6.3  | 3.2  | 3.2            | 3.0  | 3.4                            | 3.2   |  |
| 25         | 5.0                                     | 3.6            | 3.5            | 3.8            | 3.8            | 3.0  | 3.9            | 7.9  | 3.5  | 3.6            | 3.1  | 3.8                            | 3.4   |  |
| 30         | 5.3                                     | 3.9            | 3.8            | 4.1            | 4.0            | 3.0  | 4.2            | 9.6  | 3.8  | 3.9            | 3.1  | 4.1                            | 4.2   |  |
| 40         | 5.6                                     | 4.6            | 4.4            | 4.6            | 4.5            | 3.1  | 4.9            | 12.9 | 4.5  | 4.7            | 3.2  | 4.8                            | 5.7   |  |
| 50         | 5.8                                     | 5.3            | 5.0            | 5.2            | 5.0            | 3.1  | 5.7            | 14.7 | 5.2  | 5.4            | 3.4  | 5.5                            | 7.4   |  |
| 60         | 6.1                                     | 6.1            | 5.8            | 5.9            | 5.6            | 3.2  | 6.6            | 15.7 | 6.0  | 6.3            | 5.0  | 6.4                            | 11.1  |  |
| 70         | 6.8                                     | 7.1            | 6.8            | 6.8            | 6.3            | 3.2  | 7.6            | 16.8 | 6.9  | 7.3            | 5.7  | 7.4                            | 14.5  |  |
| 75         | 7.6                                     | 7.8            | 7.4            | 7.3            | 6.7            | 3.2  | 8.2            | 17.5 | 7.5  | 7.9            | 5.9  | 8.1                            | 15.5  |  |
| 80         | 8.4                                     | 8.7            | 8.1            | 7.9            | 7.3            | 3.3  | 8.9            | 18.1 | 8.1  | 8.6            | 6.2  | 8.8                            | 16.5  |  |
| 90         | 10.5                                    | 11.4           | 10.3           | 9.8            | 9.0            | 3.4  | 10.8           | 19.9 | 10.2 | 10.8           | 8.6  | 11.0                           | 18.7  |  |
| 99         | 16.7                                    | 36.1           | 17.0           | 17.4           | 15.0           | 10.4 | 17.6           | 23.1 | 16.3 | 17.8           | 14.8 | 26.1                           | 22.0  |  |
| Average    | 6.5                                     | 6.8            | 5.9            | 6.1            | 5.7            | 3.3  | 6.5            | 13.0 | 5.9  | 6.2            | 4.9  | 6.6                            | 9.6   |  |
|            | Aspect percentiles (area weighted) (mm) |                |                |                |                |      |                |      |      |                |      |                                |       |  |
| 1          | 3.1                                     | 2.1            | 2.0            | 2.1            | 2.1            | 2.7  | 2.3            | 4.0  | 1.9  | 1.7            | 2.7  | 2.2                            | 2.7   |  |
| 10         | 5.1                                     | 4.0            | 3.6            | 3.5            | 3.4            | 2.9  | 3.2            | 10.6 | 3.6  | 3.2            | 3.0  | 3.4                            | 3.0   |  |
| 20         | 5.4                                     | 5.0            | 4.5            | 4.3            | 4.0            | 3.0  | 3.9            | 13.4 | 4.0  | 4.1            | 3.1  | 4.4                            | 3.1   |  |
| 25         | 5.5                                     | 5.3            | 4.9            | 4.7            | 4.3            | 3.0  | 4.2            | 14.0 | 4.3  | 4.5            | 3.1  | 4.7                            | 3.2   |  |
| 30         | 5.5                                     | 5.4            | 5.3            | 5.0            | 4.6            | 3.0  | 4.5            | 14.5 | 4.6  | 4.9            | 3.1  | 5.0                            | 3.3   |  |
| 40         | 5.7                                     | 5.8            | 5.9            | 5.7            | 5.2            | 3.1  | 5.1            | 15.3 | 5.1  | 5.6            | 3.2  | 5.5                            | 5.4   |  |
| 50         | 5.8                                     | 6.3            | 6.7            | 6.4            | 5.9            | 3.1  | 5.6            | 16.1 | 5.6  | 6.3            | 3.7  | 6.0                            | 5.8   |  |
| 60         | 6.0                                     | 7.1            | 7.6            | 7.1            | 6.6            | 3.1  | 6.3            | 16.8 | 6.1  | 7.1            | 5.4  | 6.7                            | 6.8   |  |
| 70         | 6.2                                     | 8.1            | 8.6            | 8.0            | 7.5            | 3.2  | 7.1            | 17.8 | 6.9  | 8.0            | 5.7  | 7.6                            | 12.2  |  |
| 75         | 6.3                                     | 8.6            | 9.2            | 8.5            | 8.0            | 3.2  | 7.6            | 18.5 | 7.3  | 8.5            | 5.8  | 8.1                            | 14.3  |  |
| 80         | 6.8                                     | 9.3            | 9.9            | 9.2            | 8.6            | 3.3  | 8.2            | 18.9 | 7.8  | 9.1            | 6.0  | 8.7                            | 15.6  |  |
| 90         | 9.0                                     | 11.3           | 12.0           | 11.1           | 10.5           | 3.3  | 9.8            | 20.2 | 9.6  | 11.0           | 6.9  | 10.5                           | 17.8  |  |
| 99         | 14.4                                    | 19.4           | 19.2           | 17.9           | 17.2           | 4.1  | 15.1           | 23.3 | 15.7 | 17.6           | 12.6 | 17.4                           | 21.8  |  |
| Average    | 6.4                                     | 7.5            | 7.5            | 7.1            | 6.7            | 3.1  | 6.2            | 15.7 | 6.2  | 6.9            | 4.8  | 6.8                            | 8.6   |  |

The successive degradation of the type A furnish LC is shown in Figures 7a and 7b. Cumulative distribution curves, based on numbers, indicate that a large amount of short flakes were generated in all stages of degradation. However, LC cumulative distribution curves based on area-weighted percentiles show a more uniform segregation of the five furnish types. The area-weighted percentiles proved to be better predictors of board properties than many other variables considered and will be referred to extensively during the remainder of this discussion. Width, area, and perimeter cumulative distribution curves weighted by area are shown for the successive degradation of type A flakes in Figures 8, 9, and 10, respectively. The same relative amount of degradation was incurred in all the flake descriptors as furnish degradation proceeded.

In commercial flakeboard operations, it is imperative to know when major furnish changes occur, due to flaker knife wear, change in log source, or fluctuations in thaw tank temperatures. A more direct and rather sensitive comparison of furnish degradation, especially useful in quality control operations, can be seen in Q–Q plots. This type of comparison is obtained by plotting percentile values of one furnish type against the percentile values of another furnish type.

The Q–Q plots depicting the degradation of LC for the type A furnishes are shown in Figure 11a. Any deviation from a

line having a slope of 1 indicates a difference in the furnish. As noted in the cumulative distribution plots, the Q–Q plots indicate a large increase in the short length particles for all four degraded furnishes. If the percentiles of furnish types A<sub>2</sub>, A<sub>3</sub>, and A<sub>4</sub> are plotted against the percentiles of A<sub>1</sub> rather than A, we have a better indication of the successive degradation incurred in the respective furnishes (Fig. 11b).

Cumulative distribution curves depicting the degradation of LC in furnishes B<sub>1</sub> and D<sub>1</sub> are shown in Figure 12. Data from Tables 4 through 8 can be used to plot descriptor curves for all of the measured furnishes or to approximate combinations of furnish types. Figure 13 depicts LC cumulative distributions developed for furnish combination types A+B and A+B+C.

## Flake Alignment

Flake alignment, the single most important factor affecting the bending stiffness and strength of OSB, can be measured and described in a number of ways. The simplest is the angular measurement of a representative number of flakes on the surface of the board. This is best accomplished on the top surface of the board to avoid any effects of flake scatter, which occurs when the flakes are deposited directly on the metal caul surface, and to reduce problems in discerning angular direction caused by the settlement of fine wood

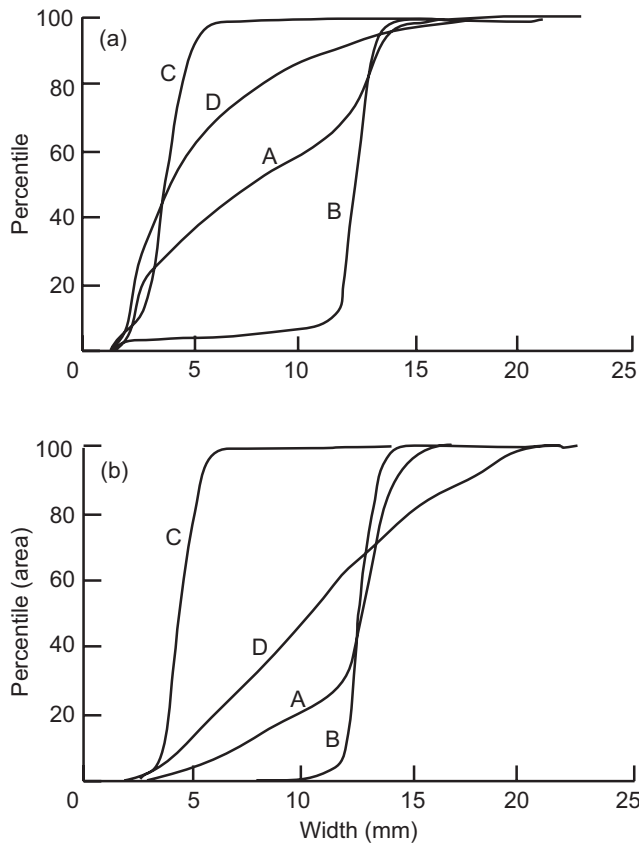


**Figure 4—Width percentiles (a) nonweighted and (b) weighted by area for the primary furnishes (A, B, C, and D).**

particles to the bottom face. Alignment can be expressed as a percentage given by the equation

$$\% \text{ Alignment} = (45 - \theta)/45 \quad (1)$$

where  $\theta$  is the average of the absolute angles the flakes make with the cardinal direction of alignment. This calculation implies that a board with random distribution of flakes has 0% alignment. The alignment data given for each furnish type in Table 9 and shown in Figure 14 are averages of 60 measurements on each of three boards. Flake alignment can also be described as the standard deviation of the angular measurements. The calculated value (Table 9) considers only the absolute values.

When the actual direction of alignment is equal to the direction used for angular alignment measurement, the sum of the positive and negative angles will equal zero. Any difference is due to orientation machine misalignment, panel trim misalignment, or simply inadequate or inaccurate sampling techniques. We consider the average cardinal alignment error in Table 9 to be too small in most cases to affect the outcome of our analysis and therefore have made no adjustment in our data for this discrepancy.

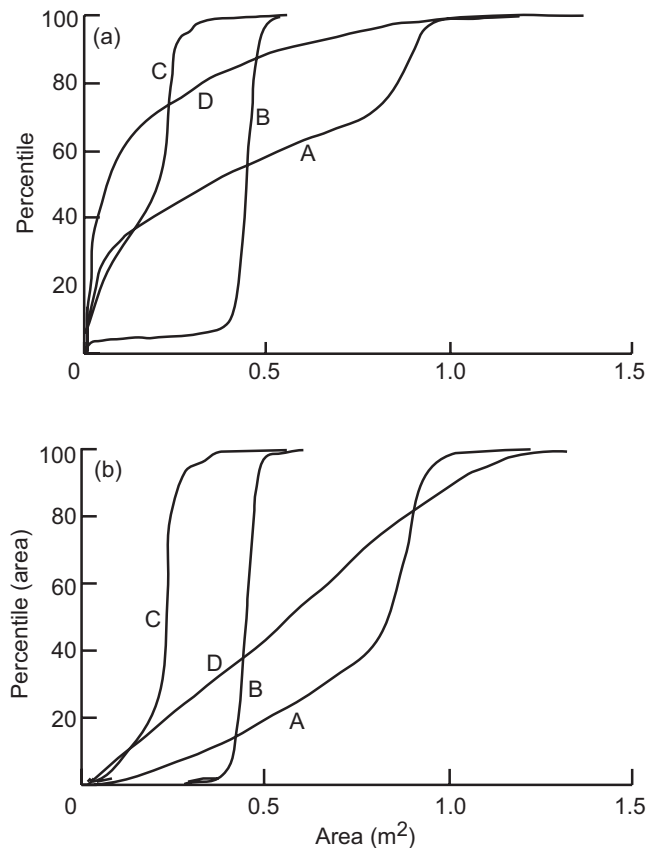


**Figure 5—Area percentiles (a) nonweighted and (b) weighted by area for the primary furnishes (A, B, C, and D).**

Alignment is closely related to the sonic velocity through the plane of the board. Sonic velocity is the speed at which sound travels through a medium. In straight-grained yellow-poplar lumber, sound travels at approximately 5.4 mm/ $\mu$ s in the longitudinal direction and 1.5 mm/ $\mu$ s in the tangential direction (Armstrong and others 1991). Sonic velocity in the random flake boards ranged from approximately 2.96 to 3.43 mm/ $\mu$ s (Table 10). Maximum sonic velocity of 5.00 mm/ $\mu$ s was measured in the Pa direction in the highly aligned A furnish boards. Minimum sonic velocity of 1.29 mm/ $\mu$ s occurred in the Pe direction of the highly aligned C furnish boards. While the sonic velocity is in itself a good indicator of flake alignment, use of the sonic velocity ratio (SVR), that is, the ratio of the sonic velocity in the Pa direction to that in the Pe direction, permits comparison of flake alignment between furnish types (Table 10; Fig. 15).

Relative to bending MOE (Table 11; Fig. 16), the SVR is a better indicator of alignment than our 60 point manual angular measurement. This is particularly true for the HA boards in both the A and D degraded furnishes. However, both the manual and SVR measurements indicate increased alignment of the B<sub>1</sub>-HA furnish compared with the B-HA furnish even though the B<sub>1</sub> boards had lower MOE-Pa than the B boards.

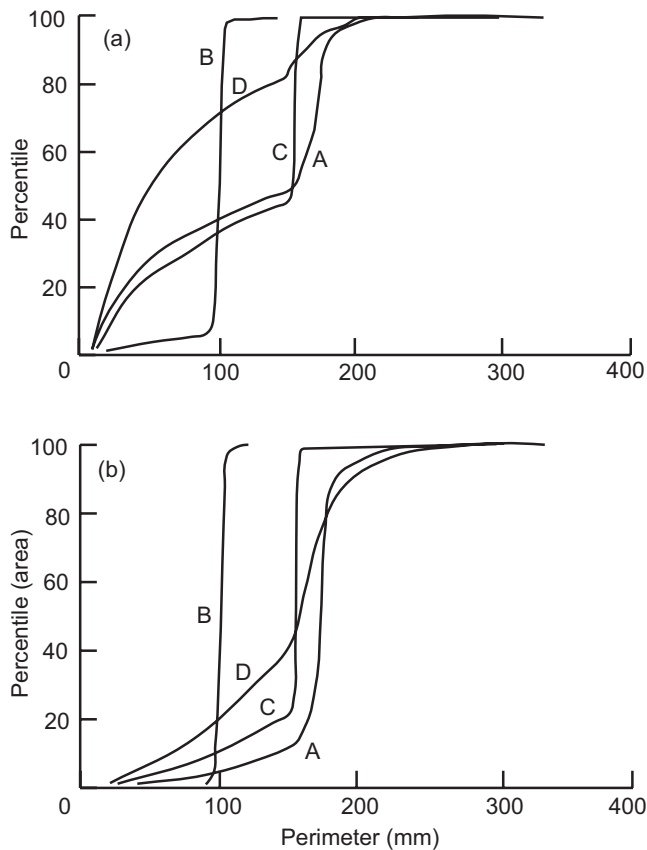


**Figure 6—Perimeter percentiles (a) nonweighted and (b) weighted by area for the primary furnishes (A, B, C, and D).**

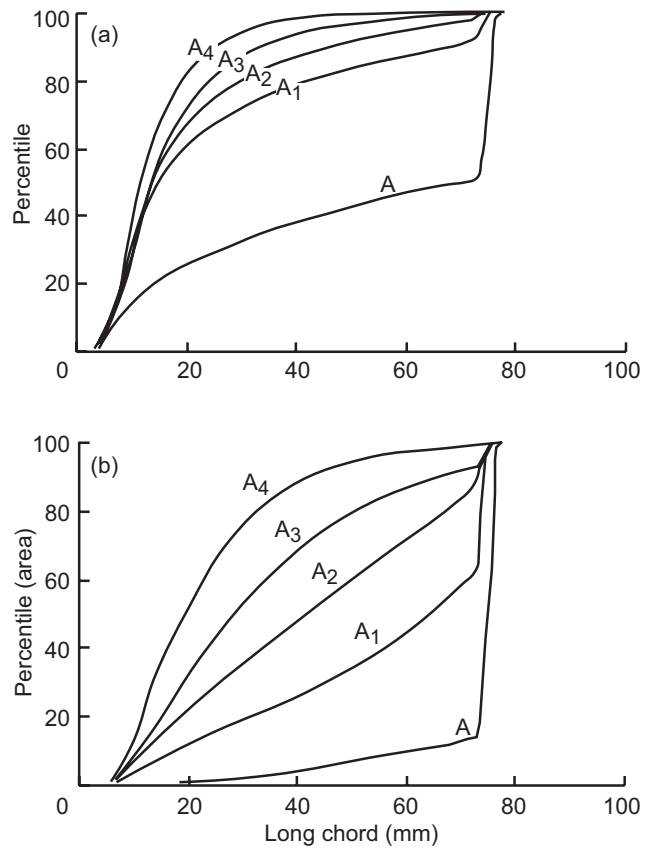


**Figure 7—Long chord percentiles (a) nonweighted and (b) weighted by area for the A and subsequent degraded furnishes.**

Still another method used to describe flake alignment is the ratio of bending stiffness in the Pa direction to that in the Pe direction. Modulus of elasticity ratios (MOE-R) are very useful in industrial quality control situations. However, because they are calculated using the same MOE-Pa value we wish to predict, they have limited usefulness in academic or research studies. Modulus of elasticity ratios (Table 11) are shown by alignment type for each flake furnish in Figure 17. These ratios of course follow the MOE-Pa very closely.

For convenience sake, it is often desirable to compare methods of alignment in terms of percentage. Figures 18 and 19 show the relationships between SVR and MOE-R, respectively, to the manually derived alignment percentage. The regression equations

$$\% \text{ Alignment} = 65.061(\ln \text{ SVR}) + 1.896 \quad (2)$$

and

$$\% \text{ Alignment} = 32.275(\ln \text{ MOE-R}) + 2.481 \quad (3)$$

derived using the data from all the furnish types are similar to those derived in earlier studies (Geimer 1981) in which the

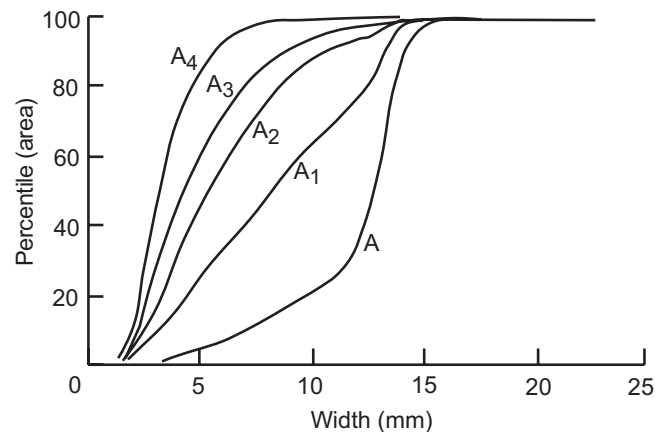


**Figure 8—Width percentiles weighted by area for the A and subsequent degraded furnishes.**

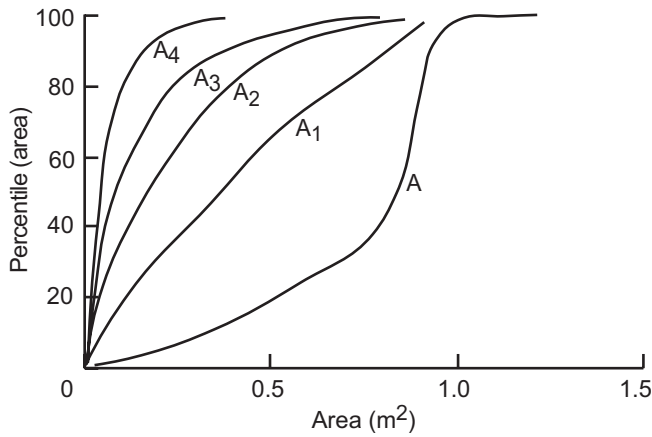


**Figure 9—Area percentiles weighted by area for the A and subsequent degraded furnishes.**

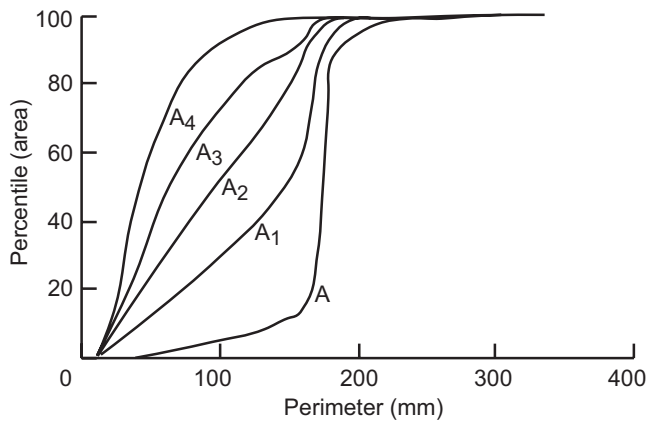


**Figure 10—Perimeter percentiles weighted by area for the A and subsequent degraded furnishes.**

SVR coefficient was determined to be 75.8 and the MOE-R coefficient was 30.7. Alignment values derived using these equations are given in Tables 10 and 11.

## Board Properties

### Bending

Average bending MOE and MOR of the boards are given in Tables 11 and 12, respectively, and are shown in Figures 16 and 20, respectively. Analysis of specimen SG data indicated that no statistically valid adjustment, like analysis of covariance, of the bending properties could be made for this variable. Average oven-dry SG for all bending specimens was 0.663. Minimum and maximum values were 0.580 and 0.761, respectively, and the standard deviation was 0.029.

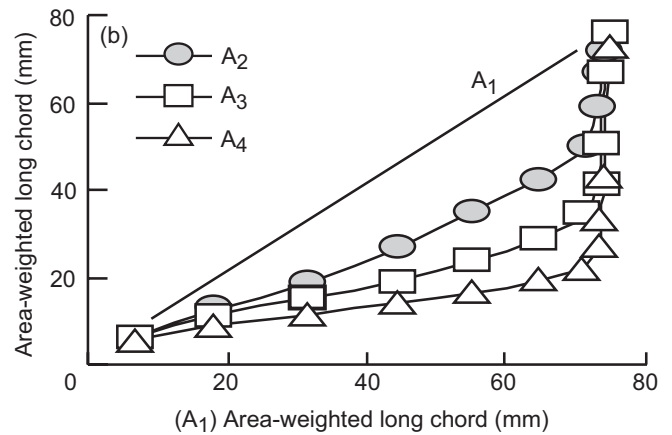
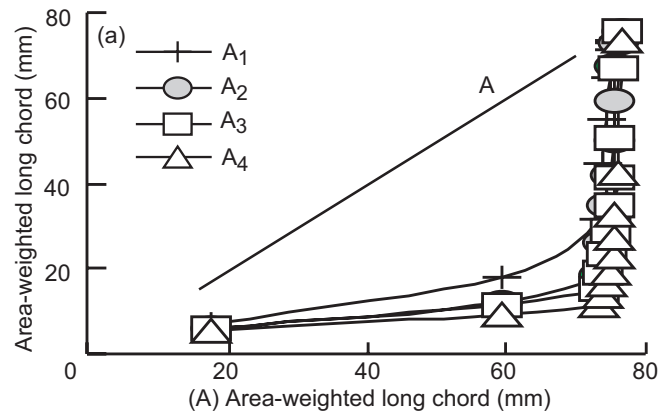


**Figure 11—Long chord percentiles of degraded A furnishes compared with (a) the primary A furnish and (b) the first stage degraded A<sub>1</sub> furnish Q-Q plots.**

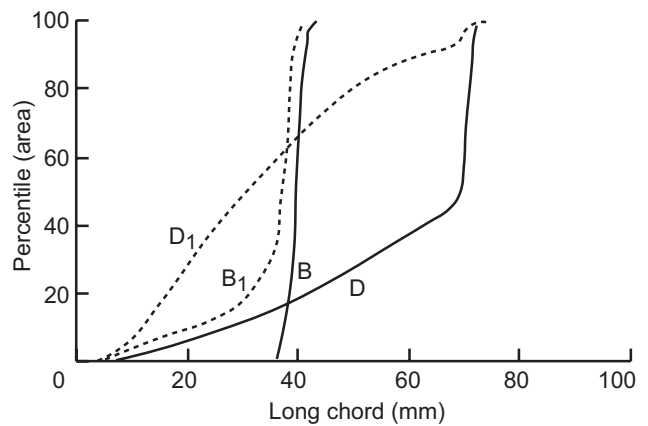


**Figure 12—Long chord percentiles weighted by area for the primary B and D and subsequent degraded furnishes.**

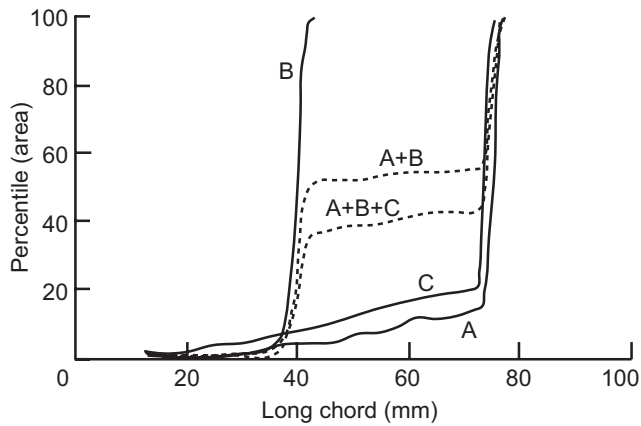


**Figure 13—Long chord percentiles weighted by area for the primary A, B, and C furnishes and combinations thereof.**

The effect of hammermill degradation can be seen in the gradual reduction of bending properties of the random boards made with the A, A<sub>1</sub>, A<sub>2</sub>, A<sub>3</sub>, and A<sub>4</sub> furnish series (Figs. 16 and 20). The MOE of 4,884 MPa in the A furnish random boards was reduced to 3,936 MPa in the A<sub>4</sub> random boards.

Modulus of elasticity reductions attributed to hammermilling were also noted in random boards made with the degraded B<sub>1</sub>, D<sub>1</sub>, and A<sub>1</sub>+B<sub>1</sub> furnishes. Interestingly, both the B and the D furnishes, which might be considered inferior in regard to flake length or amount of fines, produced random boards that had MOE properties superior to the A furnish boards. We attribute this to the reduction in flake thickness as noted previously. The relatively high MOE of the A+B and the A+B+C boards is attributed to a more favorable packing arrangement of the flakes in addition to the reduced flake thickness of the B flake component.

The overwhelming importance of flake orientation is readily apparent from the MOE-Pa of the boards. Beginning with random boards made with the highly degraded A<sub>4</sub> flake furnish, a 24% gain in random board stiffness is possible by increasing flake quality to that of the A furnish. However, a 56% gain in the MOE-Pa of the A<sub>4</sub> boards can be obtained simply by achieving a MOE-R of 2.78, as occurred in the HA boards (Table 11). Applying the same alignment procedures to the A furnish resulted in a MOE-R of 14.26 and improved the MOE-Pa of the A furnish boards by 188%.

**Table 9—Alignment derived from angular measurement**

|   | Furnish type     |                |                |                |                |       |                |       |       |                |       |                                |       |
|---|------------------|----------------|----------------|----------------|----------------|-------|----------------|-------|-------|----------------|-------|--------------------------------|-------|
|   | A                | A <sub>1</sub> | A <sub>2</sub> | A <sub>3</sub> | A <sub>4</sub> | B     | B <sub>1</sub> | C     | D     | D <sub>1</sub> | A+B   | A <sub>1</sub> +B <sub>1</sub> | A+B+C |
|   | Random           |                |                |                |                |       |                |       |       |                |       |                                |       |
| Average alignment (%)                         | 4.4              | -3.3           | 1.6            | 2.6            | 6.7            | 1.0   | 1.6            | 2.0   | -3.1  | -3.9           | 1.6   | -2.2                           | 9.5   |
| Standard deviation of average alignment       | 2.21             | 2.79           | 6.78           | 0.84           | 3.58           | 4.98  | 5.85           | 10.63 | 8.48  | 5.81           | 0.45  | 5.69                           | 8.23  |
| Standard deviation of absolute angle measures | 26.33            | 27.58          | 25.06          | 25.75          | 26.70          | 26.31 | 25.89          | 27.29 | 25.84 | 27.01          | 26.33 | 26.97                          | 25.99 |
| Average cardinal alignment (degree)           | -5.4             | 1.6            | 0.6            | 4.3            | 1.3            | 0.4   | -2.1           | 2.4   | -4.1  | 7.8            | -1.6  | 5.9                            | -2.8  |
|   | Low alignment    |                |                |                |                |       |                |       |       |                |       |                                |       |
| Average alignment (%)                         | 49.7             | 39.7           | 35.8           | 31.4           | 18.9           | 28.9  | 30.9           | 38.1  | 37.2  | 42.0           | 50.9  | 40.1                           | 38.9  |
| Standard deviation of average alignment       | 4.24             | 7.26           | 9.61           | 7.36           | 4.02           | 9.82  | 2.79           | 2.44  | 9.28  | 8.63           | 16.44 | 6.78                           | 9.88  |
| Standard deviation of absolute angle measures | 21.01            | 22.61          | 22.65          | 23.58          | 25.32          | 24.66 | 23.15          | 23.70 | 22.19 | 21.68          | 19.67 | 23.38                          | 23.83 |
| Average cardinal alignment (degree)           | -2.4             | 1.3            | -0.3           | -1.5           | -7.2           | -3.8  | 2.4            | -3.5  | 2.0   | 0.5            | 5.0   | 0.9                            | 2.7   |
|   | High alignment   |                |                |                |                |       |                |       |       |                |       |                                |       |
| Average alignment (%)                         | 78.0             | 62.2           | 68.2           | 69.5           | 45.3           | 57.3  | 61.6           | 74.2  | 55.1  | 63.5           | 69.3  | 65.9                           | 76.0  |
| Standard deviation of average alignment       | 2.64             | 6.56           | 5.99           | 3.81           | 6.10           | 7.19  | 8.18           | 3.14  | 3.94  | 9.72           | 9.76  | 2.81                           | 1.89  |
| Standard deviation of absolute angle measures | 8.76             | 19.04          | 15.95          | 13.49          | 22.57          | 19.92 | 15.17          | 11.39 | 18.86 | 15.29          | 15.09 | 15.40                          | 11.29 |
| Average cardinal alignment (degree)           | -0.6             | 0.4            | -1.0           | -1.8           | -1.8           | -4.1  | -1.0           | -0.3  | -0.7  | -0.6           | 0.2   | -2.1                           | 1.5   |
|   | Medium alignment |                |                |                |                |       |                |       |       |                |       |                                |       |
| Average alignment (%)                         |                  |                |                |                |                | 42.1  |                |       |       |                |       |                                |       |
| Standard deviation of average alignment       |                  |                |                |                |                | 4.17  |                |       |       |                |       |                                |       |
| Standard deviation of absolute angle measures |                  |                |                |                |                | 21.52 |                |       |       |                |       |                                |       |
| Average cardinal alignment (degree)           |                  |                |                |                |                | 1.1   |                |       |       |                |       |                                |       |

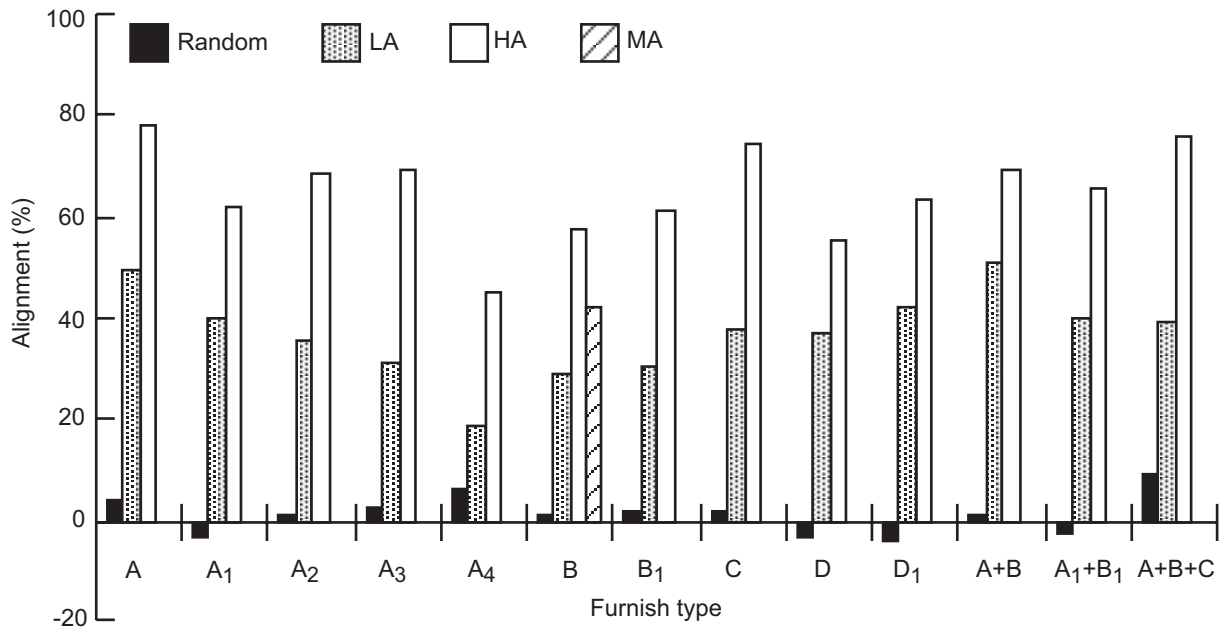


Figure 14—Percentage alignment obtained from angular measurements on boards from the various furnishes (LA, low alignment; HA, high alignment; MA, medium alignment).

Table 10— Sonic velocity data by furnish type<sup>a</sup>

| Alignment                         | Furnish type |                |                |                |                |       |                |       |       |                |       |                                |       |
|-----------------------------------|--------------|----------------|----------------|----------------|----------------|-------|----------------|-------|-------|----------------|-------|--------------------------------|-------|
|                                   | A            | A <sub>1</sub> | A <sub>2</sub> | A <sub>3</sub> | A <sub>4</sub> | B     | B <sub>1</sub> | C     | D     | D <sub>1</sub> | A+B   | A <sub>1</sub> +B <sub>1</sub> | A+B+C |
| Pa (mm/μs)                        |              |                |                |                |                |       |                |       |       |                |       |                                |       |
| Random                            | 3.428        | 3.322          | 3.189          | 3.051          | 2.957          | 3.408 | 3.089          | 3.281 | 3.423 | 3.090          | 3.413 | 3.266                          | 3.318 |
| Low                               | 4.342        | 3.917          | 3.814          | 3.657          | 3.352          | 3.926 | 3.734          | 4.001 | 3.968 | 3.639          | 4.197 | 4.009                          | 4.134 |
| High                              | 5.002        | 4.525          | 4.526          | 4.008          | 3.676          | 4.304 | 4.253          | 4.729 | 4.560 | 4.029          | 4.735 | 4.509                          | 4.585 |
| Medium                            | 4.164        |                |                |                |                |       |                |       |       |                |       |                                |       |
| Pe (mm/μs)                        |              |                |                |                |                |       |                |       |       |                |       |                                |       |
| Random                            | 3.317        | 3.188          | 3.090          | 2.928          | 2.954          | 3.290 | 3.072          | 3.101 | 3.295 | 3.048          | 3.309 | 3.160                          | 3.234 |
| Low                               | 2.189        | 2.252          | 2.298          | 2.363          | 2.448          | 2.382 | 2.322          | 2.097 | 2.394 | 2.393          | 2.208 | 2.352                          | 2.289 |
| High                              | 1.433        | 1.637          | 1.721          | 2.010          | 2.058          | 1.950 | 1.641          | 1.294 | 1.733 | 1.930          | 1.521 | 1.896                          | 1.461 |
| Medium                            | 2.309        |                |                |                |                |       |                |       |       |                |       |                                |       |
| Pa/Pe = SVR                       |              |                |                |                |                |       |                |       |       |                |       |                                |       |
| Random                            | 1.034        | 1.042          | 1.033          | 1.042          | 1.001          | 1.036 | 1.007          | 1.058 | 1.039 | 1.014          | 1.032 | 1.034                          | 1.026 |
| Low                               | 1.985        | 1.739          | 1.660          | 1.548          | 1.369          | 1.648 | 1.609          | 1.911 | 1.657 | 1.520          | 1.901 | 1.706                          | 1.808 |
| High                              | 3.492        | 2.773          | 2.634          | 1.994          | 1.786          | 2.214 | 2.595          | 3.656 | 2.637 | 2.089          | 3.116 | 2.378                          | 3.139 |
| Medium                            | 1.804        |                |                |                |                |       |                |       |       |                |       |                                |       |
| % = 67.367 (log <sub>e</sub> SVR) |              |                |                |                |                |       |                |       |       |                |       |                                |       |
| Random                            | 2            | 3              | 2              | 3              | 0              | 2     | 0              | 4     | 3     | 1              | 2     | 2                              | 2     |
| Low                               | 46           | 37             | 34             | 29             | 21             | 34    | 32             | 44    | 34    | 28             | 43    | 36                             | 40    |
| High                              | 84           | 69             | 65             | 46             | 39             | 53    | 64             | 87    | 65    | 50             | 77    | 58                             | 77    |
| Medium                            | 40           |                |                |                |                |       |                |       |       |                |       |                                |       |

<sup>a</sup>Pa, parallel; Pe, perpendicular; SVR, sonic velocity ratio.

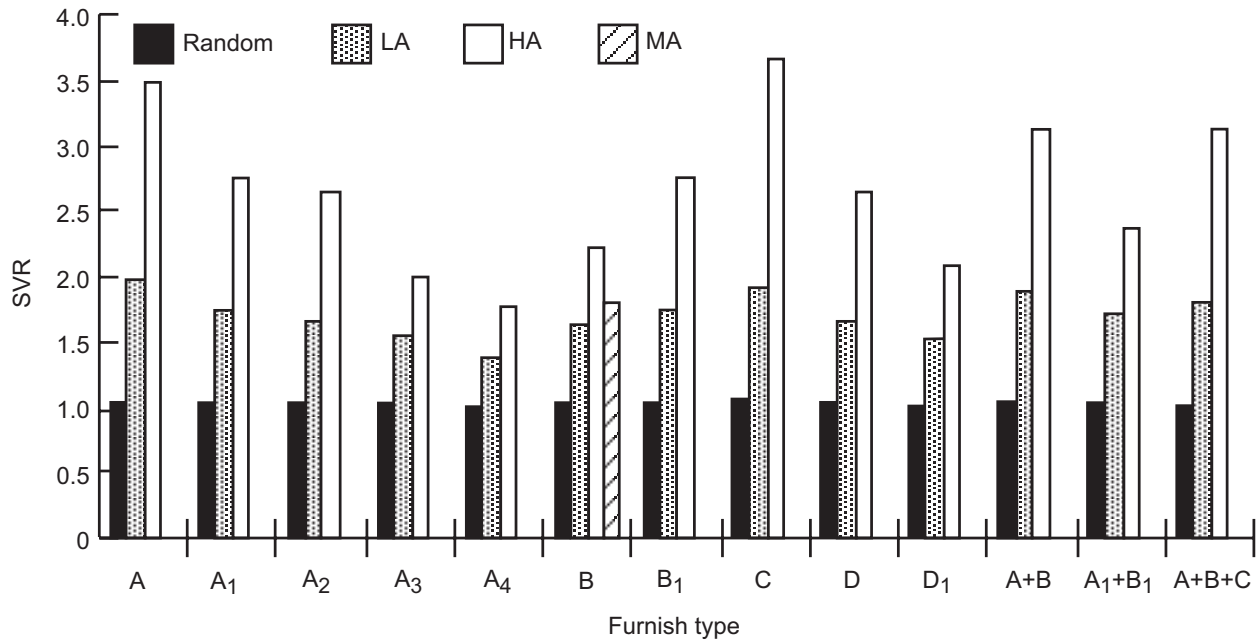


Figure 15—Sonic velocity ratio (SVR) by furnish type (LA, low alignment; HA, high alignment; MA, medium alignment).

Table 11—Modulus of elasticity data by furnish type

| Alignment <sup>a</sup> | Furnish type                        |                |                |                |                |       |                |        |        |                |        |                                |        |
|------------------------|-------------------------------------|----------------|----------------|----------------|----------------|-------|----------------|--------|--------|----------------|--------|--------------------------------|--------|
|                        | A                                   | A <sub>1</sub> | A <sub>2</sub> | A <sub>3</sub> | A <sub>4</sub> | B     | B <sub>1</sub> | C      | D      | D <sub>1</sub> | A+B    | A <sub>1</sub> +B <sub>1</sub> | A+B+C  |
|                        | MOE (MPa)                           |                |                |                |                |       |                |        |        |                |        |                                |        |
| Random-average         | 4,884                               | 4,867          | 4,551          | 4,126          | 3,936          | 5,315 | 4,235          | 4,258  | 5,120  | 4,505          | 5,395  | 4,987                          | 5,028  |
| Random-Pa              | 4,838                               | 5,010          | 4,516          | 4,286          | 4,034          | 5,505 | 4,367          | 4,643  | 5,298  | 4,608          | 5,516  | 4,999                          | 5,171  |
| Random-Pe              | 4,930                               | 4,723          | 4,585          | 3,965          | 3,838          | 5,125 | 4,102          | 3,873  | 4,941  | 4,401          | 5,275  | 4,976                          | 4,884  |
| Low-Pa                 | 10,423                              | 8,171          | 7,217          | 6,297          | 5,723          | 7,447 | 6,435          | 7,941  | 9,170  | 7,240          | 9,779  | 8,033                          | 9,297  |
| Low-Pe                 | 2,195                               | 2,689          | 2,701          | 2,953          | 3,103          | 2,609 | 2,643          | 2,137  | 3,356  | 3,252          | 2,747  | 2,804                          | 2,712  |
| High-Pa                | 14,043                              | 11,457         | 9,538          | 7,791          | 6,125          | 9,917 | 8,274          | 13,009 | 11,515 | 8,354          | 12,193 | 10,664                         | 12,342 |
| High-Pe                | 1,000                               | 1,448          | 1,425          | 1,931          | 2,206          | 1,908 | 1,563          | 1,034  | 1,977  | 1,885          | 1,471  | 1,701                          | 1,287  |
| Medium-Pa              |                                     |                |                |                |                | 8,469 |                |        |        |                |        |                                |        |
| Medium-Pe              |                                     |                |                |                |                | 2,517 |                |        |        |                |        |                                |        |
|                        | MOE-R (Pa/Pe) <sup>b</sup>          |                |                |                |                |       |                |        |        |                |        |                                |        |
| Random                 | 0.98                                | 1.06           | 0.99           | 1.08           | 1.05           | 1.07  | 1.06           | 1.20   | 1.07   | 1.05           | 1.05   | 1.00                           | 1.06   |
| Low                    | 4.75                                | 3.04           | 2.67           | 2.13           | 1.84           | 2.85  | 2.43           | 3.72   | 2.73   | 2.23           | 3.56   | 2.86                           | 3.43   |
| High                   | 14.05                               | 7.91           | 6.69           | 4.04           | 2.78           | 5.20  | 5.29           | 12.58  | 5.83   | 4.43           | 8.29   | 6.27                           | 9.59   |
| Medium                 |                                     |                |                |                |                | 3.37  |                |        |        |                |        |                                |        |
|                        | % = 32.275 (log <sub>e</sub> MOE-R) |                |                |                |                |       |                |        |        |                |        |                                |        |
| Random                 | -1                                  | 2              | -1             | 3              | 2              | 2     | 2              | 6      | 2      | 2              | 2      | 0                              | 2      |
| Low                    | 53                                  | 38             | 33             | 26             | 21             | 35    | 30             | 44     | 34     | 27             | 43     | 36                             | 42     |
| High                   | 89                                  | 70             | 64             | 47             | 35             | 56    | 56             | 86     | 60     | 50             | 71     | 62                             | 76     |
| Medium                 |                                     |                |                |                |                | 41    |                |        |        |                |        |                                |        |

<sup>a</sup> Pa, parallel; Pe, perpendicular.

<sup>b</sup> MOE-R, modulus of elasticity ratios.

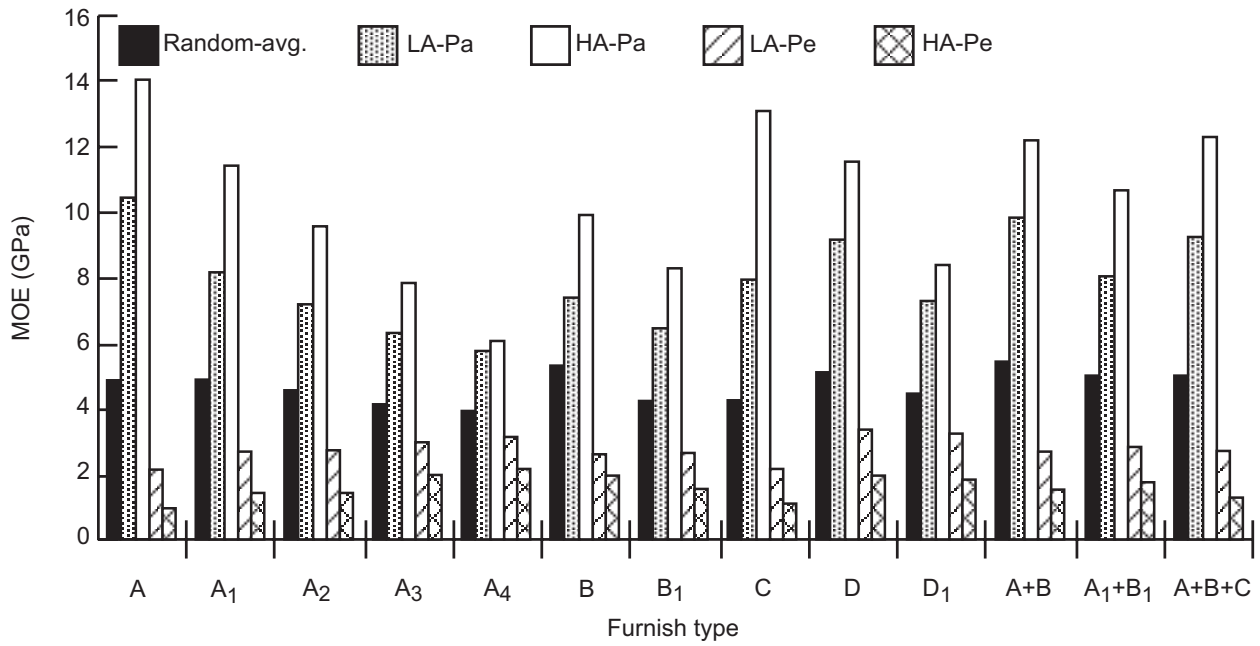


Figure 16—Modulus of elasticity by furnish type and alignment direction (LA, low alignment; HA, high alignment; Pa, parallel; Pe, perpendicular).

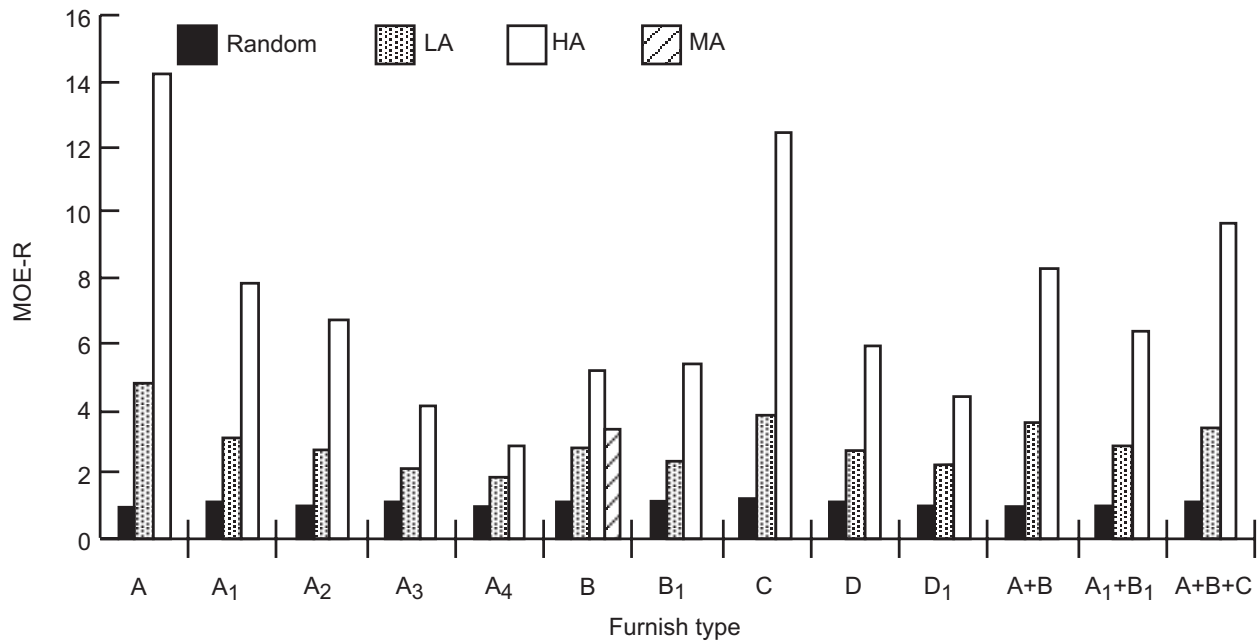


Figure 17—Modulus of elasticity ratio (MOE-R) by furnish type and alignment (LA, low alignment; HA, high alignment; MA, medium alignment).

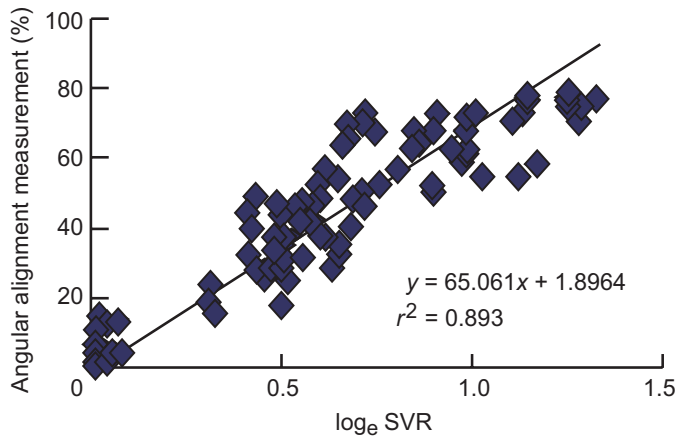


Figure 18—Relationship between alignment percentage and the natural log of sonic velocity ratio (SVR) (Eq. (2)).

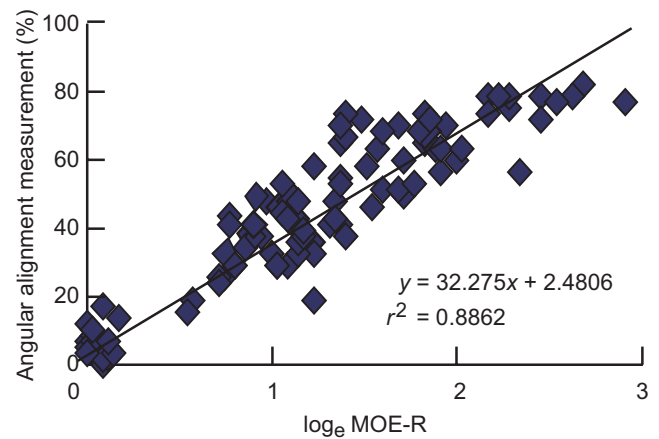


Figure 19—Relationship between alignment percentage and the natural log of MOE ratio (MOE-R) (Eq. (3)).

Table 12—Modulus of rupture data by furnish type

| Alignment <sup>a</sup> | Furnish type       |                |                |                |                |      |                |      |      |                |      |                                |       |
|------------------------|--------------------|----------------|----------------|----------------|----------------|------|----------------|------|------|----------------|------|--------------------------------|-------|
|                        | A                  | A <sub>1</sub> | A <sub>2</sub> | A <sub>3</sub> | A <sub>4</sub> | B    | B <sub>1</sub> | C    | D    | D <sub>1</sub> | A+B  | A <sub>1</sub> +B <sub>1</sub> | A+B+C |
|                        | MOR (MPa)          |                |                |                |                |      |                |      |      |                |      |                                |       |
| Random-average         | 33.2               | 32.0           | 31.6           | 27.5           | 24.5           | 34.6 | 26.7           | 29.5 | 31.1 | 26.1           | 36.3 | 30.7                           | 34.6  |
| Random-Pa              | 29.9               | 32.0           | 30.7           | 27.3           | 25.2           | 34.0 | 27.9           | 32.0 | 31.0 | 26.5           | 37.1 | 32.1                           | 37.1  |
| Random-Pe              | 36.5               | 32.0           | 32.4           | 27.6           | 23.7           | 35.2 | 25.5           | 26.9 | 31.2 | 25.6           | 35.4 | 29.3                           | 32.1  |
| Low-Pa                 | 58.6               | 49.1           | 39.0           | 34.9           | 30.0           | 41.1 | 34.0           | 46.1 | 59.7 | 38.9           | 55.1 | 44.5                           | 58.0  |
| Low-Pe                 | 15.9               | 21.0           | 18.3           | 20.8           | 19.1           | 19.4 | 18.9           | 17.2 | 27.1 | 21.8           | 21.8 | 21.3                           | 20.9  |
| High-Pa                | 67.4               | 62.7           | 49.3           | 39.7           | 33.0           | 52.9 | 38.8           | 74.5 | 72.4 | 41.6           | 63.5 | 54.7                           | 65.7  |
| High-Pe                | 8.7                | 12.6           | 12.5           | 16.0           | 16.4           | 16.2 | 12.6           | 9.1  | 16.6 | 13.0           | 14.4 | 13.0                           | 11.2  |
| Medium-Pa              |                    |                |                |                |                | 42.2 |                |      |      |                |      |                                |       |
| Medium-Pe              |                    |                |                |                |                | 18.8 |                |      |      |                |      |                                |       |
|                        | MOR-R <sup>b</sup> |                |                |                |                |      |                |      |      |                |      |                                |       |
| Random-ratio           | 0.82               | 1.00           | 0.95           | 0.99           | 1.06           | 0.97 | 1.09           | 1.19 | 1.00 | 1.04           | 1.05 | 1.10                           | 1.15  |
| Low-ratio              | 3.67               | 2.34           | 2.13           | 1.68           | 1.57           | 2.12 | 1.80           | 2.68 | 2.20 | 1.79           | 2.53 | 2.09                           | 2.77  |
| High-ratio             | 7.78               | 4.97           | 3.94           | 2.48           | 2.01           | 3.26 | 3.07           | 8.21 | 4.36 | 3.21           | 4.42 | 4.21                           | 5.87  |
| Medium-ratio           |                    |                |                |                |                | 2.24 |                |      |      |                |      |                                |       |

<sup>a</sup>Pa, parallel; Pe, perpendicular.

<sup>b</sup>MOR-R, modulus of rigidity ratios.

Modulus of rupture responds to the flake furnish and alignment variables in a manner similar to MOE. This is to be expected in a wood composite. The relation between mean values of MOR and MOE has an  $r^2 = 0.967$  and is shown in Figure 21. When the values of individual boards were predicted,  $r^2 = 0.939$ .

### Shear

Average Minnesota shear properties for the boards are given in Table 13. All tests were conducted parallel to the

alignment direction. Shear properties were related to SG; however, this relationship varied with both furnish type and alignment. Shear properties adjusted to 0.640 SG using an average adjustment factor of 17,321(0.640 – SG) are shown in Figure 22. In general, shear strength decreased with furnish degradation and increased with flake alignment. Boards constructed solely or partially with furnish B showed high shear strength. This is partially attributed to the thinner flakes of the B furnish.

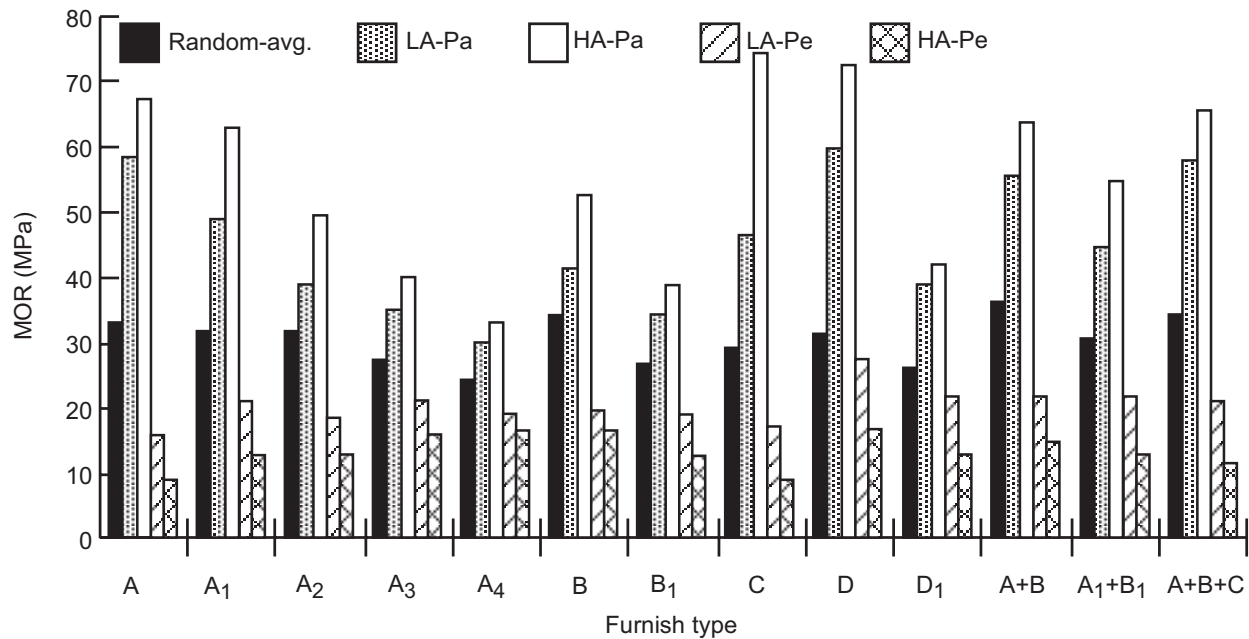


Figure 20—Modulus of rupture by furnish type and alignment direction (LA, low alignment; HA, high alignment; Pa, parallel; Pe, perpendicular).

### Dimensional Stability

Water absorption, for all furnish types combined, averaged 6.2%, 8.3%, and 15.0% when equilibrated to 50%, 65%, and 90% RH, respectively (Table 14; Fig. 23). No practical difference could be detected in WA of the different furnishes due to degree of alignment; however, there was a trend for a slight increase in WA with flake degradation (Table 15). As experienced in other studies (Geimer 1982), WA declined slightly with increasing SG (Fig. 24).

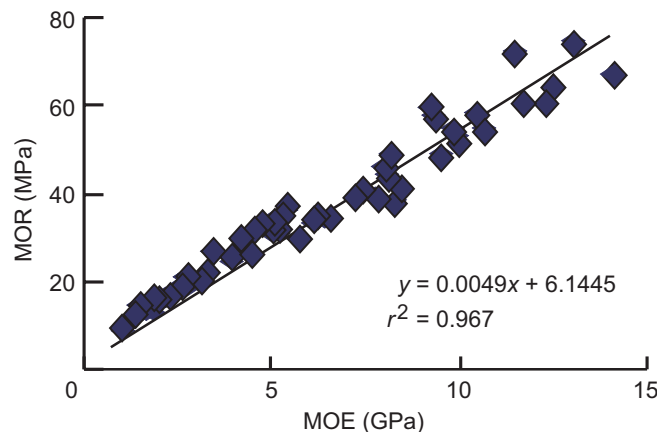


Figure 21—Correlation of modulus of rupture to modulus of elasticity.

No practical difference could be seen in TS of boards from the same flake furnish with different alignment. The TS data used in Tables 15 and 16 and Figures 25 and 26 are averages of alignment types. Of the four prime furnishes, type C showed the highest TS (Fig. 25). In general, increases in TS occurred with flake degradation, although these were not always significantly different from other furnish types (Table 15). With the exception of the B<sub>1</sub> furnish, all furnishes increased in thickness when dried to an OD2 condition following the VPS exposure (Table 16). This may have been a result of additional swelling in the wet state following VPS measurement and prior to OD2 redrying or the breaking of adhesive bonds with accompanying springback caused by high stresses during drying. Thickness swelling was strongly related to WA (Fig. 26).

Linear expansion was, of course, directly affected by both degree of flake alignment and test direction (Table 17). Within a furnish, the boards with the highest alignment had the lowest LE-Pa (Fig. 27). The very pronounced linear shrinkage of the specimen when oven-dried following the VPS exposure was very interesting (Fig. 28). This appeared at first to result from the additional thickness expansion occurring from VPS to OD2 exposures. However, the extent of shrinkage was not well correlated with the measured TS.

**Table 13—Minnesota shear and specific gravity (SG) by furnish type**

| Alignment | Furnish type |                |                |                |                |       |                |       |       |                |       |                                |       |  |
|-----------|--------------|----------------|----------------|----------------|----------------|-------|----------------|-------|-------|----------------|-------|--------------------------------|-------|--|
|           | A            | A <sub>1</sub> | A <sub>2</sub> | A <sub>3</sub> | A <sub>4</sub> | B     | B <sub>1</sub> | C     | D     | D <sub>1</sub> | A+B   | A <sub>1</sub> +B <sub>1</sub> | A+B+C |  |
|           | Shear (MPa)  |                |                |                |                |       |                |       |       |                |       |                                |       |  |
| Random    | 4,010        | 3,873          | 3,776          | 3,616          | 3,387          | 4,271 | 3,599          | 3,567 | 3,028 | 2,848          | 4,090 | 3,167                          | 4,584 |  |
| Low       | 5,138        | 5,258          | 3,966          | 3,706          | 3,629          | 4,026 | 3,729          | 3,192 | 5,452 | 3,682          | 5,512 | 4,395                          | 5,549 |  |
| High      | 4,016        | 4,863          | 4,506          | 4,455          | 3,812          | 4,559 | 3,772          | 4,972 | 5,265 | 3,182          | 5,350 | 3,948                          | 5,052 |  |
| Medium    |              |                |                |                |                | 4,513 |                |       |       |                |       |                                |       |  |
|           | SG           |                |                |                |                |       |                |       |       |                |       |                                |       |  |
| Random    | 0.664        | 0.670          | 0.649          | 0.660          | 0.646          | 0.667 | 0.650          | 0.650 | 0.668 | 0.655          | 0.665 | 0.649                          | 0.671 |  |
| Low       | 0.685        | 0.681          | 0.673          | 0.653          | 0.661          | 0.655 | 0.659          | 0.665 | 0.680 | 0.671          | 0.689 | 0.673                          | 0.696 |  |
| High      | 0.655        | 0.663          | 0.653          | 0.643          | 0.634          | 0.663 | 0.646          | 0.684 | 0.664 | 0.643          | 0.668 | 0.647                          | 0.682 |  |
| Medium    |              |                |                |                |                | 0.667 |                |       |       |                |       |                                |       |  |

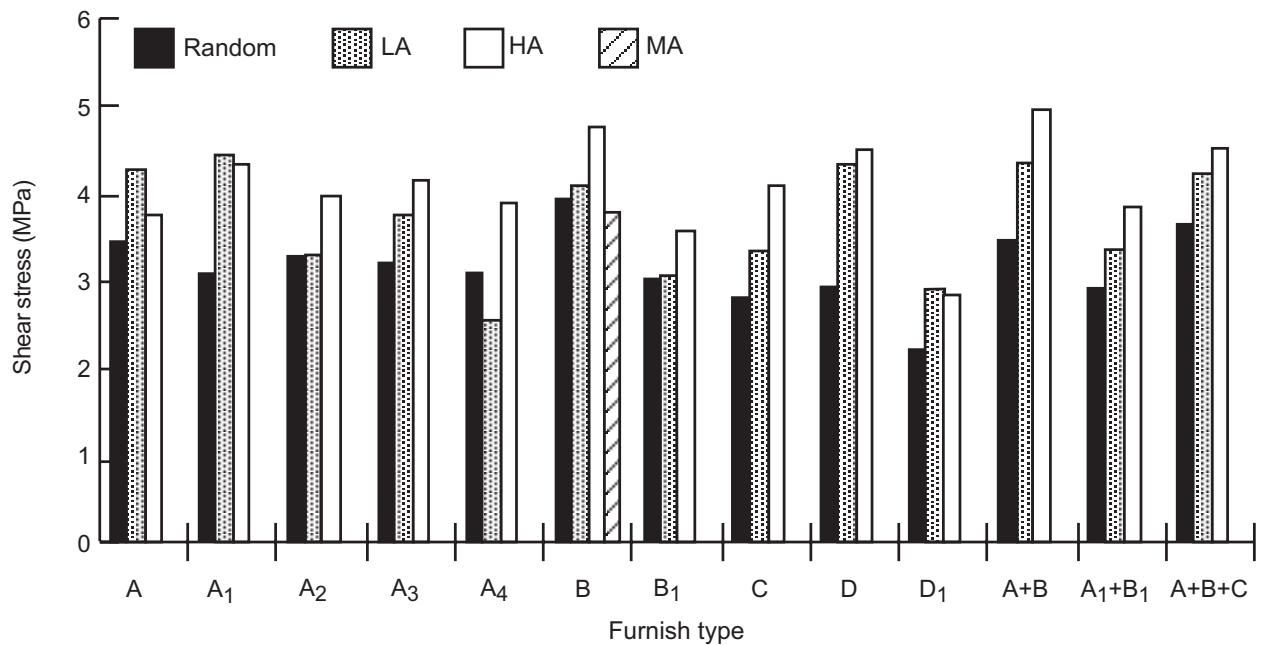


**Figure 22—Shear stress by furnish type and alignment (values have been adjusted for specific gravity; LA, low alignment; HA, high alignment; MA, medium alignment).**

**Table 14—Water adsorption by furnish type**

| Environment      | Furnish type         |                |                |                |                |      |                |      |      |                |      |                                |       |         |
|------------------|----------------------|----------------|----------------|----------------|----------------|------|----------------|------|------|----------------|------|--------------------------------|-------|---------|
|                  | A                    | A <sub>1</sub> | A <sub>2</sub> | A <sub>3</sub> | A <sub>4</sub> | B    | B <sub>1</sub> | C    | D    | D <sub>1</sub> | A+B  | A <sub>1</sub> +B <sub>1</sub> | A+B+C | Average |
|                  | Water adsorption (%) |                |                |                |                |      |                |      |      |                |      |                                |       |         |
| 50% RH           | 6.0                  | 6.3            | 6.4            | 6.3            | 6.4            | 6.2  | 6.4            | 6.4  | 6.0  | 6.4            | 6.0  | 6.1                            | 6.0   | 6.2     |
| 65% RH           | 8.1                  | 8.3            | 8.5            | 8.4            | 8.5            | 8.2  | 8.4            | 8.5  | 8.1  | 8.5            | 7.9  | 8.1                            | 8.0   | 8.3     |
| 90% RH           | 15.2                 | 15.3           | 15.5           | 14.9           | 15.1           | 14.7 | 15.3           | 15.0 | 15.1 | 15.3           | 14.4 | 14.9                           | 14.3  | 15.0    |
| VPS <sup>a</sup> | 95.7                 | 94.9           | 100.7          | 99.6           | 101.2          | 99.9 | 97.0           | 92.7 | 96.0 | 103.4          | 93.8 | 98.7                           | 92.8  | 97.4    |

<sup>a</sup>VPS, vacuum pressure soak.

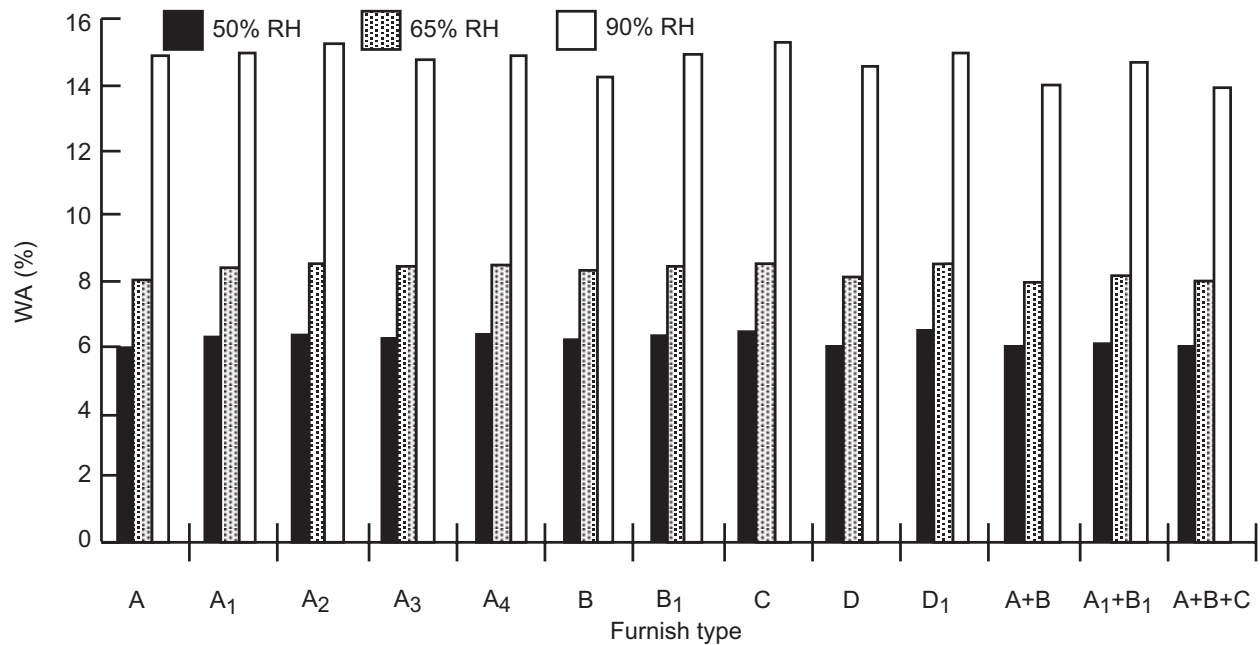


Figure 23—Water absorption (WA) by furnish type at three equilibrated exposures.

Table 15—Tukey’s test separation of furnish by water adsorption and thickness swell properties

| Environment      | Significance level | Furnish types (Low to High) |         |                |                                   |                                   |                                   |                                   |                |                |                                   |                |                |                |
|------------------|--------------------|-----------------------------|---------|----------------|-----------------------------------|-----------------------------------|-----------------------------------|-----------------------------------|----------------|----------------|-----------------------------------|----------------|----------------|----------------|
|                  |                    | (A+B+C)                     | (A+B)   | A              | D                                 | (A <sub>1</sub> +B <sub>1</sub> ) | B                                 | A <sub>1</sub>                    | A <sub>3</sub> | A <sub>4</sub> | A <sub>2</sub>                    | B <sub>1</sub> | D <sub>1</sub> | C              |
| Water adsorption |                    |                             |         |                |                                   |                                   |                                   |                                   |                |                |                                   |                |                |                |
| 50% RH           | 0.0001             | (A+B+C)                     | (A+B)   | A              | D                                 | (A <sub>1</sub> +B <sub>1</sub> ) | B                                 | A <sub>1</sub>                    | A <sub>3</sub> | A <sub>4</sub> | A <sub>2</sub>                    | B <sub>1</sub> | D <sub>1</sub> | C              |
| 65% RH           | 0.0001             | (A+B)                       | (A+B+C) | D              | A                                 | (A <sub>1</sub> +B <sub>1</sub> ) | B                                 | A <sub>1</sub>                    | B <sub>1</sub> | A <sub>3</sub> | A <sub>4</sub>                    | C              | D <sub>1</sub> | A <sub>2</sub> |
| 90% RH           | 0.0023             | (A+B+C)                     | (A+B)   | B              | A <sub>3</sub>                    | (A <sub>1</sub> +B <sub>1</sub> ) | C                                 | D                                 | A <sub>4</sub> | A              | A <sub>1</sub>                    | D <sub>1</sub> | B <sub>1</sub> | A <sub>2</sub> |
| Thickness swell  |                    |                             |         |                |                                   |                                   |                                   |                                   |                |                |                                   |                |                |                |
| 50% RH           | 0.0003             | (A+B+C)                     | (A+B)   | B              | D                                 | A                                 | D <sub>1</sub>                    | (A <sub>1</sub> +B <sub>1</sub> ) | A <sub>1</sub> | A <sub>3</sub> | C                                 | A <sub>4</sub> | B <sub>1</sub> | A <sub>2</sub> |
| 60% RH           | 0.001              | (A+B)                       | (A+B+C) | D              | B                                 | A                                 | (A <sub>1</sub> +B <sub>1</sub> ) | D <sub>1</sub>                    | A <sub>1</sub> | B <sub>1</sub> | C                                 | A <sub>3</sub> | A <sub>2</sub> | A <sub>4</sub> |
| 90% RH           | 0.0001             | (A+B)                       | B       | (A+B+C)        | D                                 | D <sub>1</sub>                    | (A <sub>1</sub> +B <sub>1</sub> ) | A                                 | A <sub>3</sub> | B <sub>1</sub> | A <sub>1</sub>                    | A <sub>4</sub> | C              | A <sub>2</sub> |
| VPS <sup>a</sup> | 0.0001             | D                           | A       | (A+B)          | (A <sub>1</sub> +B <sub>1</sub> ) | B                                 | A <sub>1</sub>                    | (A+B+C)                           | D <sub>1</sub> | B <sub>1</sub> | A <sub>2</sub>                    | A <sub>3</sub> | A <sub>4</sub> | C              |
| OD2 <sup>b</sup> | 0.0001             | D                           | B       | B <sub>1</sub> | (A+B)                             | A <sub>1</sub>                    | A                                 | (A+B+C)                           | A <sub>2</sub> | D <sub>1</sub> | (A <sub>1</sub> +B <sub>1</sub> ) | A <sub>3</sub> | A <sub>4</sub> | C              |

<sup>a</sup>VPS, vacuum pressure soak.

<sup>b</sup>OD2, second oven-dry.

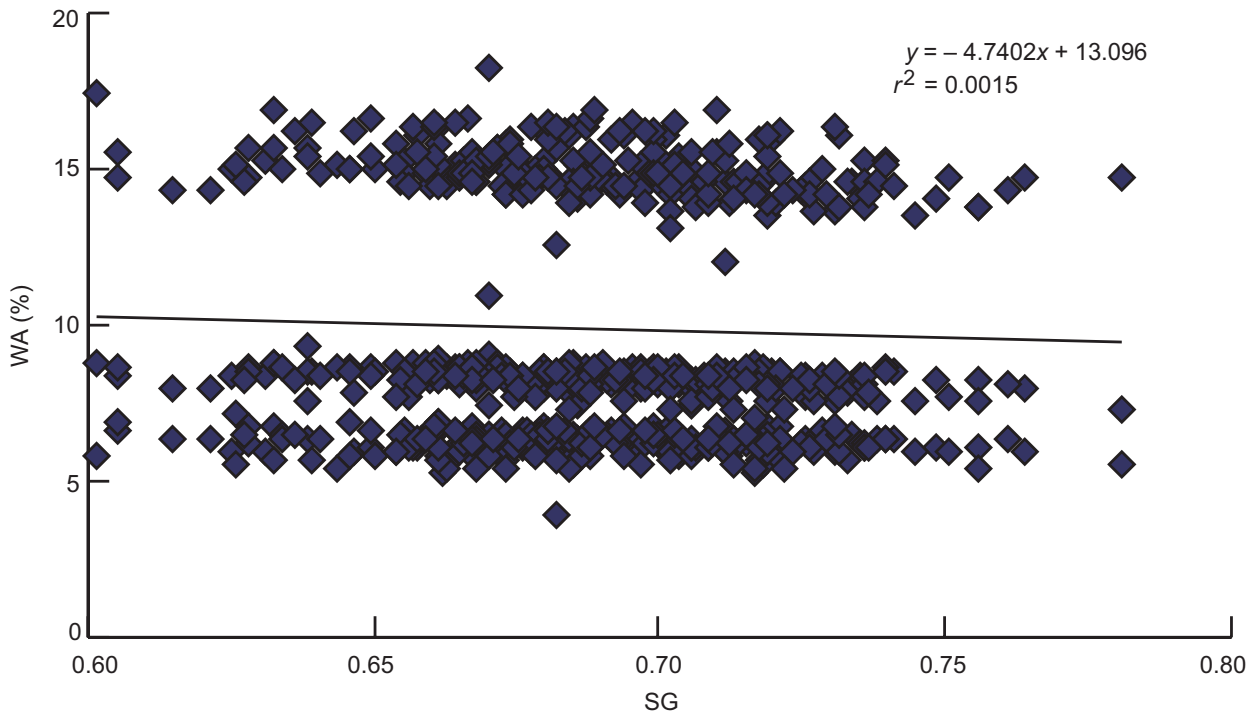


Figure 24—Water absorption (WA) compared with specific gravity (SG) (data taken from all board types and three exposure levels).

Table 16—Thickness swell by furnish type

| Environment      | Furnish type        |                |                |                |                |      |                |      |      |                |      |                                |       |         |
|------------------|---------------------|----------------|----------------|----------------|----------------|------|----------------|------|------|----------------|------|--------------------------------|-------|---------|
|                  | A                   | A <sub>1</sub> | A <sub>2</sub> | A <sub>3</sub> | A <sub>4</sub> | B    | B <sub>1</sub> | C    | D    | D <sub>1</sub> | A+B  | A <sub>1</sub> +B <sub>1</sub> | A+B+C | Average |
|                  | Thickness swell (%) |                |                |                |                |      |                |      |      |                |      |                                |       |         |
| 50% RH           | 2.4                 | 2.6            | 2.7            | 2.6            | 2.7            | 2.3  | 2.7            | 2.6  | 2.4  | 2.5            | 2.2  | 2.5                            | 2.2   | 2.5     |
| 65% RH           | 4.0                 | 4.1            | 4.4            | 4.3            | 4.4            | 3.8  | 4.3            | 4.3  | 3.8  | 4.1            | 3.6  | 4.1                            | 3.7   | 4.1     |
| 90% RH           | 12.8                | 13.3           | 13.9           | 13.1           | 13.4           | 11.5 | 13.1           | 13.9 | 11.7 | 12.5           | 11.4 | 12.8                           | 11.6  | 12.7    |
| VPS <sup>a</sup> | 20.2                | 21.5           | 23.1           | 23.2           | 23.5           | 21.2 | 22.7           | 24.8 | 17.7 | 22.0           | 20.6 | 21.1                           | 22.0  | 21.8    |
| OD2 <sup>b</sup> | 24.0                | 24.0           | 25.1           | 27.5           | 30.1           | 21.9 | 22.7           | 30.6 | 19.8 | 25.5           | 23.0 | 26.4                           | 24.8  | 25.0    |

<sup>a</sup>VPS, vacuum pressure soak.

<sup>b</sup>OD2, second oven-dry.

## Models

Several models pertaining to MOE of single layer OSB have been explored previously (Geimer 1979, 1980, 1986). The relationship

$$(\text{MOE Pa} \times \text{MOE Pe})^{1/2} = \text{MOE Random} \quad (4)$$

has consistently predicted bending properties more accurately and with less variation than the relationship

$$(\text{MOE Pa} + \text{MOE Pe})/2 = \text{MOE Random} \quad (5)$$

Analysis of the data in this study shows that predictions using Equation (4) were an average 8% low with a standard deviation of 10% while predictions using Equation (5) averaged 20% high with a standard deviation of 16%.

Useful equations (Geimer 1986) relating to Equation (4) are

$$(\text{MOE Pa})/\text{MOE Random} = \text{MOE-R}^p \quad (6)$$

$$(\text{MOE Pa})/\text{MOE Random} = \text{SVR}^b \quad (7)$$

$$\text{MOE-R} = \text{SVR}^d \quad (8)$$

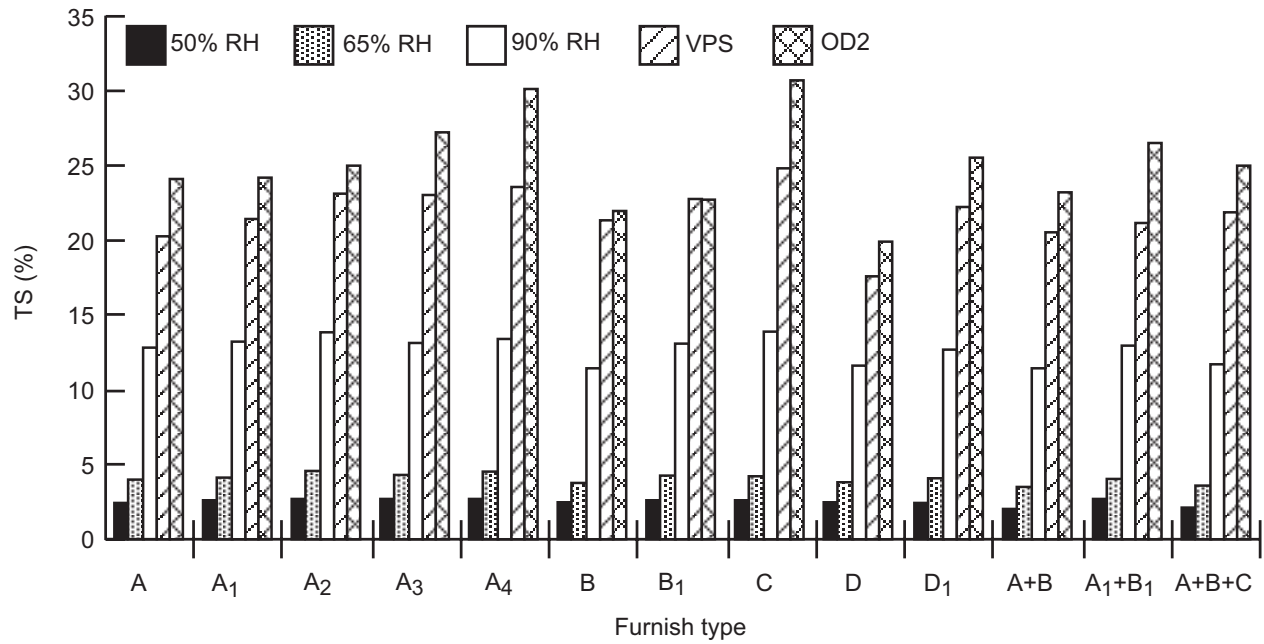


Figure 25—Thickness swell (TS) at five exposure levels (VPS, vacuum pressure soak; OD2, second oven-dry).

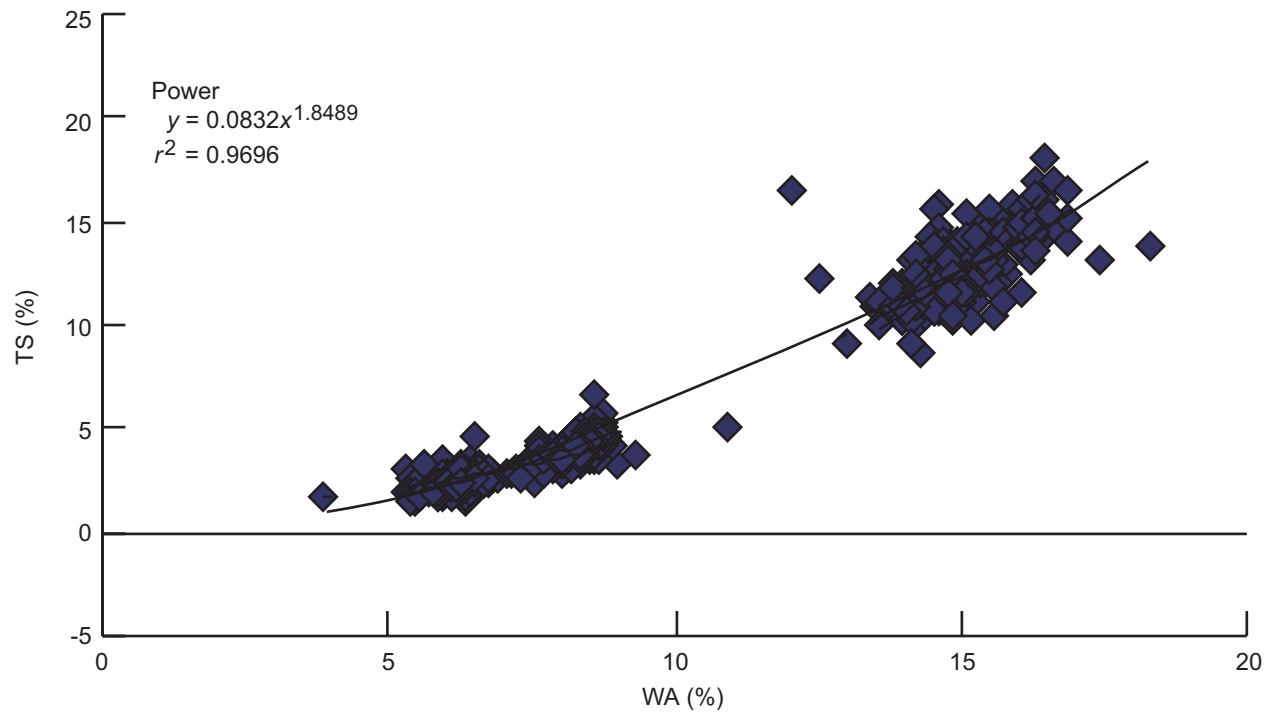


Figure 26—Thickness swell (TS) estimated using a power function of water absorption (WA) (no vacuum pressure soak).

**Table 17—Linear expansion by furnish type<sup>a</sup>**

| Environment | Linear expansion (%) |                |                |                |                |        |                |        |        |                |        |                                |        |
|-------------|----------------------|----------------|----------------|----------------|----------------|--------|----------------|--------|--------|----------------|--------|--------------------------------|--------|
|             | A                    | A <sub>1</sub> | A <sub>2</sub> | A <sub>3</sub> | A <sub>4</sub> | B      | B <sub>1</sub> | C      | D      | D <sub>1</sub> | A+B    | A <sub>1</sub> +B <sub>1</sub> | A+B+C  |
|             | Random               |                |                |                |                |        |                |        |        |                |        |                                |        |
| 50% RH      | 0.151                | 0.145          | 0.138          | 0.152          | 0.157          | 0.155  | 0.165          | 0.131  | 0.152  | 0.149          | 0.147  | 0.138                          | 0.148  |
| 65% RH      | 0.192                | 0.192          | 0.183          | 0.203          | 0.204          | 0.196  | 0.214          | 0.171  | 0.191  | 0.200          | 0.185  | 0.173                          | 0.198  |
| 90% RH      | 0.223                | 0.225          | 0.208          | 0.245          | 0.246          | 0.234  | 0.263          | 0.197  | 0.214  | 0.255          | 0.215  | 0.191                          | 0.217  |
| VPS         | 0.242                | 0.186          | 0.235          | 0.301          | 0.298          | 0.243  | 0.303          | 0.243  | 0.222  | 0.295          | 0.236  | 0.203                          | 0.242  |
| OD2         | -0.197               | -0.166         | -0.165         | -0.151         | -0.075         | -0.180 | -0.189         | -0.119 | -0.134 | -0.090         | -0.182 | -0.144                         | -0.183 |
|             | LA-Pa                |                |                |                |                |        |                |        |        |                |        |                                |        |
| 50% RH      | 0.098                | 0.118          | 0.118          | 0.124          | 0.122          | 0.136  | 0.142          | 0.095  | 0.118  | 0.133          | 0.077  | 0.098                          | 0.105  |
| 65% RH      | 0.118                | 0.136          | 0.141          | 0.134          | 0.138          | 0.198  | 0.174          | 0.115  | 0.151  | 0.157          | 0.119  | 0.134                          | 0.122  |
| 90% RH      | 0.133                | 0.148          | 0.155          | 0.152          | 0.150          | 0.191  | 0.202          | 0.104  | 0.171  | 0.183          | 0.113  | 0.103                          | 0.131  |
| VPS         | 0.150                | 0.163          | 0.182          | 0.178          | 0.181          | 0.222  | 0.242          | 0.091  | 0.197  | 0.207          | 0.121  | 0.109                          | 0.146  |
| OD2         | -0.156               | -0.135         | -0.108         | -0.169         | -0.106         | -0.156 | -0.142         | -0.122 | -0.151 | -0.145         | -0.160 | -0.174                         | -0.175 |
|             | LA-Pe                |                |                |                |                |        |                |        |        |                |        |                                |        |
| 50% RH      | 0.290                | 0.281          | 0.236          | 0.241          | 0.205          | 0.259  | 0.220          | 0.244  | 0.236  | 0.247          | 0.294  | 0.230                          | 0.284  |
| 65% RH      | 0.411                | 0.351          | 0.279          | 0.293          | 0.241          | 0.319  | 0.270          | 0.300  | 0.315  | 0.297          | 0.368  | 0.278                          | 0.349  |
| 90% RH      | 0.564                | 0.488          | 0.335          | 0.426          | 0.301          | 0.446  | 0.410          | 0.411  | 0.428  | 0.407          | 0.522  | 0.382                          | 0.488  |
| VPS         | 0.671                | 0.613          | 0.496          | 0.533          | 0.441          | 0.574  | 0.511          | 0.560  | 0.488  | 0.507          | 0.621  | 0.494                          | 0.608  |
| OD2         | -0.256               | -0.195         | -0.076         | -0.072         | 0.005          | -0.144 | -0.099         | 0.064  | -0.046 | -0.097         | -0.248 | -0.068                         | -0.092 |
|             | HA-Pa                |                |                |                |                |        |                |        |        |                |        |                                |        |
| 50% RH      | 0.082                | 0.087          | 0.100          | 0.095          | 0.107          | 0.102  | 0.111          | 0.073  | 0.083  | 0.101          | 0.071  | 0.096                          | 0.088  |
| 65% RH      | 0.109                | 0.116          | 0.109          | 0.112          | 0.121          | 0.128  | 0.137          | 0.090  | 0.103  | 0.117          | 0.100  | 0.116                          | 0.109  |
| 90% RH      | 0.112                | 0.129          | 0.116          | 0.094          | 0.121          | 0.139  | 0.150          | 0.075  | 0.118  | 0.128          | 0.106  | 0.130                          | 0.126  |
| VPS         | 0.156                | 0.140          | 0.103          | 0.103          | 0.123          | 0.172  | 0.150          | 0.066  | 0.125  | 0.130          | 0.110  | 0.138                          | 0.139  |
| OD2         | -0.083               | -0.159         | -0.171         | -0.180         | -0.147         | -0.159 | -0.218         | -0.133 | -0.129 | -0.155         | -0.131 | -0.120                         | -0.106 |
|             | HA-Pe                |                |                |                |                |        |                |        |        |                |        |                                |        |
| 50% RH      | 0.674                | 0.589          | 0.522          | 0.360          | 0.300          | 0.426  | 0.430          | 0.690  | 0.593  | 0.375          | 0.774  | 0.456                          | 0.641  |
| 65% RH      | 0.906                | 0.766          | 0.680          | 0.455          | 0.377          | 0.541  | 0.557          | 0.903  | 0.761  | 0.464          | 1.042  | 0.586                          | 0.855  |
| 90% RH      | 1.427                | 1.164          | 0.986          | 0.673          | 0.502          | 0.795  | 0.876          | 1.385  | 1.089  | 0.695          | 1.636  | 0.858                          | 1.289  |
| VPS         | 1.634                | 1.343          | 1.266          | 0.785          | 0.681          | 0.948  | 1.019          | 1.711  | 1.223  | 0.836          | 1.778  | 0.964                          | 1.525  |
| OD2         | -0.047               | 0.049          | 0.101          | -0.012         | 0.090          | -0.045 | 0.013          | 0.311  | -0.123 | 0.013          | -0.084 | 0.081                          | 0.087  |

<sup>a</sup>VPS, vacuum pressure soak; OD2, second ovdndry; LA, low alignment; HA, high alignment; Pa, parallel; Pe, perpendicular.

where MOE-R is the ratio of MOE-Pa to MOE-Pe, SVR is the ratio of sonic velocity Pa to sonic velocity Pe, and  $\beta$ ,  $\rho$ , and  $\delta$  are constants varying with furnish type.

From (Kolsky 1963)

$$MOE = SG(V^2) \tag{9}$$

where  $V$  is the sonic velocity measured in the same direction as the modulus. Theoretically, then, the MOE-R is equal to the square of the SVR, ( $\delta = 2$ ) and the ratio of MOE-Pa/MOE-Random is equal to the square root of the MOE-R, ( $\rho = 0.5$ ). This implies that  $\beta$  is equal to 1 since  $\beta = (\rho) \times (\delta)$ .

In reality, the exponents vary somewhat with the furnish type (Table 18). The constants  $\delta$  and  $\rho$  averaged 1.9795 and 0.4256, respectively, for all boards.

A variation of Equation (7) useful in predicting bending properties of aligned boards (Geimer 1979) is

$$\text{Strength or stiffness} = e^\mu SG^\alpha SVR^{\pm\beta} \tag{10}$$

where  $SG$  is specific gravity, and  $\mu$ ,  $\alpha$ , and  $\beta$  are constants varying with furnish type.

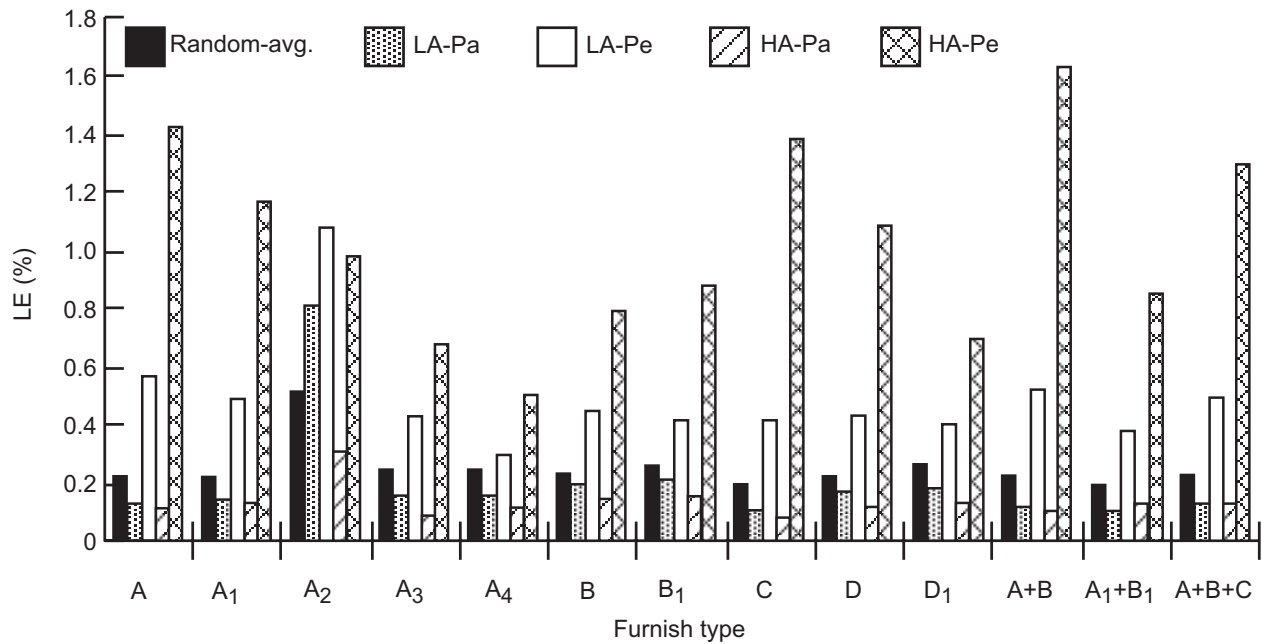


**Figure 27—Linear expansion (LE) at 90% RH by furnish type and alignment direction (LA, low alignment; HA, high alignment; Pa, parallel; Pe, perpendicular).**

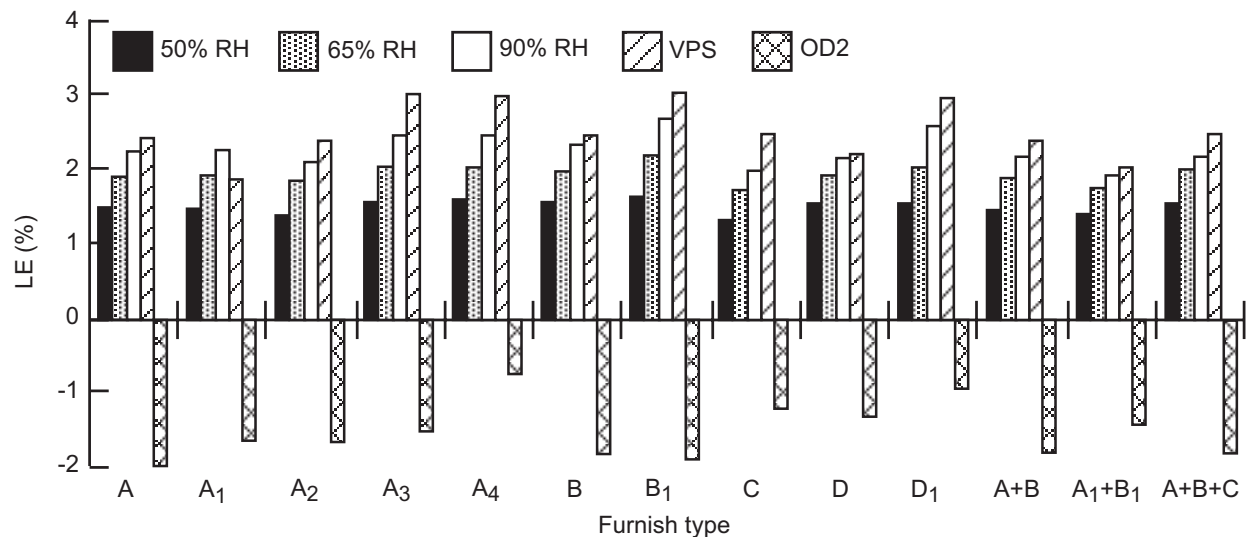


**Figure 28—Linear expansion (LE) of random boards at five exposure levels (VPS, vacuum pressure soak; OD2, second ovdry).**

Since SVR equals 1 in a random board, MOE in a random board is equal to  $\epsilon^{\mu} SG^{\alpha}$ . Changing the sign of  $\beta$  permits us to reinforce prediction precision by using the Pa and Pe data in the same equation. This equation can also be used to estimate bending MOR if the proper constants are defined. As with the relation between MOE and MOR (Fig. 21), there is an excellent correlation between MOR-R and MOE-R (Fig. 29).

The following regression equation has an  $r^2 = 0.90$ :

$$\text{MOR-R} = 0.6285 (\text{MOE-R}) + 0.552 \quad (11)$$

The constants  $\beta$ ,  $\rho$ , and  $\delta$  used to describe MOR relations are given in Table 19.

**Table 18—Exponential values  $\rho$ ,  $\beta$ , and  $\delta$  by furnish type for Equations 6, 7, and 8<sup>a</sup> using MOE data**

| Equation  | Exponent and coefficient    | Value of exponent and coefficient by furnish type |                 |                 |                 |                 |                 |                 |                 |                 |                 |                 |                                |                 |                 |
|---|-----------------------------|---|-----------------|-----------------|-----------------|-----------------|-----------------|-----------------|-----------------|-----------------|-----------------|-----------------|--------------------------------|-----------------|-----------------|
|   |                             | A   | A <sub>1</sub>  | A <sub>2</sub>  | A <sub>3</sub>  | A <sub>4</sub>  | B               | B <sub>1</sub>  | C               | D               | D <sub>1</sub>  | A+B             | A <sub>1</sub> +B <sub>1</sub> | A+B+C           | All             |
| Eq. (6) (MOE Pa)/<br>MOE random<br>= MOE-R <sup>p</sup> | Rho ( $\rho$ )<br>$r^2$     | 0.4148<br>0.977                                   | 0.4242<br>0.994 | 0.4031<br>0.984 | 0.4788<br>0.991 | 0.4785<br>0.959 | 0.3653<br>0.989 | 0.4168<br>0.989 | 0.4479<br>0.998 | 0.4878<br>0.985 | 0.4553<br>0.967 | 0.4071<br>0.987 | 0.4228<br>0.997                | 0.4197<br>0.987 | 0.4256<br>0.982 |
| Eq. (7) (MOE Pa)/<br>MOE random =<br>SVR <sup>b</sup>   | Beta ( $\beta$ )<br>$r^2$   | 0.9011<br>0.977                                   | 0.8606<br>0.991 | 0.7891<br>0.972 | 0.9341<br>0.997 | 0.8550<br>0.932 | 0.7615<br>0.985 | 0.7341<br>0.970 | 0.8815<br>0.993 | 0.9026<br>0.975 | 0.9055<br>0.960 | 0.7665<br>0.979 | 0.8792<br>0.993                | 0.8348<br>0.974 | 0.8436<br>0.975 |
| Eq. (8) MOE-R =<br>SVR <sup>b</sup>                     | Delta ( $\delta$ )<br>$r^2$ | 2.1645<br>0.993                                   | 2.0292<br>0.998 | 1.9577<br>0.988 | 1.9373<br>0.992 | 1.8038<br>0.990 | 2.0802<br>0.992 | 1.6790<br>0.988 | 1.9692<br>0.997 | 1.8550<br>0.994 | 1.9891<br>0.993 | 1.8875<br>0.996 | 2.0745<br>0.992                | 1.9952<br>0.993 | 1.9795<br>0.990 |

<sup>a</sup>Individual MOE parallel (Pa) values and the average MOE random value were used with each furnish type; SVR, sonic velocity ratio; MOE-R, modulus of elasticity ratios.

## Predicting Board Properties Using Flake Characteristics

Normally at this stage, plots of properties versus potential predictors are made to determine what predictors are useful in a regression. For example, the MOE for LA-Pa boards (Table 11) can be plotted against the area-weighted LC median (Table 4) for each furnish (Fig. 30). Although we did look at many of these plots, the large number of flake characteristics, weighting schemes, percentiles, alignments, and board properties made the use of this method very cumbersome. In addition, even though two different variables may be highly correlated to the property in question, the very nature of multiple regression restricts the usefulness of the second variable if the property predicting information in the second variable is already supplied by the first variable. For these reasons, we used a stepwise regression program available in SAS software (SAS Institute, Cary, NC) (SAS 1990) to determine the relative effectiveness of various independent variables in predicting a property.

In Equation (7), we can see that bending MOE is dependent on the MOE property of a random board and the ability to align flakes. We have also seen that the MOE of a random board (Eq. (10) with the SVR term omitted) is dependent on board SG. Furthermore, the data presented herein show that flake furnish does affect both the bending properties of the random board and the ability to achieve alignment. This suggests that we should incorporate an additional term or terms that reflect these relationships into the prediction equation.

This general form of the model, as in Equation (10), was input along with the variable terms that were to be analyzed. Using natural logs of the strength or stiffness properties converts the equation into a linear model. Each independent variable was examined, and the program determined which one improved prediction the most when added to the

equation. This procedure was continued with the remaining variables until improvement in predicting precision did not justify adding terms. The terms included averages of LC, width, area, perimeter, and aspect ratio; the 25th, 50th, 75th, 90th, and 95th percentiles for LC, width, area, perimeter, and aspect ratio; and the area-weighted 25th, 50th, 75th, 90th, and 95th percentiles for LC, width, area, perimeter, and aspect ratio for all furnish types. In addition, all of the above values were available in the natural log and squared formats. Sonic velocity ratio, angular alignment percentages, SG, and thickness were also input in both the normal and natural log formats. Both normal and logarithmic forms of MOE were predicted.

### Predicting Modulus of Elasticity

Equation (10) was used as the general format for predicting MOE. Since the relationship between flake characteristics and alignment depends to a high degree on the type of alignment equipment used, the use of SVR permits analysis of the data in a general fashion. The specific relationships between flake characteristics and SVR are dealt with later.

Equation (10) is readily analyzed when the terms are converted to logarithms. Exploratory analysis showed the equation to be superior to regressions that used linear or combinations of logarithmic and linear formats. Using the reciprocal of the SVR for the perpendicular values permits the inclusion of both Pa and Pe data in the same equation and strengthens the analysis (Fig. 31). Because, as mentioned previously, a good correlation between SG and board MOE could not be obtained, we elected to omit SG in our preliminary analysis. The  $r^2$  values for selected regression equations using flake characterization cumulative distribution values (and combinations thereof), by themselves and with SVR, to predict flakeboard MOE are given in Table 20. In all cases, the cumulative distribution values referred to in Table 20 are weighted by area. Both dependent and independent variables were in the logarithmic format.

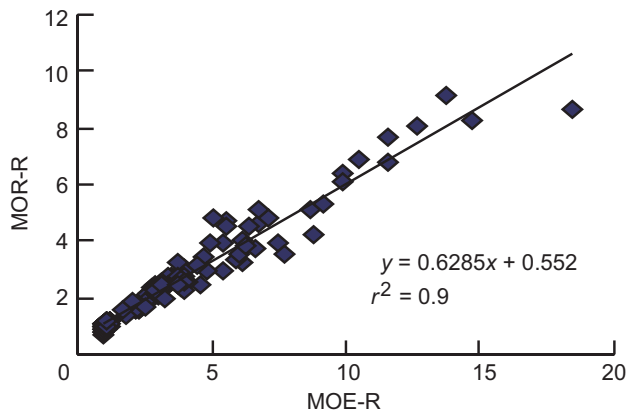


Figure 29—Correlation of MOR ratios (MOR-R) to MOE ratios (MOE-R).

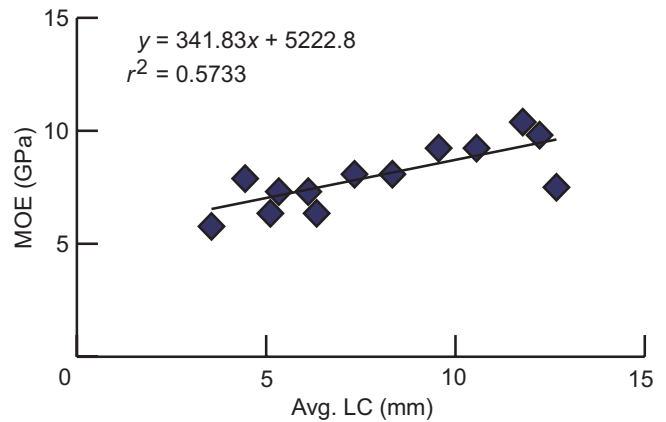


Figure 30—Relationship between average MOE and the weighted long chord (LC) median (values are from the LA-Pa data for each furnish type).

Table 19—Exponential values  $\rho$ ,  $\beta$ , and  $\delta$  by furnish type for Equations 6, 7, and 8<sup>a</sup> using MOR data

| Equation  | Exponent and coefficient    | Value of exponent and coefficient by furnish type |                 |                 |                 |                 |                 |                 |                 |                 |                 |                 |                                |                 |                 |
|---|-----------------------------|---|-----------------|-----------------|-----------------|-----------------|-----------------|-----------------|-----------------|-----------------|-----------------|-----------------|--------------------------------|-----------------|-----------------|
|   |                             | A   | A <sub>1</sub>  | A <sub>2</sub>  | A <sub>3</sub>  | A <sub>4</sub>  | B               | B <sub>1</sub>  | C               | D               | D <sub>1</sub>  | A+B             | A <sub>1</sub> +B <sub>1</sub> | A+B+C           | All             |
| Eq. (6) (MOR Pa)/<br>MOR random =<br>MOR-R <sup>p</sup> | Rho ( $\rho$ )<br>$r^2$     | 0.3680<br>0.930                                   | 0.4350<br>0.981 | 0.3109<br>0.916 | 0.4176<br>0.981 | 0.4305<br>0.906 | 0.2956<br>0.919 | 0.3558<br>0.940 | 0.4421<br>0.993 | 0.6265<br>0.967 | 0.4617<br>0.919 | 0.3992<br>0.970 | 0.4221<br>0.985                | 0.3974<br>0.961 | 0.4103<br>0.928 |
| Eq. (7) (MOR Pa)/<br>MOR random =<br>SVR <sup>b</sup>   | Beta ( $\beta$ )<br>$r^2$   | 0.6107<br>0.858                                   | 0.6816<br>0.967 | 0.4407<br>0.865 | 0.5343<br>0.979 | 0.5414<br>0.850 | 0.4254<br>0.838 | 0.4085<br>0.862 | 0.7117<br>0.990 | 0.9555<br>0.958 | 0.7044<br>0.892 | 0.5275<br>0.940 | 0.6702<br>0.974                | 0.6207<br>0.924 | 0.6096<br>0.884 |
| Eq. (8) MOR-R =<br>SVR <sup>b</sup>                     | Delta ( $\delta$ )<br>$r^2$ | 1.6990<br>0.967                                   | 1.5703<br>0.990 | 1.4337<br>0.967 | 1.2706<br>0.985 | 1.2669<br>0.952 | 1.4558<br>0.932 | 1.1796<br>0.968 | 1.6090<br>0.996 | 1.5251<br>0.990 | 0.990<br>0.972  | 1.3361<br>0.990 | 1.5774<br>0.976                | 1.5821<br>0.986 | 1.4977<br>0.968 |

<sup>a</sup>Pa, parallel; SVR, sonic velocity ratio; MOR-R, modulus of rigidity ratios.

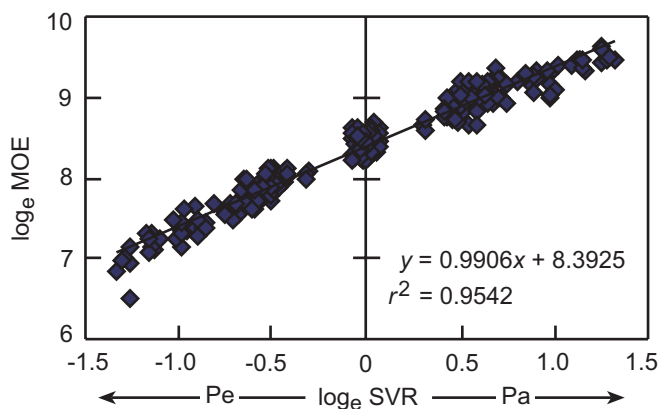


Figure 31—Strengthened predictions of MOE from sonic velocity ratios (SVR) because of combined parallel (Pa) and perpendicular (Pe) values.

Basic prediction accuracy using only SVR to predict the MOE of the combined Pa and Pe data was represented by  $r^2 = 0.95$ . This very good precision is attributed to large changes in MOE in direct response to flake alignment. Very limited predictive capabilities are observed when the flake characterization data is used by itself to predict MOE of the combined data. This is because we are trying to simultaneously predict increases in MOE-Pa and decreases in MOE-Pe in addition to both HA and LA levels of MOE with the same characteristic. However, the flake characteristic data becomes significant when we use them in conjunction with the SVR to describe the combined data. In this case, the SVR accounts for the differences due to degree and direction of alignment, and the flake characteristic data is only concerned with the residuals. Despite its significance, little improvement in the prediction of the combined data is obtained by including flake characterization with SVR data since the SVR is such a dominant factor.

**Table 20— $r^2$  values for MOE predictive equations<sup>a</sup>**

| Variable <sup>b</sup>    | $r^2$   |                        |                       |                        |                       |                        |                       |                        |                       |                        |                       |                        | Residual percentile |
|--------------------------|---|------------------------|-----------------------|------------------------|-----------------------|------------------------|-----------------------|------------------------|-----------------------|------------------------|-----------------------|------------------------|---------------------|
|                          | log <sub>e</sub> MOE = log <sub>e</sub> SVR + log <sub>e</sub> (variable) |                        |                       |                        |                       |                        |                       |                        |                       |                        |                       |                        |                     |
|                          | Combined data   |                        | Random                |                        | LA-Pa                 |                        | HA-Pa                 |                        | LA-Pe                 |                        | Ha-Pe                 |                        |                     |
|                          | Vari-<br>able<br>only   | SVR +<br>vari-<br>able | Vari-<br>able<br>only | SVR +<br>vari-<br>able | Vari-<br>able<br>only | SVR +<br>vari-<br>able | Vari-<br>able<br>only | SVR +<br>vari-<br>able | Vari-<br>able<br>only | SVR +<br>vari-<br>able | Vari-<br>able<br>only | SVR +<br>vari-<br>able |                     |
| SVR                      | —   | 0.95                   | —                     | 0.04                   | —                     | 0.62                   | —                     | 0.76                   | —                     | 0.41                   | —                     | 0.73                   | —                   |
| 25% LC                   | 0.002   | 0.96                   | 0.21                  | 0.24                   | 0.54                  | 0.63                   | 0.79                  | 0.83                   | 0.38                  | 0.43                   | 0.48                  | 0.74                   | 0.046               |
| 50% LC                   | 0.003   | 0.96                   | 0.19                  | 0.23                   | 0.57                  | 0.66                   | 0.80                  | 0.84                   | 0.22                  | 0.42                   | 0.47                  | 0.74                   | 0.056               |
| 75% LC                   | 0.004   | 0.96                   | 0.24                  | 0.28                   | 0.66                  | 0.70                   | 0.79                  | 0.85                   | 0.12                  | 0.54                   | 0.41                  | 0.74                   | 0.083               |
| 90% LC                   | 0.002   | 0.96                   | 0.09                  | 0.13                   | 0.41                  | 0.66                   | 0.44                  | 0.80                   | 0.03                  | 0.51                   | 0.23                  | 0.73                   | 0.044               |
| 25% width                | 0.007   | 0.96                   | 0.52                  | 0.56                   | 0.47                  | 0.68                   | 0.39                  | 0.82                   | 0.09                  | 0.43                   | 0.07                  | 0.75                   | 0.147               |
| 50% width                | 0.009   | 0.96                   | 0.64                  | 0.67                   | 0.59                  | 0.74                   | 0.47                  | 0.84                   | 0.03                  | 0.49                   | 0.08                  | 0.75                   | 0.206               |
| 75% width                | 0.011   | 0.97                   | 0.63                  | 0.67                   | 0.52                  | 0.75                   | 0.38                  | 0.85                   | 0.00                  | 0.54                   | 0.03                  | 0.76                   | 0.235               |
| 90% width                | 0.010   | 0.96                   | 0.53                  | 0.57                   | 0.36                  | 0.74                   | 0.22                  | 0.84                   | 0.02                  | 0.57                   | 0.00                  | 0.76                   | 0.225               |
| 25% area                 | 0.006   | 0.96                   | 0.47                  | 0.51                   | 0.63                  | 0.69                   | 0.70                  | 0.85                   | 0.23                  | 0.42                   | 0.27                  | 0.75                   | 0.125               |
| 50% area                 | 0.007   | 0.96                   | 0.53                  | 0.57                   | 0.72                  | 0.75                   | 0.76                  | 0.88                   | 0.16                  | 0.46                   | 0.27                  | 0.75                   | 0.159               |
| 75% area                 | 0.010   | 0.96                   | 0.59                  | 0.63                   | 0.74                  | 0.78                   | 0.68                  | 0.88                   | 0.05                  | 0.57                   | 0.17                  | 0.76                   | 0.201               |
| 90% area                 | 0.010   | 0.96                   | 0.54                  | 0.58                   | 0.65                  | 0.78                   | 0.52                  | 0.86                   | 0.00                  | 0.62                   | 0.09                  | 0.75                   | 0.221               |
| 25% perimeter            | 0.003   | 0.96                   | 0.27                  | 0.31                   | 0.58                  | 0.64                   | 0.81                  | 0.85                   | 0.34                  | 0.42                   | 0.44                  | 0.75                   | 0.066               |
| 50% perimeter            | 0.004   | 0.96                   | 0.26                  | 0.30                   | 0.63                  | 0.68                   | 0.84                  | 0.87                   | 0.22                  | 0.43                   | 0.44                  | 0.74                   | 0.079               |
| 75% perimeter            | 0.006   | 0.96                   | 0.33                  | 0.37                   | 0.73                  | 0.74                   | 0.82                  | 0.88                   | 0.10                  | 0.59                   | 0.35                  | 0.75                   | 0.121               |
| 90% perimeter            | 0.005   | 0.96                   | 0.19                  | 0.23                   | 0.54                  | 0.71                   | 0.53                  | 0.83                   | 0.01                  | 0.59                   | 0.18                  | 0.73                   | 0.098               |
| 25% aspect               | 0.004   | 0.96                   | 0.17                  | 0.21                   | 0.00                  | 0.69                   | 0.05                  | 0.77                   | 0.22                  | 0.51                   | 0.22                  | 0.75                   | 0.080               |
| 50% aspect               | 0.004   | 0.96                   | 0.25                  | 0.29                   | 0.01                  | 0.67                   | 0.02                  | 0.79                   | 0.10                  | 0.47                   | 0.17                  | 0.75                   | 0.090               |
| 75% aspect               | 0.002   | 0.96                   | 0.15                  | 0.19                   | 0.00                  | 0.64                   | 0.02                  | 0.79                   | 0.03                  | 0.42                   | 0.15                  | 0.74                   | 0.050               |
| 90% aspect               | 0.002   | 0.96                   | 0.17                  | 0.21                   | 0.00                  | 0.63                   | 0.01                  | 0.79                   | 0.01                  | 0.42                   | 0.13                  | 0.74                   | 0.050               |
| 25%,50%,75% LC           | 0.004   | 0.96                   | 0.28                  | 0.32                   | 0.71                  | 0.71                   | 0.92                  | 0.92                   | 0.41                  | 0.55                   | 0.52                  | 0.75                   | 0.085               |
| 25%,50%,75% width        | 0.011   | 0.97                   | 0.65                  | 0.69                   | 0.59                  | 0.76                   | 0.48                  | 0.85                   | 0.29                  | 0.58                   | 0.20                  | 0.76                   | 0.237               |
| 25%,50%,75% area         | 0.011   | 0.97                   | 0.62                  | 0.66                   | 0.75                  | 0.78                   | 0.76                  | 0.88                   | 0.41                  | 0.66                   | 0.36                  | 0.77                   | 0.235               |
| 25%,50%,75%<br>perimeter | 0.006   | 0.96                   | 0.37                  | 0.41                   | 0.77                  | 0.77                   | 0.93                  | 0.93                   | 0.38                  | 0.61                   | 0.46                  | 0.76                   | 0.128               |
| 25%,50%,75% aspect       | 0.006   | 0.96                   | 0.45                  | 0.49                   | 0.43                  | 0.69                   | 0.54                  | 0.79                   | 0.48                  | 0.54                   | 0.52                  | 0.75                   | 0.130               |
| Average LC               | 0.003   | 0.96                   | 0.26                  | 0.29                   | 0.72                  | 0.72                   | 0.92                  | 0.92                   | 0.26                  | 0.46                   | 0.52                  | 0.74                   | 0.080               |
| Average width            | 0.010   | 0.96                   | 0.65                  | 0.69                   | 0.53                  | 0.73                   | 0.41                  | 0.85                   | 0.02                  | 0.50                   | 0.04                  | 0.76                   | 0.220               |
| Average area             | 0.009   | 0.96                   | 0.60                  | 0.63                   | 0.75                  | 0.78                   | 0.72                  | 0.89                   | 0.09                  | 0.52                   | 0.20                  | 0.75                   | 0.200               |
| Average perimeter        | 0.005   | 0.96                   | 0.35                  | 0.38                   | 0.77                  | 0.77                   | 0.92                  | 0.93                   | 0.21                  | 0.50                   | 0.44                  | 0.75                   | 0.110               |

<sup>a</sup> SVR, sonic velocity ratio; LA, low alignment; HA, high alignment; Pa, parallel; Pe, perpendicular; LC, long chord.

<sup>b</sup> All variables weighted by area.

Separating the data by alignment and test direction variables allows us to directly observe the effect of the flake characterization data. The SVR values were of course little help in predicting MOE of the random boards. Surprisingly, flake width was the best prediction variable for random boards. This implies, since the correlation was positive, that increased stiffness, in most cases, results from distribution of flake to flake stresses across a wider area rather than from

improvement in the packing arrangement. The area data also showed very good potential for the prediction of random board bending properties. Area percentiles also showed good accuracy in prediction of both the HA-Pa and LA-Pa boards. The best predictors of MOE in aligned boards were LC and perimeter. These flake characteristics are, of course, related to the relative ease in aligning long flakes.

Cumulative distribution aspect ratios showed very poor predictive capability. This is because the aspect ratio changes very little with flake length; that is, flake width generally decreases as flake length decreases. Weighting the aspect percentiles by area does not accomplish much, since a long, wide flake may have the same aspect ratio as a short, narrow flake, and on average, the same number of flakes would be contained in each percentile.

Accuracy of prediction was less for LA boards than for HA boards and less for MOE-Pe than for MOE-Pa. When used to predict MOE-Pe, single descriptors all produced a negative coefficient. Predictions were not markedly improved by the addition of three or more percentiles of the same flake descriptor. Multiple descriptors could prove to be more useful in situations where small changes are made in a common flake furnish or the furnish is changed by the addition of a batch of geometrically uniform flakes.

In many cases, the flake descriptor average was a good predictor. The influence of average flake thickness was not readily or consistently apparent. This is probably due to the limited fluctuation of this variable in our study and its effect being masked by the other variables under consideration. In general, the best results were obtained with mid-range cumulative distribution values. This is of course because the curves are usually more dispersed in this area.

Another method used to determine the best flake characterization term to add to the model was to regress the residuals developed in predictions made using only the SVR. The  $r^2$  values are shown in Table 20 for selected variables. The  $r^2$  values in this case pertain only to the 4% variation not explained by SVR. The results are in agreement with the previous conclusions. Width is the best predictor followed closely by area. This is reasonable considering that length and perimeter have been shown to have a very large influence on alignment and are therefore incorporated in the prediction equation through the SVR.

Because past work has indicated that length as well as width is important in achieving high quality bending properties and because of the contribution of area in predicting the bending properties in the aligned boards, we chose the area-weighted 75th area percentile as the most appropriate variable to use in our prediction equation:

$$MOE = e^{\mu} SG^{\alpha} SVR^{\pm\beta} (\text{area-weighted 75th \% Area})^{\gamma} \quad (12)$$

Values for the exponential terms of  $\mu$ ,  $\beta$ , and  $\gamma$  have been ascertained using the entire combined data (Table 21). As in Table 20, both dependent and independent variables are in the logarithmic format. Specific gravity was included in the regression equation determining the exponents. One must remember that even though the area-weighted 75th area percentile term is highly significant, it does not contribute much to the prediction of the aligned boards because of the

**Table 21—Exponential values for predictive equations**

| <sup>a</sup> (Eq. (12)) MOE = e <sup>μ</sup> SG <sup>α</sup> SVR <sup>±β</sup> (area-weighted 75th % area) <sup>γ</sup>                                       |                   |       |                |       |                |
|---|-------------------|-------|----------------|-------|----------------|
|   | μ                 | α     | β              | γ     | r <sup>2</sup> |
| Combined  | 8.603             | 1.529 | 1.015          | 0.071 | 0.97           |
| Random  | 8.179             | 1.015 | —              | 0.117 | 0.65           |
| <sup>b</sup> (Eq. (13)) SVR = e <sup>μ<sub>2</sub></sup> (area-weighted 25th % LC) <sup>δ</sup>   |                   |       |                |       |                |
|   | μ <sub>2</sub>    | δ     | r <sup>2</sup> |       |                |
| HA <sup>b</sup>   | -0.309            | 0.360 | 0.75           |       |                |
| LA <sup>b</sup>   | -0.079            | 0.172 | 0.76           |       |                |
| <sup>c</sup> (Eq. (14)) MOE = e <sup>μ±βμ<sub>2</sub></sup> SG <sup>α</sup> (area-weighted 25th % LC) <sup>±βδ</sup> (area-weighted 75th % area) <sup>γ</sup> |                   |       |                |       |                |
|   | μ+βμ <sub>2</sub> | α     | βδ             | γ     | r <sup>2</sup> |
| HA  | 8.290             | 1.529 | 0.366          | 0.071 | 0.87           |
| LA  | 8.523             | 1.529 | 0.175          | 0.071 | 0.85           |

<sup>a</sup>Both dependent and independent variables are in the logarithmic format.  
<sup>b</sup>HA, high alignment; LA, low alignment.  
<sup>c</sup>Exponential variables defined by combining Equations (12) and (13). Value for e exponent for Pa (+) data.

very strong influence of the SVR term. If the SVR is omitted in the regression, the area-weighted 75th area percentile accounts for approximately 65% of the variation in the MOE of random boards. Exponents  $\mu$  and  $\gamma$  are given for the random board data in Table 21.

**Predicting Sonic Velocity Ratio**

The relative importance of flake characteristics in predicting SVR is shown in Table 22. As indicated in our previous discussion, LC and perimeter are the geometric variables most closely associated with alignment. This relationship is of course dependent on the type of alignment machine and the operating circumstances. It is conceivable that the positive correlation of flake length to alignment could be altered in electrostatic, pneumatic, or other alignment devices and that the influence of length is reduced as the aspect ratio approaches one. In our study, the entire difference between HA and LA levels resulted from a 64-cm decrease in free-fall difference. Interestingly, the same relative ordering between LA and HA levels was maintained for all the furnish types (Fig. 32).

As was the case in predicting MOE, accuracy does not substantially improve with the addition of cumulative distribution values of the same characteristic such as the 25th, 50th, and 75th LC. In these circumstances, one of the terms is quite often negative to counteract overprediction by the other two variables. Average values by themselves proved to be relatively useful in predicting SVR. Our choice for the best all around predictor of SVR was the 25th percentile of LC.

**Table 22— $r^2$  values for sonic velocity ratio (SVR) predictive equations<sup>a</sup>**

| Variable <sup>b</sup> | $r^2$  |       |
|-----------------------|--|-------|
|                       | $\log_e \text{SVR} = \log_e (\text{variable})$ |       |
|                       | LA-Pa  | HA-Pa |
| 25% LC                | 0.76   | 0.75  |
| 50% LC                | 0.66   | 0.74  |
| 75% LC                | 0.71   | 0.66  |
| 90% LC                | 0.39   | 0.32  |
| 25% width             | 0.38   | 0.21  |
| 50% width             | 0.39   | 0.24  |
| 75% width             | 0.27   | 0.15  |
| 90% width             | 0.13   | 0.05  |
| 25% area              | 0.67   | 0.53  |
| 50% area              | 0.66   | 0.53  |
| 75% area              | 0.57   | 0.41  |
| 90% area              | 0.39   | 0.26  |
| 25% perimeter         | 0.76   | 0.73  |
| 50% perimeter         | 0.71   | 0.73  |
| 75% perimeter         | 0.71   | 0.63  |
| 90% perimeter         | 0.41   | 0.33  |
| 25% aspect            | 0.07   | 0.15  |
| 50% aspect            | 0.02   | 0.11  |
| 75% aspect            | 0.02   | 0.13  |
| 90% aspect            | 0.01   | 0.10  |
| 25%,50%,75% LC        | 0.89   | 0.83  |
| 25%,50%,75% width     | 0.45   | 0.34  |
| 25%,50%,75% area      | 0.68   | 0.56  |
| 25%,50%,75% perimeter | 0.86   | 0.78  |
| 25%,50%,75% aspect    | 0.68   | 0.66  |
| Average LC            | 0.85   | 0.82  |
| Average width         | 0.33   | 0.18  |
| Average area          | 0.62   | 0.45  |
| Average perimeter     | 0.82   | 0.76  |

<sup>a</sup>LA, low alignment; HA, high alignment; Pa, parallel; LC, long chord.

<sup>b</sup>All variables weighted by area.

The equation

$$\text{SVR} = e^{\mu_2} (\text{area-weighted 25th \% LC})^{\delta} \quad (13)$$

describes our HA data with an  $r^2 = 0.75$ , when  $\mu_2 = -0.309$  and  $\delta = 0.360$ , and our LA data with an  $r^2 = 0.76$ , when  $\mu_2 = -0.079$  and  $\delta = 0.172$  (Table 21). Since furnish characteristics cannot be used to describe the effort made in achieving alignment, different coefficients are needed to describe the relationship between SVR and flake characteristics for each type (HA, MA, and LA) of alignment. Prediction of SVR for both HA and LA are compared with measured values in Table 23.

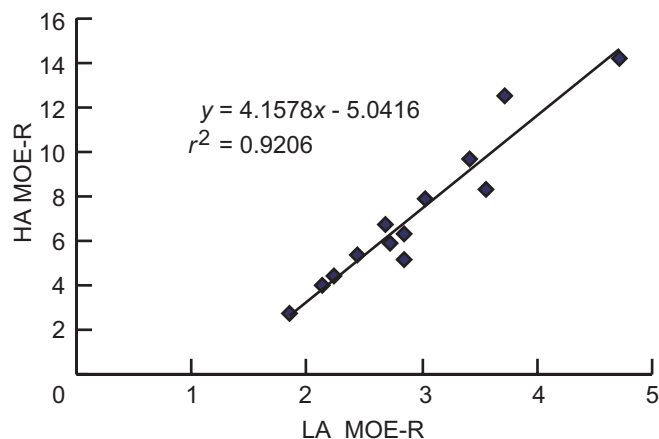


**Figure 32—High alignment (HA) MOE ratios (MOE-R) compared with low alignment (LA) MOE-R.**

Substituting Equation (13) into Equation (12), we have

$$\text{MOE} = e^{\mu \pm \beta \mu_2} \text{SG}^{\alpha} (\text{area-weighted 25th \% LC})^{\pm \beta \delta} \times (\text{area-weighted 75th \% Area})^{\gamma} \quad (14)$$

If the various exponents are known, it is then possible to predict the changes of MOE with changes in furnish characteristic. Values of  $\mu \pm \beta \mu_2$ ,  $\pm \beta \delta$ , and  $\gamma$  for LA and HA in Equation (14) have been derived by combining exponents obtained in Equations (12) and (13) (Table 21). Keep in mind that Equation (12) used the combined data and Equation (13) used subsets of the data.

In Table 24, predicted MOE is compared with measured MOE for random, LA, and HA boards. The predicted values for random boards were derived using combined data exponents in Table 21 and setting the SVR to 1 in Equation (12). Predicted values for aligned boards were derived using the exponents for Equation (14) shown in Table 21. Remember that a negative  $\beta$  is used in predicting Pe values.

Prediction errors for SVR and MOE-Pa are shown as a percentage of measured values in Figures 33 and 34, respectively. Maximum error of 25% occurred in the prediction of type B furnish. In this case, the MOE prediction error can be attributed to overprediction of the SVR for furnish B. Prediction accuracy of HA and LA boards would increase, of course, had we used exponents from Equation (12) derived from the HA or LA boards, respectively. This would be the case in a commercial operation where alignment devices are usually maintained to provide a constant degree of flake alignment. Prediction values are also affected by the choice of format and the logarithmic or actual scale terms used in the equations. We elected to use the logarithmic format to be consistent with our analytical techniques.

**Table 23—Sonic velocity ratio (SVR) predictions by furnish type**

|                     | Furnish type |                |                |                |                |       |                |       |       |                |       |                                |       |
|---------------------|--------------|----------------|----------------|----------------|----------------|-------|----------------|-------|-------|----------------|-------|--------------------------------|-------|
|                     | A            | A <sub>1</sub> | A <sub>2</sub> | A <sub>3</sub> | A <sub>4</sub> | B     | B <sub>1</sub> | C     | D     | D <sub>1</sub> | A+B   | A <sub>1</sub> +B <sub>1</sub> | A+B+C |
| LA-Pa <sup>a</sup>  |              |                |                |                |                |       |                |       |       |                |       |                                |       |
| SVR                 | 1.985        | 1.739          | 1.660          | 1.548          | 1.369          | 1.648 | 1.609          | 1.911 | 1.657 | 1.520          | 1.901 | 1.706                          | 1.808 |
| Estimated SVR (log) | 1.937        | 1.732          | 1.575          | 1.505          | 1.430          | 1.733 | 1.690          | 1.933 | 1.795 | 1.524          | 1.740 | 1.699                          | 1.744 |
| HA-Pa <sup>a</sup>  |              |                |                |                |                |       |                |       |       |                |       |                                |       |
| SVR                 | 3.492        | 2.773          | 2.634          | 1.994          | 1.786          | 2.214 | 2.595          | 3.656 | 2.637 | 2.089          | 3.116 | 2.378                          | 3.139 |
| Estimated SVR (log) | 3.458        | 2.737          | 2.243          | 2.039          | 1.833          | 2.742 | 2.599          | 3.444 | 2.948 | 2.093          | 2.762 | 2.630                          | 2.777 |

<sup>a</sup>LA, low alignment; HA, high alignment; Pa, parallel.

**Table 24—Modulus of elasticity predictions in megapascals by furnish type<sup>a</sup>**

|                  | Furnish type |                |                |                |                |        |                |        |        |                |        |                                |        |
|------------------|--------------|----------------|----------------|----------------|----------------|--------|----------------|--------|--------|----------------|--------|--------------------------------|--------|
|                  | A            | A <sub>1</sub> | A <sub>2</sub> | A <sub>3</sub> | A <sub>4</sub> | B      | B <sub>1</sub> | C      | D      | D <sub>1</sub> | A+B    | A <sub>1</sub> +B <sub>1</sub> | A+B+C  |
| LA-Pa            |              |                |                |                |                |        |                |        |        |                |        |                                |        |
| Measured average | 10,423       | 8,171          | 7,217          | 6,297          | 5,723          | 7,447  | 6,435          | 7,941  | 9,170  | 7,240          | 9,779  | 8,033                          | 9,297  |
| Estimated        | 9,605        | 8,155          | 7,100          | 6,027          | 5,607          | 7,593  | 6,966          | 8,096  | 8,413  | 6,477          | 8,425  | 7,796                          | 8,289  |
| HA-Pa            |              |                |                |                |                |        |                |        |        |                |        |                                |        |
| Measured average | 14,043       | 11,457         | 9,538          | 7,791          | 6,125          | 9,917  | 8,274          | 13,009 | 11,515 | 8,354          | 12,193 | 10,664                         | 12,342 |
| Estimated        | 16,717       | 13,080         | 9,221          | 7,796          | 6,594          | 12,471 | 10,325         | 15,679 | 13,260 | 8,663          | 12,404 | 11,721                         | 12,933 |
| LA-Pe            |              |                |                |                |                |        |                |        |        |                |        |                                |        |
| Measured average | 2,195        | 2,689          | 2,701          | 2,953          | 3,103          | 2,609  | 2,643          | 2,137  | 3,356  | 3,252          | 2,747  | 2,804                          | 2,712  |
| Estimated        | 2,543        | 2,785          | 2,850          | 2,835          | 2,813          | 2,553  | 2,591          | 2,280  | 2,762  | 2,900          | 2,917  | 2,659                          | 2,897  |
| HA-Pe            |              |                |                |                |                |        |                |        |        |                |        |                                |        |
| Measured average | 1,000        | 1,448          | 1,425          | 1,931          | 2,206          | 1,908  | 1,563          | 1,034  | 1,977  | 1,885          | 1,471  | 1,701                          | 1,287  |
| Estimated        | 1,274        | 1,598          | 1,995          | 2,089          | 2,105          | 1,612  | 1,643          | 1,285  | 1,629  | 1,905          | 1,802  | 1,564                          | 1,742  |
| Random           |              |                |                |                |                |        |                |        |        |                |        |                                |        |
| Measured average | 4,884        | 4,867          | 4,551          | 4,126          | 3,936          | 5,315  | 4,235          | 4,258  | 5,120  | 4,505          | 5,395  | 4,987                          | 5,028  |
| Estimated        | 4,709        | 4,649          | 4,251          | 4,208          | 3,837          | 4,523  | 4,157          | 4,152  | 4,689  | 4,170          | 4,704  | 4,305                          | 4,633  |

<sup>a</sup>LA, low alignment; HA, high alignment; Pa, parallel; Pe, perpendicular.

### Predicting Shear Values

Analysis of data indicated that the same model used to predict MOE was also useful in predicting shear stress. This supports previous investigations (Geimer 1981). Prediction accuracy using selected independent variables is shown in Table 25. Since SG was highly related to shear strength, we included this along with SVR in our analysis. Shear strength like MOE was correlated with width and area. To be consistent, we picked the area-weighted 75th area percentile as an additional factor, which relates furnish type to board strength.

The equation

$$\text{Shear stress} = e^{\mu} \text{SG}^{\alpha} \text{SVR}^{\beta} (\text{area-weighted 75\% area})^{\gamma} \quad (15)$$

fits our data with an  $r^2 = 0.39$  when  $\mu = 5.93$ ,  $\alpha = 0.736$ ,  $\beta = 0.203$ , and  $\gamma = 0.111$ . Thickness when added to the equation showed a positive correlation to shear strength and was highly significant. We elected to omit this characteristic because we felt both the data and the improvement made in prediction accuracy were limited.

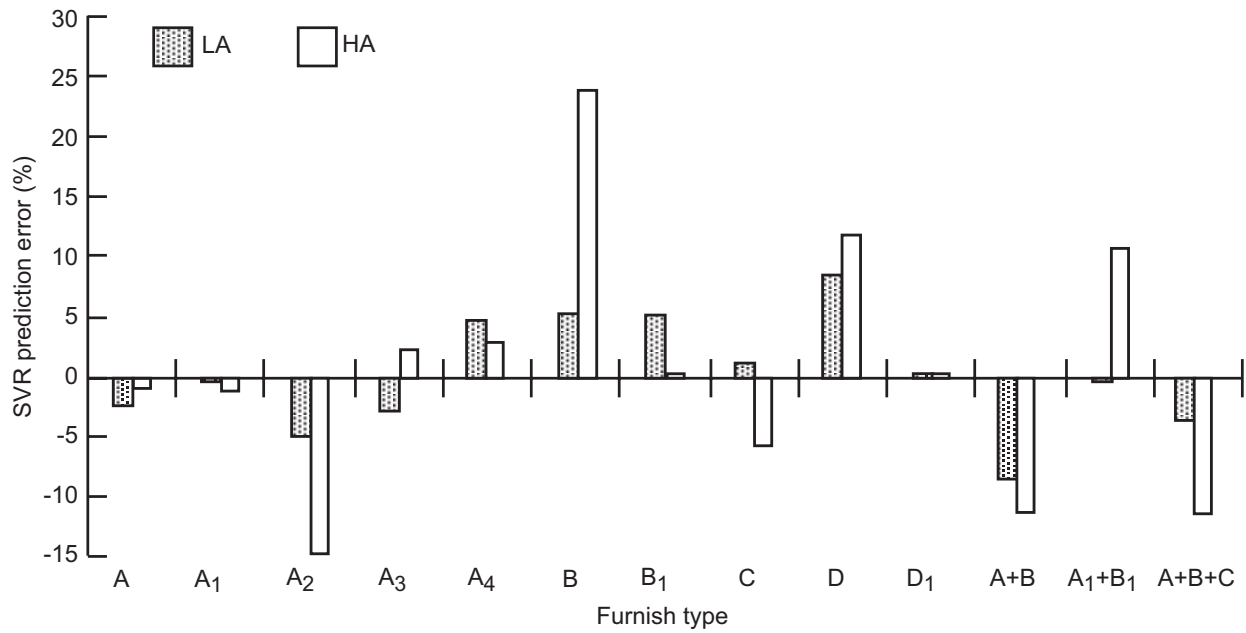


**Figure 33—Prediction error for sonic velocity ratios (SVR) (percentages are based on measured values; LA, low alignment; HA, high alignment).**

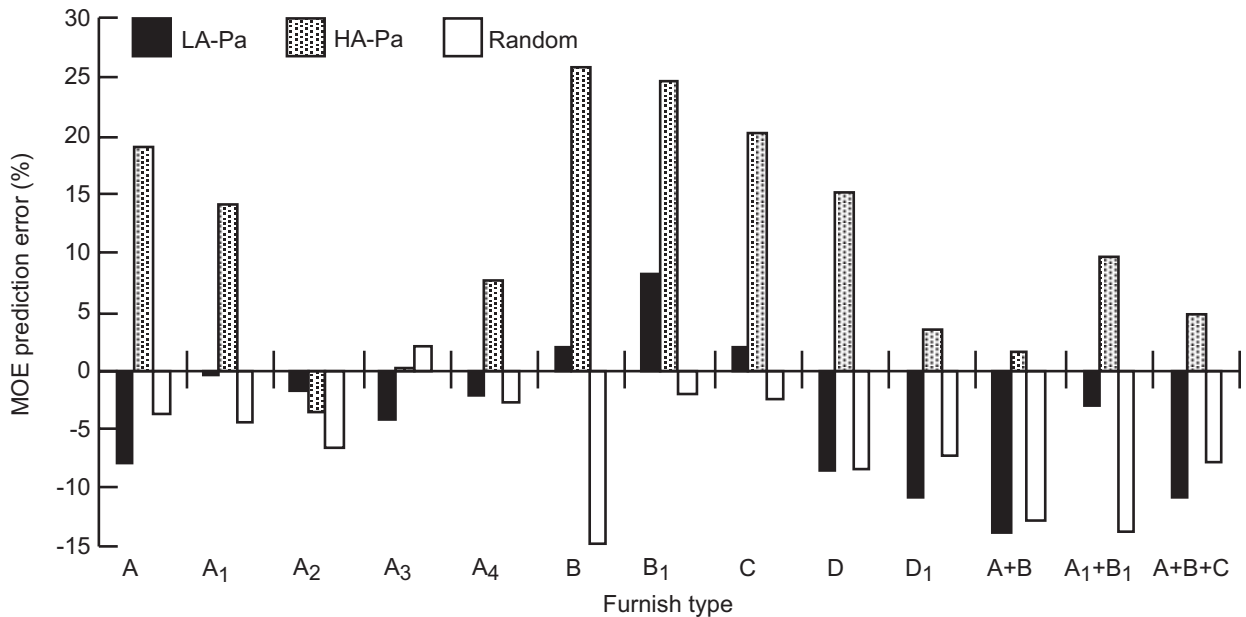


**Figure 34—Prediction error for MOE (percentages are based on measured values; LA, low alignment; HA, high alignment; Pa, parallel).**

### Predicting Dimensional Stability

**Water Adsorption**—Water adsorption predictions were quite poor especially at the lower RH exposures. The (area-weighted) width percentiles were the most significant. This is probably because the width percentiles vary considerably between furnish types. At 90% RH, specific gravity was the single most important factor and predicted WA:

$$WA = \mu + \alpha(SG) \tag{16}$$

with  $r^2 = 0.09$ . Addition of the natural log of average width increased prediction to  $r^2 = 0.13$ .

**Table 25— $r^2$  values for shear predictive equations<sup>a</sup>**

| Variable <sup>b</sup> | $r^2$<br>$\log_e \text{ shear} = \log_e \text{ SG} + \log_e \text{ SVR} + \log_e (\text{variable})$ |                        |                                  |                              |                              | Residual variable |
|-----------------------|---|------------------------|----------------------------------|------------------------------|------------------------------|-------------------|
|                       | Combined data   |                        | Random<br>SG, SVR, +<br>variable | LA<br>SG, SVR, +<br>variable | HA<br>SG, SVR, +<br>variable |                   |
|                       | Variable<br>only  | SG, SVR, +<br>variable |                                  |                              |                              |                   |
| SVR                   | —   | 0.29                   | 0.02                             | 0.36                         | 0.18                         | —                 |
| 25% LC                | 0.10  | 0.30                   | 0.12                             | 0.36                         | 0.18                         | 0.05              |
| 50% LC                | 0.14  | 0.32                   | 0.13                             | 0.40                         | 0.24                         | 0.09              |
| 75% LC                | 0.14  | 0.33                   | 0.09                             | 0.43                         | 0.26                         | 0.10              |
| 90% LC                | 0.06  | 0.30                   | 0.03                             | 0.37                         | 0.21                         | 0.04              |
| 25% width             | 0.16  | 0.36                   | 0.19                             | 0.47                         | 0.21                         | 0.14              |
| 50% width             | 0.24  | 0.41                   | 0.25                             | 0.63                         | 0.23                         | 0.23              |
| 75% width             | 0.22  | 0.41                   | 0.14                             | 0.67                         | 0.22                         | 0.22              |
| 90% width             | 0.15  | 0.37                   | 0.05                             | 0.64                         | 0.21                         | 0.16              |
| 25% area              | 0.19  | 0.36                   | 0.24                             | 0.46                         | 0.22                         | 0.14              |
| 50% area              | 0.22  | 0.38                   | 0.22                             | 0.57                         | 0.22                         | 0.18              |
| 75% area              | 0.23  | 0.39                   | 0.15                             | 0.68                         | 0.23                         | 0.20              |
| 90% area              | 0.21  | 0.39                   | 0.09                             | 0.70                         | 0.23                         | 0.20              |
| 25% perimeter         | 0.12  | 0.31                   | 0.14                             | 0.37                         | 0.19                         | 0.07              |
| 50% perimeter         | 0.16  | 0.33                   | 0.15                             | 0.42                         | 0.25                         | 0.11              |
| 75% perimeter         | 0.16  | 0.34                   | 0.09                             | 0.48                         | 0.27                         | 0.12              |
| 90% perimeter         | 0.09  | 0.31                   | 0.02                             | 0.43                         | 0.22                         | 0.06              |
| 25% aspect            | 0.05  | 0.35                   | 0.06                             | 0.59                         | 0.21                         | 0.08              |
| 50% aspect            | 0.05  | 0.35                   | 0.06                             | 0.54                         | 0.20                         | 0.08              |
| 75% aspect            | 0.01  | 0.30                   | 0.02                             | 0.41                         | 0.18                         | 0.01              |
| 90% aspect            | 0.01  | 0.30                   | 0.03                             | 0.39                         | 0.19                         | 0.02              |
| 25%,50%,75% LC        | 0.16  | 0.34                   | 0.13                             | 0.43                         | 0.27                         | 0.11              |
| 25%,50%,75% width     | 0.26  | 0.43                   | 0.41                             | 0.69                         | 0.23                         | 0.25              |
| 25%,50%,75% area      | 0.23  | 0.40                   | 0.25                             | 0.68                         | 0.25                         | 0.20              |
| 25%,50%,75% perimeter | 0.17  | 0.34                   | 0.16                             | 0.49                         | 0.28                         | 0.13              |
| 25%,50%,75% aspect    | 0.27  | 0.45                   | 0.36                             | 0.61                         | 0.30                         | 0.27              |
| Average LC            | 0.16  | 0.33                   | 0.14                             | 0.42                         | 0.27                         | 0.10              |
| Average width         | 0.21  | 0.40                   | 0.19                             | 0.60                         | 0.22                         | 0.20              |
| Average area          | 0.24  | 0.39                   | 0.20                             | 0.64                         | 0.23                         | 0.20              |
| Average perimeter     | 0.18  | 0.32                   | 0.15                             | 0.49                         | 0.27                         | 0.13              |

<sup>a</sup>SG, specific gravity; SVR, sonic velocity ratio; LA, low alignment; HA, high alignment; LC, long chord.

<sup>b</sup>All variables weighted by area.

**Thickness Swell**—Using the format

$$TS = e^{\mu} (WA)^{\lambda} (SG)^{\alpha} \quad (17)$$

the natural log of thickness swell was predicted with an accuracy of  $r^2 = 97$ . Specific gravity was slightly significant at the 0.026 level while WA was highly significant at the 0.0001 level. The 50th width percentile (area-weighted) was the best additional furnish predictor. However, approximately the same fractional percentage increase in  $R^2$  values could be obtained with many other furnish characteristic variables. Equation (17) is the logarithmic form of the TS prediction equation used in a previous study (Geimer 1982). The new equation accounts for the absence of TS when the WA is 0.

**Linear Expansion**—Since LE is highly dependent on alignment, the SVR is a dominant variable in the prediction equation:

$$LE = e^{\mu} SG^{\alpha} SVR^{\pm\beta} WA^{\lambda} \quad (18)$$

By itself, the natural log of SVR can predict the natural log of LE with  $r^2 = 0.80$ . Addition of the WA term increases the  $r^2$  value to 0.86. Specific gravity is not significant and adds little to the prediction accuracy. As was the case with MOE prediction, the value of a furnish characterization variable is overshadowed by the SVR. The 50th width percentile (area-weighted) was the first choice among flake characteristics, but it only increased prediction accuracy to 0.87.

## Determining Sample Sizes

Determination of flake sample sizes that are needed to predict board properties, such as MOE, MOR, shear, and dimensional stability, is not a simple calculation. The easiest way to determine minimum sample size simulates the effects of different sample sizes obtained from the current data set. The board property in question along with SVR is calculated from a randomly selected flake sample of size  $n$ , for a particular furnish type, using the equations developed in this study. Repeating this procedure a number of times establishes the prediction variability for sample size  $n$ . Finally, using different values for  $n$ , a sample size that provides a variability suitable for the board property in some end-use condition is obtained. Because of its complexity and the range of end-use conditions to be considered, a simulation of this sort is not considered here. However, the data from this study are available from the authors.

## Conclusions

Although the average value of any one flake geometric descriptor, such as LC or width, is significantly different between screen fractions of a flake furnish, these values are highly dependent on the other flake dimensions (1/8 screen and larger) and consequently vary with furnish type.

Modern image analysis techniques provide a method to directly characterize a flake furnish using individual flake dimensions. By ranking the data from smallest to largest and determining percentile values, cumulative distribution curves can be constructed to compare factors such as LC, width, area, perimeter, etc., between flake furnishes. Geometric characteristics of individual flakes become more meaningful when weighted by their respective area.

The geometric predictor most useful in evaluating flake alignment is the area-weighted LC. The SVR, a measure of flake alignment, can be predicted with an  $r^2 = 0.75$  using the area-weighted 25th LC percentile. It is extremely important to relate flake furnish with extent of alignment, as this factor (SVR) was shown by itself to predict MOE of boards from the 13 furnish types with  $r^2 = 0.95$ . The relation of flake furnish to alignment given herein is of course only valid when using similar alignment equipment. This study points out the importance of developing equipment that can align relatively small particles. Width and area were important flake characteristics in considering the bending properties of a random board. The area-weighted 75th area percentile accounted for 59% of the MOE variability among the random boards of the 13 furnish types. Use of the area-weighted 25th LC percentile and the area-weighted 75th area percentile in conjunction with SG data allowed us to predict MOE of the HA boards from all furnish types with  $r^2 = 0.87$ . Prediction of MOE for the LA boards was done with  $r^2 = 0.85$ .

The same general logarithmic-type equation used to predict bending MOE was also found useful in predicting shear stress. Incorporation of SG, SVR, and the area-weighted 75th area percentile permitted the prediction of shear stress in the 13 furnish types with  $r^2 = 0.39$ .

Linear expansion, like MOE, is highly dependent on flake alignment. If the SVR and the change in WA are known, LE could be predicted with  $r^2 = 0.86$ . The area-weighted 50th width percentile was the flake characteristic most important in predicting LE once SVR and WA were accounted for. The area-weighted 50th width percentile was also the most useful flake characteristic to predict TS once WA and SG were accounted for.

## References

- Armstrong, J.P.; Patterson, D.W.; Sneckenberger, J.E. 1991. Comparison of three equations for predicting stress wave velocity as a function of grain angle. *Wood and Fiber Science*. 23(1): 32–43.
- ASTM. 1991. Standard methods for evaluating the properties of wood-based fiber and particle panel materials. ASTM D1037–91. Philadelphia, PA: American Society for Testing and Materials.

- Dai, C.; Steiner, P.R.** 1994a. Spatial structure of wood composites in relation to processing and performance characteristics. Pt. 2. Modeling and simulation of a randomly-formed flake layer network. *Wood Science and Technology*. 28: 135–146.
- Dai, C.; Steiner, P.R.** 1994b. Spatial structure of wood composites in relation to processing and performance characteristics. Pt. 3. Modeling the formation of multi-layered random flake mats. *Wood Science and Technology*. 28: 229–239.
- Geimer, R.L.** 1976. Flake alignment in particleboard as affected by machine variables and particle geometry. Res. Pap. FPL–275. Madison, WI: U.S. Department of Agriculture, Forest Service, Forest Products Laboratory.
- Geimer, R.L.** 1979. Data basic to the engineering design of reconstituted flakeboard. In: Proceedings, 13th Washington State University international symposium on particleboard.; 1979 April; Pullman, WA. Pullman, WA: Washington State University; 3: 105–125.
- Geimer, R.L.** 1980. Predicting flakeboard properties. In: Improvements in bending properties by aligning a mixture of flakes. Proceedings, 14th Washington State University international symposium on particleboard; 1980 April; Pullman, WA. Pullman, WA: Washington State University; 14: 59–76.
- Geimer, R.L.** 1981. Predicting shear and internal bond properties of flakeboard. *Holz als Roh-und Werkstoff*. 39(10): 410–415.
- Geimer, R.L.** 1982. Dimensional stability of flakeboards as affected by board specific gravity and flake alignment. *Forest Products Journal*. 32(8): 44–52.
- Geimer, R.L.** 1986. Mechanical property ratios, A measure of flake alignment. Res. Pap. FPL–RP–468. Madison, WI: U.S. Department of Agriculture, Forest Service, Forest Products Laboratory.
- Geimer, R.L.; Link, C.L.** 1988. Flake classification by image analysis. Res. Pap. FPL–RP–486. Madison, WI: U.S. Department of Agriculture, Forest Service, Forest Products Laboratory. 25 p.
- Geimer, R.L.; Price, E.W.** 1978. Construction variables considered in fabrication of a structural flakeboard. Gen. Tech. Rep. WO–5. Washington, DC: U.S. Department of Agriculture, Forest Service.
- Geimer, R.L.; Lehmann, W.F.; McNatt, J.D.** 1974. Engineering properties of structural particleboards from forest residues. In: Proceedings, 8th Washington State University symposium on particleboard; 1974 March; Pullman, WA. Pullman, WA: Washington State University; 8: 119–143.
- Geimer, R.L.; McDonald, K.A.; Bechtel, F.K.; Wood, J.E.** 1993. Measurement of flake alignment in flakeboard with grain angle indicator. Res. Pap. FPL–RP–518. Madison, WI: U.S. Department of Agriculture, Forest Service, Forest Products Laboratory.
- Heebink, B.G.; Schaeffer, E.L.; Chern, J.; Haskell, J.H.** 1977. Structural flakeboards using ring flakes from fingerling chips. Res. Pap. FPL–RP–296. Madison, WI: U.S. Department of Agriculture, Forest Service, Forest Products Laboratory.
- Kolsky, H.** 1963. *Stress waves in solids*. New York, NY: Dover Publications, Inc.
- Lang, E.M.; Wolcott, M.P.** 1995. Modeling the consolidation of a wood strand mat. In: *Mechanics of cellulosic materials*. New York, NY: Applied Mechanics Division, American Society of Mechanical Engineers; 209: 153–176.
- Lehmann, W.F.; Geimer, R.L.** 1974. Properties of structural particleboards from Douglas-Fir residues. *Forest Products Journal*. 24(10): 17–25.
- Lu, C.; Steiner, P.R.; Lam, F.** 1998. Simulation study of wood-flake composite mat structures. *Forest Products Journal*. 48(5): 89–93.
- SAS.** 1990. *SAS/STAT Software, Version 6, 1st ed.* Cary, NC: SAS Institute, Inc.
- Spelter, H.; McKeever, D.; Durbak, I.** 1997. Review of wood-based panel sector in United States and Canada. Gen. Tech. Rep. FPL–GTR–99. Madison, WI: U.S. Department of Agriculture, Forest Service, Forest Products Laboratory. 45 p.
- Steiner, P.R.; Dai, C.** 1993. Spatial structure of wood composites in relation to processing and performance characteristics. Pt. 1. Rationale for model development. *Wood Science and Technology*. 28: 45–51.
- Suchland, O.; Xu, H.** 1989. A simulation of the horizontal density distribution in a flakeboard. *Forest Products Journal*. 39(5): 29–33.
- Tansey, P.** 1994. In the eye of a panels whirlwind. *Wood Based Panels International*. 14(3):9–10.
- Turner, H.D.** 1954. Effect of particle size on strength and dimensional stability of resin bonded wood particleboard panels. *Forest Products Journal*. 4(4): 210–223.
- Winistorfer, P.M.; Xu, W.** 1996. Layer water absorption of medium density fiberboard and oriented strandboard. *Forest Products Journal*. 46(6): 69–72.
- Winistorfer, P.M.; Young, T.M.; Walker, E.** 1996. Modeling and comparing vertical density gradients. *Wood and Fiber Science*. 28(1): 133–141.